Preface

This report is written as a Master's Thesis at the Department of Civil and Environmental Engineering at Norwegian University of Science and Technology (NTNU) as part of the Master of Science (MSc) degree in Geotechnics and Geohazards. The study is carried out in the spring semester of 2021 under the supervision of Professor Gudmund Reidar Eiksund.

This report is continuation of the research done in fall semester of 2020 for the TBA4510-Geotechnical Engineering, Specialization Project. Working as a Structural Engineer for over twelve years, my interest for the field of dynamic analysis grew.

Working as a Structural Engineer at Multiconsult AS, I came recently across two projects where building had basement and a seismic analysis was required to perform. Especially, the case where one of the parallel basement walls had earth pressure.
I was more eager to carry out dynamic analysis and combine structural engineering with geotechnical engineering knowledge.

During this course, I received generous assistance from my supervisor, and I am grateful to him for giving me the opportunity to write about this topic under his supervision.

I would like to express my sincere gratitude to Professor Amir M. Kaynia who shared his opinions about results of this report.

I would also like to thank Corneliu Athanasiu my colleague at Multiconsult AS for sharing his thoughts about modelling of the base shear force in the PLAXIS 2D analysis presented in this Thesis.

Hijratullah Niazi

Trondheim, 24 June 2021

Summary

This Master's Thesis studies earthquake analysis by using the simplified approach proposed by the Eurocode 8. Three different models will be studied, model 1, in which earth pressure is along one of the longitudinal basement walls and in which it is assumed that the basement floor is semi-rigid, model 2, which has a basement, and earth pressure along both basement walls and in which it is assumed that the basement is rigid, finally, model 3, which is constructed on grade without a basement. The objective of this report is to study if the simplified method according to the EC8 can be used in case of one sided or two-sided earth pressure, and to examine if results from the EC8 method corresponds with the results from a Finite Element Method (FEM) program, PLAXIS 2D.

This report has mainly two parts. The first part calibrates the PLAXIS 2D model results with those obtained when using the one-dimensional programs DEEPSOIL and EERA. In this part, a representative soil model is constructed in PLAXIS 2D and results are then compared with those from DEEPSOIL and EERA. The Accelerogram and Pseudo Spectral Acceleration (PSA) on the surface of the model obtained from PLAXIS 2D show a good match with results from DEEPSOIL and EERA.

The calibrated model in part 1, is used for further analysis in Part 2. In this part, three different models are constructed and analyzed. The base shear force results obtained from PLAXIS 2D show that model 1 has the highest base shear force, 55,6 kN/m, model 2 has the lowest, 15,4 kN/m, and model 3 has a base shear force of 23,0 kN/m. The results according to the EC8 show that, model 1 and model 3 have 25,6 kN/m, and model 2 has a base shear force of 25,3 kN/m.

The results from EC8 and PLAXIS 2D suggest that, the simplified method according to EC8 provides relatively close results to FEM program when the model does not have a basement and is located on grade, as model 3. In the case of model 1, the EC8 method provides a lower base shear force than that provided by PLAXIS 2D. Furthermore, results show that in the case of model 2, the EC8 method provides a higher value than PLAXIS 2D.

EC8 suggests three methods for computing the fundamental period of a building T_1. Alternative 2, described in EC8 in section 4.3.3.2.2 (5), has been used to assess if the EC8 results gets better. As expected, results obtained for model 1 were increased from 25,6 kN/m to 27,8 kN/m. This implies that the simplified approach according to EC8 does not account for a building's stiffness, and therefore does not provide results that are close to those found using a FEM program such as PLAXIS 2D. Based on this report's findings for the selected *Time Series*, Kobe, it can be concluded that for the case of model 1 and model 2, analysis based on the FEM method is required to obtain more accurate results.

Sammendrag

Denne masteroppgaven studerer jordskjelvanalyse ved å bruke forenklet metode i henhold til Eurokode 8. Tre forskjellige modeller blir studert, modell 1 hvor jordtrykk er langs en av de langsgående kjellerveggene og hvor det antas at kjelleretasjen er semirigid, modell 2, som har kjeller, og jordtrykk langs begge kjellervegger og hvor det antas at kjelleren er stiv, til slutt, modell 3, som er konstruert på overflaten uten kjeller. Målet med denne rapporten er å undersøke om den forenklede metoden i henhold til EC8 kan brukes i tilfelle med ett eller tosidig jordtrykk, og å undersøke om resultatene fra EC8-metoden er i samsvarer med resultatene fra et Elementmetode program (FEM), PLAXIS 2D.

Denne rapporten består hovedsakelig av to deler. Den første delen kalibrerer PLAXIS 2D modellresultatene med de som oppnås ved bruk av endimensjonalt programmer DEEPSOIL og EERA. I denne delen konstrueres en representativ jordmodell i PLAXIS 2D, og resultatene blir deretter sammenlignet med DEEPSOIL og EERA. Akselerasjon og Pseudo Spektral Akselerasjon på overflate av modellen hentet fra PLAXIS 2D, viser godt samsvar med DEEPSOIL og EERA.

Den kalibrerte modellen i del 1, brukes videre i analyse i del 2. I denne delen konstrueres og analyseres tre forskjellige modeller. Baseskjær resultat fra PLAXIS 2D viser at modell 1 har den høyeste baseskjær, 55,6 kN/m, modell 2 har den laveste 15,4 kN/m, og modell 3 har en baseskjær på 23,0 kN/m. Resultatene i henhold til EC8 viser at modell 1 og modell 3 har 25,6 kN/m, og modell 2 har en baseskjær på 25,3 kN/m.

Resultatene fra EC8 og PLAXIS 2D foreslår at den forenklede metoden i henhold til EC8 gir relativt bra resultater med FEM programmet når modellen ikke har kjeller og ligger på overflaten, som i modell 3. For modell 1, EC8 metode gir en lavere baseskjær enn den som er gitt av PLAXIS 2D. Videre viser resultatene at i tilfelle av modell 2 gir EC8-metode høyere baseskjær enn PLAXIS 2D.

EC8 foreslår tre metoder for å beregne første egensvingendeperiode til et bygg T_1. Alternative 2 beskrevet i EC8-4.3.3.2.2 (5), har blitt benyttet for å studere om EC8 resultatene blir bedret. Som forventet ble resultatene for modell økt fra 25,6 kN/m til 27,8 kN/m. Dette betyr at den forenklede metoden i henhold til EC8 ikke tar høyde for bygningens stivhet, og gir derfor ikke resultater som ligner på analysen med FEM programmet PLAXIS 2D.

Basert på denne rapportens resultat for den valgte tidsserien, Kobe, kan det konkluderes med at for tilfelle av modell 1 og modell 2 kreves analyse basert på elementmetoden for å oppnå mer nøyaktige resultater.

List of Figures

Figure 1: Deformation produced by body waves: (a) p-wave, (b) SV-wave, (Kramer, 1996) ..7
Figure 2: Deformations produced by surface waves: (a) Rayleigh wave, (b) Love wave, (Kramer, 1996) ..7
Figure 3: Free vibration of underdamped, critically damped, and overdamped systems, (K.Chopra, 2012) ..9
Figure 4: Ground response nomenclature: (a) soil overlying bedrock, (b) no soil overlying bedrock, (Kramer, 1996) ..10
Figure 5: Examples of common problems typically analyzed by two-dimensional plane strain dynamic response analysis: (a) cantilever retaining wall, (b) earth dam, (c) tunnel, (Kramer, 1996) ..11
Figure 6: Schematic representation of stress-strain model used in EL model, (EERA Manual) ..12
Figure 7: Equivalent-Linear Model, (a) Hysteresis stress-strain curve, (b) Variation of secant shear modulus and damping ration with shear strain amplitude (EERA Manual) ..12
Figure 8: A hysteretic loop in one cycle of soil shearing, (SRBULOV, 2008) ..14
Figure 9: Stiffness parameters of Hardening Soil model with small-strain stiffness in a triaxial test, (Bentley-12, 2021) ..17
Figure 10: Characteristic stiffness-strain behavior of soil, (Bentley-12, 2021) ..17
Figure 11: Results from the Hardin-Drnevich relationship compare to test data by Santos & Correia (2001), (Bentley-12, 2021) ..18
Figure 12: Hysteretic behavior in the HSsmall model, (A. Laera, 2017) ..19
Figure 13: Modulus reduction curves, (A. Laera, 2017) ..20
Figure 14: Damping curve, (A. Laera, 2017) ..20
Figure 15: Role of damping ratio ξ in free vibration of a SDOF system, (Bentley-12, 2021) 22
Figure 16: Node selection for input signal on dummy plate, (Bentley-05, 2014) ..23
Figure 17: Dynamic steps and the input signal, (Bentley-02, 2012) ..25
Figure 18: Dynamic steps and the input signal, (Bentley-02, 2012) ..25
Figure 19: Max number of steps stored, Reference Manual (Bentley-10, 2020) ..26
Figure 20: Iteration of shear modulus and damping ratio with shear strain in equivalent linear analysis, (EERA Manual) ..28
Figure 21: Normalized variation of complex shear modulus amplitude with critical damping ratio (Model 1), (EERA manual) ..29
Figure 22: Normalized variation of energy dissipated per loading cycle as a function of critical damping ratio for model 1 and 2, (EERA manual) ..30
Figure 23: Shape of the elastic response spectrum (NS-EN 1998-1, figure 3.1) ..33
Figure 24: Horizontal elastic response spectra for use in Norway for ground type A to E (NS-EN 1998-1, figure NA.3(903)) ..34

Figure 25: SDOF system with ground excitation, illustration by Hijratullah Niazi, after Dimensjonering for JORDSKJELV (Øystein Løset, et al 2010) 37
Figure 26: Input File Parameters, SeismoMatch 38
Figure 27: Input multiple source accelerogram, SeismoMatch 39
Figure 28: Different Accelerogram files, SeismoMatch 39
Figure 29: Analysis Control Definition-1, DEEPSOIL 40
Figure 30: Analysis Control Definition-2, DEEPSOIL 41
Figure 31: Soil column, PLAXIS 2D 42
Figure 32: Model 1 45
Figure 33: Model 2 45
Figure 34: Model 3 46
Figure 35: Points selected for output result-Part 1 48
Figure 36: PSA response spectra at point A 49
Figure 37: Acceleration at point A, without Rayleigh damping 50
Figure 38: Acceleration at point A with Rayleigh damping coefficients 51
Figure 39: PSA response spectra at point A (with Rayleigh damping) 51
Figure 40: PSA response at point A, PLAXIS, DEEPSOIL and EERA 52
Figure 41: Acceleration at point A, PLAXIS, DEEPSOIL and EERA 53
Figure 42: Input and output signal at point B 54
Figure 43: Input and output signal at point B for $\delta t = 0{,}02$ 55
Figure 44: Input and output signal at point B for Compliant base boundary 56
Figure 45: Accelerogram at 3,6m from the surface level, (A. Laera, 2017) 58
Figure 46: PSA spectrum at 3.6 m from the surface level, (A. Laera, 2017) 59
Figure 47: Generated mesh with selected nodes-Model 1 60
Figure 48: Generated mesh with selected nodes-Model 2 60
Figure 49: Generated mesh with selected nodes-Model 3 60
Figure 50: Time history of displacement at point 1-Model 1 61
Figure 51: Frequency representation (spectrum)-Model 1 61
Figure 52: Time history of displacement at point 1-Model 2 62
Figure 53: Frequency representation (spectrum)-Model 2 62
Figure 54: Time history of displacement at point 1-Model 3 63
Figure 55: Frequency representation (spectrum)-Model 3 63
Figure 56: Shear Base Force obtained from FEM-Design 67
Figure 57: Dynamic time interval 79
Figure 58: Rayleigh damping coefficients 80
Figure 59: Base Shear Force, Model 1 81
Figure 60: Base Shear Force, Model 2 81
Figure 61: Base Shear Force, Model 3 82
Figure 62: Base Shear Force-Model 3 for interface R=0,6 82
Figure 63: Base Shear Force, Model 1 without Rayleigh damping 83

Figure 64: Input and output signal at point B-Part 1 84
Figure 65: Base Shear Force-Model 3 for Max number of steps store=50 84
Figure 66: Wall numbering 85
Figure 67: PSA Model 1 85
Figure 68: PSA Model 2 86
Figure 69: PSA Model 3 86
Figure 70: Displacement at top of Model 1 87
Figure 71: Output Time Series at point B, SeismoMatch 88
Figure 72: Output Response Spectra at point B, SeismoMatch 88
Figure 73: PSA at point A, DEEPSOIL 89
Figure 74: Acceleration at point A, DEEPSOIL 89
Figure 75: Earthquake tab sheet, (EERA) 90
Figure 76: Profile tab sheet, (EERA) 90
Figure 77: Variation of G, Vs and unit weight of soil with depth. Profile tab sheet, (EERA) 91
Figure 78: Mat1 tab sheet, (EERA) 92
Figure 79: Iteration tab sheet, (EERA) 92
Figure 80: Design Spectrum-Model 1 94
Figure 81: Design Spectrum-Model 2 96
Figure 82: Design Spectrum-Model 3 98
Figure 83: Design Spectrum for alternative computation of fundamental period $(T1)$-Model 1 99
Figure 84: Design Spectrum, for behavior factor $q = 2{,}0$ -Model 2 100
Figure 85: Mass of Model 1 and Model 3, illustration by Hijratullah Niazi 101
Figure 86: Mass of Model 2, illustration by Hijratullah Niazi 101
Figure 87: Ground types, (CEN, 2004), (TableNA.3.1) 102
Figure 88: Design concepts, structural ductility classes and upper limit reference values of the behavior factors, (CEN, 2004), (Table NA.6.1) 102
Figure 89: Seismic zones in southern Norway, $ag\ 40Hz$ in $m/s2$, (CEN, 2004), Fig NA.3(901) 103
Figure 90: Generating Ground Response Analysis 104
Figure 91: Check Dynamic Time Interval at the base of model 105
Figure 92: Plotting Frequency Representation (Spectrum) 106
Figure 93: Plot Base Shear Force 107

List of Tables

Table 1: Values of importance factor (NS-EN 1998-1, table NA.4(091)) 32
Table 2: Values of the parameters describing the recommended elastic response spectra (NS-EN 1998-1, Tabell NA.3.3) 33
Table 3: Values of parameters describing the vertical elastic response spectrum (CEN, 2004), Table NA.3.4 34
Table 4: Soil material parameter 43
Table 5: Boundary conditions 44
Table 6: Stage construction for Part 1 44
Table 7: Stage construction for Part 2-Model 1 and Model 2 46
Table 8: Stage construction for Part 2-Model 3 47
Table 9: Material properties of concrete 47
Table 10: Comparison PSA in PLAXIS 2D and DEEPSOIL 49
Table 11: Comparison Accelerogram in PLAXIS 2D and DEEPSOIL 50
Table 12: Comparison Accelerogram in PLAXIS 2D (with Rayleigh damping) and DEEPSOIL 52
Table 13: Comparison PSA in PLAXIS 2D (with Rayleigh damping) and DEEPSOIL 52
Table 14: Summary PSA, PLAXIS, DEEPSOIL and EERA 53
Table 15: Summary comparison Accelerogram PLAXIS 2D, DEEPSOIL and EERA 53
Table 16: Summary building natural frequency 64
Table 17: Base shear force-Model 1 68
Table 18: Base shear force -Model 2 68
Table 19: Base shear force -Model 3 68
Table 20: Base shear force, Model 3 for Interface R=0,6 68
Table 21: Base Shear Force, Model 1 without Rayleigh damping coefficient 69
Table 22: Base Shear Force-Model 3 for Max number of steps stored=50 69
Table 23: Summary Base Shear Force 70
Table 24: Base shear force-Alternative method for computation of fundamental period-Model 1 71
Table 25: Base shear force for different behavior factor q, Model 2 73
Table 26: Material parameter Hssmall model 77
Table 27: Summary Base Shear Force-Model 3 for interface R=0,6 83
Table 28: Summary Base Shear Force, Model 1 without Rayleigh damping 83

Acronyms

CEN	European Committee for Standardization
DCH	Ductility class high
DCL	Ductility class low
DCM	Ductility class medium
EA	Axial stiffness
EERA	Equivalent-linear Earthquake Response Analysis
EI	Inertial stiffness
EL	Equivalent linear
FEM	Finite element method
FFT	Fast Fourier Transform
GW	Ground Water level from top of the soil
HSsmall	Hardening Soil Small strain
N_{SPT}	Standard Penetration Test blow-count
PGA	Peak Ground Acceleration
PI	Plasticity index
P_{NCR}	Reference probability of exceedance in 50 years of the reference seismic action for the no-collapse requirement
PSA	Pseudo Spectral Acceleration
SDOF	Single Degree of Freedom
SH	S-waves horizontal direction
SV	S-waves vertical direction
T_{NCR}	Reference return period of the reference seismic action for the no-collapse requirement
w	Weight of the structure elements

List of Symbols

α	Rayleigh coefficient (section 2.5.1)
β	Lower bound factor for the horizontal design spectrum (section 2.5.3)
β	Rayleigh coefficient (section 2.5.1)
λ	Correction factor
Δt	Time interval (for full calculation phase)
h_i	Thickness of each soil layer
A_c	Total effective are of the shear walls in the first storey of the building
A_{loop}	Area of hysteresis loop
c'_{ref}	Cohesion (effective)
c_{cr}	Critical damping coefficient
E_{50}^{ref}	Secant stiffness in standard drained triaxial test
E_D	Dissipated energy
E_S	Energy accumulated at the maximum shear strain
E_{oed}^{ref}	Tangent stiffness for primary oedometer loading
E_{ur}^{ref}	Unloading/reloading stiffness from drained triaxial test
F_b	Base shear force
F_i	Force at floor
G^*	Complex shear modulus
G_s	Secant shear modulus
G_t	Tangent shear modulus
$[K]$	Stiffness matrix
K_0	Coefficient of earth pressure at rest
$[M]$	Mass matrix
R_{int}	Interface
R_γ	Ratio of effective shear strain to maximum shear strain
$S_d\ (T)$	Design elastic response spectra
$S_e(T)$	Elastic response spectrum
T_1	Fundamental period of vibration of the building for lateral motion
T_B	Lower limit of the period of the constant spectral acceleration branch
T_C	Upper limit of the period of the constant spectral acceleration branch
T_D	Value defining the beginning of constant displacement response range of the spectrum
$V_{s,30}$	Average value of propagation velocity of S waves in the upper 30m of the soil profile at shear strain of 10^{-5} or less
V_s	Shear wave velocity
W_D	Dissipated energy

W_S	Maximum strain energy
a_g	Design ground acceleration on type ground A
a_{gR}	Reference peak ground acceleration on type ground A
a_{vg}	Design ground acceleration in the vertical direction
f_1	Fundamental frequency
p_{ref}	Atmospheric pressure, $p_{ref} = 100\ kpa$
$\dot{u}\ (t)$	Velocity
$\ddot{u}\ (t)$	Acceleration
u_i	Deformation of floor
v_i	Shear wave velocity (at a shear strain level of 10^{-5} or less)
$\dot{\gamma}$	Shear strain rate
$\gamma_{0,7}$	Threshold shear strain at which Gs=0,722 G0
γ_I	Importance factor
γ_c	strain amplitude
γ_{eff}	Effective shear strain
γ_{sat}	Soil unit weight, saturated
γ_{unsat}	Soil unit weight, unsaturated
δ_t	Dynamic elementary time step
λ_s	Length of share wave
ν_{ur}	Poisson's ratio
σ_1'	Major effective principle stress
σ_3'	Minor effective principle stress
τ_c	Shear stress
ω_n	Natural angular frequency
c	Damping constant
d	Lateral displacement of the top of the building
f	Frequency
g	Gravity
G	Shear modulus
H	Height of the structure
k	Spring constant, spring stiffness
m	Mass of the structure (equation (2.11))
m	Number of sub-steps (equation (2.29))
m	Power for stress-level dependency of stiffness (equation (2.13), (2.14), (2.15),(2.16))
n	Max steps
p	Force
q	Behavior factor
S	Soil factor

T	Vibration of a linear SDOF system
$u\,(t)$	Displacement
γ	Shear strain
η	Damping correction factor (section 2.5.3)
η	Viscosity (section 2.4.1)
ν	Poisson's ratio
ξ	Damping ratio
ρ	Density
τ	Shear stress
φ	Friction angle
ψ	Dilatancy angle
ω	Angular frequency

TABLE OF CONTENTS

Preface i
Summary iii
Sammendrag v
List of Figures vii
List of Tables x
Acronyms xi
List of Symbols xii

1 INTRODUCTION 1
1.1 BACKGROUND 1
1.2 OBJECTIVES 2
1.3 APPROACH 3
1.4 LIMITATIONS 4
1.5 THESIS OUTLINE 5

2 LITERATURE 6
2.1 Geodynamics 6
2.2 Seismic Waves 6
2.3 Free Vibration 8
2.4 Ground Response Analysis 10
2.4.1 Equivalent Linear Analysis 11
2.4.2 Non-Linear Analysis 13
2.4.3 Shear Modulus 14
2.5 Analyzing Method 15
2.5.1 Finite Element Method 15
2.5.2 One-Dimensional Analysis 27
2.5.3 Eurocode 8 31

3 METHODOLOGY 38

4 ANALYSIS AND RESULTS 48
4.1 Part 1 48
4.2 Summary and Discussion 57
4.3 Part 2 60
4.4 Free Vibration Analysis 61
4.5 Calculation of Base Shear Force 65
4.5.1 Eurocode 8 65
4.5.2 PLAXIS 2D 68
4.6 Discussion 70

5 CONCLUSION 72

6 RECOMMENDATION FOR FURTHER WORK 74

7 BIBLIOGRAPHY 75
8 APPENDICES 77
8.1 Appendix A 77
8.2 Appendix B 81
8.3 Appendix C 88
8.4 Appendix D 89
8.5 Appendix E 90
8.6 Appendix F 93
8.7 Appendix G 104

1 INTRODUCTION

1.1 BACKGROUND

Although Norway has low seismicity compared to the other regions, it is still mandatory to check structures for earthquake loads. According to Eurocode 8, this applies to all structures unless a structure satisfies the rules for omission of earthquake design. EC8 consists of six parts, each part deals with a different type of structures. NS-EN 1998-1 deals with design of structures for earthquake resistance. In this Thesis, the relevant part of EC8-1 will be studied.

Engineers mostly prefer to use a simple, and reliable approach, which provides approximate values. The EC8 method offers a simplified approach for earthquake calculations, and because of its simplicity and good approximation, it is still attractive to Design Engineers. On the other hand, Finite Element Method (FEM) analysis programs offer more realistic values but requires extensive knowledge of the program. Additionally, performing analysis takes more time than the simplified approach proposed by the EC8 method.

In this Thesis, three different models will be analyzed both with the simplified method according to the EC8 method and with a FEM program, PLAXIS 2D. Model 1 has earth pressure on one of the longitudinal basement walls, model 2 has a basement and earth pressure along both longitudinal basement walls, and model 3 is located on grade without a basement. Obtained results from both methods will be studied and compared.

Problem Formulation

This Thesis will focus on earthquake analysis according to the simplified method proposed by the EC8 method, and three different models will be studied. The numerical analysis is performed in PLAXIS 2D, which is a FEM-based program. The results from the EC8 method and PALXIS 2D will be compared, and PLAXIS 2D will be used as a tool for comparison purposes.

First, FEM program, PLAXIS 2D model should be calibrated with a one-dimensional program. Hence, ground response analysis will be performed in PLAXIS 2D where Accelerogram and Pseudo Spectral Acceleration (PSA) at the surface of the model will be compared with results from one-dimensional programs. Two different one-dimensional programs will be used, DEEPSOIL and EERA. The results from PLAXIS 2D will be compared with those from DEEPSOIL and EERA, where calibrated model input parameters will be used for further analysis.

Task Description

- Perform free field site response analysis in PLAXIS 2D and compare output results for accelerogram and PSA at the surface of the model with the one-dimensional program, DEEPSOIL and EERA
- Construct three different models and carry out dynamic analysis in PLAXIS 2D
- Perform free vibration analysis in PLAXIS 2D, use obtained natural frequency of the structures in the EC8 equations for comparison of obtained base shear force between EC8 and PLAXIS 2D
- Calculate the base shear force according to the simplified method proposed in the EC8 and compare results for the three models with those from FEM program, PLAXIS 2D

1.2 OBJECTIVES

The main objective of this report is to study how results based on EC8 method corresponds to results obtained from a FEM program. Furthermore, to examine which case according to the EC8 method provides conservative or nonconservative results.

The objectives of this report are summarized in the following:

1. Calibrate the PLAXIS 2D model and compare the results from PLAXIS 2D with one-dimensional programs. Perform ground response analysis in PLAXIS 2D, DEEPSOIL and EERA. Compare the obtained accelerogram and PSA results from PLAXIS 2D with DEEPSOIL and EERA. The objective of this comparison is to ensure that input parameters in PLAXIS 2D are reasonably correct. The aim of using two different one-dimensional programs is to study if PLAXIS 2D results correspond with both DEEPSOIL and EERA.
2. Construct three different models in PLAXIS 2D, use the calibrated model properties for further analysis, and perform earthquake analysis. Compare the results from PLAXIS 2D with results obtained using the EC8 method.
3. Use different variables and study the influence of parameters on results obtained from PLAXIS 2D. The aim is to study if using different variables will influence output results in PLAXIS 2D.
4. Obtain the natural frequency of each model from PLAXIS 2D, use the values in the EC8 calculations for base shear force, and discuss the results.
5. Compute the fundamental period of vibration of the building T_1 according to the equation (4.9) described in section 4.3.3.2.2 (5) in EC8 and discuss the results.
6. Use different values for the behavior factor q in the EC8 calculations and discuss the results.

1.3 APPROACH

The approach used to achieve the research objectives is summarized as follow:

Phase 1: PLAXIS 2D model calibration: The selection of boundary conditions and material properties calculation are made according to recommendations from PLAXIS. The time series is generated in SeismoMatch for a particular location in the city of Trondheim, where peak ground acceleration value and ground type are taken from EC8 and are used as input in SeismoMatch. The generated plots from SeismoMatch is used as the input time series for DEEPSOIL, EERA and PLAXIS 2D for further calculations. A soil column is modelled in PLAXIS 2D, where output results at the top of the model, Accelerogram and PSA are compared with the results from DEEPSOIL and EERA.

Phase 2: Construct models in PLAXIS 2D: Three different models will be constructed and analyzed in PLAXIS 2D, where material properties and boundary conditions are according to the calibrated model performed earlier. The time series generated in SeismoMatch will be used as the input signal motion at the base of the model in PLAXIS 2D. All models have same width, height, and mass, but each model is different in relation to the surface and basement. Model 1 has earth pressure on one of its longitudinal basement walls, model 2 has a basement and earth pressure on both basement walls, and model 3 is on grade without a basement.

Phase 3: Comparison of the base shear force: The same peak ground acceleration, and ground type, used for calibration will be used as the input for the EC8 calculations. Three calculations will be performed, one for each model. According to the EC8 assumptions, model 1 and model 3 are the same in regard to their height and mass, whilst, model 2 has less mass and one floor less height, since mass and height are taken from top of the rigid basement and not from top of the foundation. Base shear force results from EC8 will be compared with PLAXIS 2D.

Phase 4: Studying of parameters in PLAXIS 2D: Several parameters will be changed in PLAXIS 2D and the effect will be studied. For section 4.1 Part 1, the effect of defining Rayleigh damping coefficients, incorrect dynamic time intervals, and simulation for a different type of boundary condition at the base of the model will be studied. For section 4.5.2 PLAXIS 2D, the effect of the interface, modelling without defining Rayleigh damping coefficients, and selecting lower numbers for *Max number of steps stored* in the dynamic phase, will be studied. Results when using the changed parameters will be compared with the original results for each part.

Phase 5: Studying of parameters in EC8: Fundamental period T_1 will be calculated according to an alternative method described in section 4.3.3.2.2 (5) in EC8. Calculation of base shear force in EC8 will be performed for two different behavior factor q values, and the results will be discussed.

1.4 LIMITATIONS

Earthquake analysis is a broad topic. Due to scope of this report and time constraints, relevant theories and analysis methods are included. Hence, this report has certain limitations which are as follow:

- Since only PLAXIS 2D is used for the FEM analysis part, no literature and analysis regarding PLAXIS 3D is added in this report
- Liquefication is not part of the analysis, no literature and analysis regarding liquefication is presented in this report
- The analysis performed in this report does not consider accumulation of the pore pressure, hence it is not relevant to model the dissipation of pore overpressure after an earthquake
- Calculations for Distribution of the horizontal seismic forces according to the section 4.3.3.2.3 in EC8 is not included in this report
- The analysis performed in this report is limited to the earthquake loads in Norway, and relevant Norwegian National Annex values are used
- In this report, only one *Time Series*, Kobe, is used as input signal motion
- This Thesis considers only Part 1 of the NS-EN 1998, other parts are not included
- Analysis according to the EC8 method is carried out only for the *Lateral force method analysis*, and analysis according to other methods are included in this report

1.5 THESIS OUTLINE

Contents of this Thesis are divided into eight chapters, summary of each chapters is presented below.

Chapter 1: Introduction: An overall overview of Thesis is given in this chapter, it describes Background, Objectives, Approach, and report Limitations.

Chapter 2: Literature Review: Relevant and selected literature regarding earthquake, the PLAXIS 2D Dynamic module, and the EC8 will be discussed in this chapter.

Chapter 3: Methodology: In this chapter, the methodology of how each program is used in this report will be discussed. Additionally, it will be discussed in detail how models are constructed in PLAXIS 2D for the dynamic analysis, material parameters are computed, selection of boundary conditions, and at the end procedure for generating of plots.

Chapter 4: Analysis and Results: This chapter will cover analysis carried out in PLAXIS 2D and calculations according to the EC8 method. Results from both methods will be then compared.

Chapter 5: Discussion and Conclusion: Results obtained from PLAXIS 2D and EC8 method will be discussed and based on the obtained results conclusion will be provided.

Chapter 6: Recommendation for Further work: Recommendations for possible further work will be given.

Chapter 7: Bibliography: In this section, all used references for this report will be given. Several PLAXIS 2D documents has been used for this report besides other literature sources.

Chapter 8: Appendices:

Generally, all detailed calculations, graphs and other material which are not covered in other chapters are attached in this section. The Appendix G in this report, shows useful tips for the PLAXIS 2D, this might help reader to know how certain curves are generated in the PLAXIS 2D.

2 LITERATURE

Geotechnical Earthquake Engineering in comparison to other Civil Engineering disciplines is quite young. The study of earthquakes, their effect on people and their environment is becoming more and more important task for the design engineers to consider it during design phase, especially when the structure is in the seismic zone. This section will cover related literature to the earthquake analysis according to the methods proposed in the EC8 and the PLAXIS 2D.

2.1 Geodynamics

Geodynamics deals with the dynamics of the earth, understanding of plate tectonics and geologic phenomena. It is important to understand all aspects of geodynamics when designing a structure in a seismic zone. Ground motion resulting from earthquakes especially with large magnitude can be disastrous dynamics disturbance which will affect human made structures.

As a result of formation of the fracture in the earth's crust, earthquake occurs, and formation of such fractures are caused by the tectonic forces. These forces have caused the formation of mountains, valleys, and oceans. The tectonic movement sets up elastic strains in the crustal rock, when the ability of the rock to sustain the elastic strain is exceeded, a fracture is initiated at the weakness zone of the rock. Fracturing relieves elastic strain energy stored in the rock, and consequently gives rise to the elastic waves which propagate outwards from the source of the fault. Since ground motions induced by the earthquake forces cause excitation of the structure, it is therefore important to study and analyze such forces. Measurement of the ground acceleration is generally common to obtain, velocity and displacement histories can be derived from the acceleration history by numerical integration process. It is therefore important to obtain the time histories of ground displacement to assess effect of the earthquake wave motion. (L.Humar, 2012)

Geodynamics is an extensive topic, in this assignment only topics related to the earthquake analysis according to the EC8 method which is the scope of this report will be discussed in the following sections.

2.2 Seismic Waves

When earthquake, volcanic eruptions, large landslides, or large man-made explosions occurs, seismic waves which are waves of the energy travel through the earth's layers. These waves are studied by geophysicists and it's called seismologist, and they are recorded by a seismometer, hydrophone (in water), or accelerometer. (Wikipedia-1, 2021)
There are different types of seismic waves, *body*, and *surface* waves. Body waves which travel through the interior of the earth are two types, *p-waves*, and *s-waves*. Figure 1

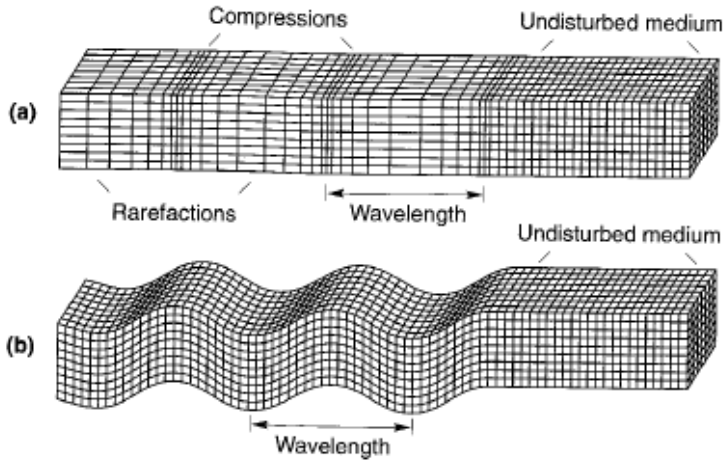

Figure 1: Deformation produced by body waves: (a) p-wave, (b) SV-wave, (Kramer, 1996)

P-waves are also known as primary, compressional or longitudinal waves. These types of waves are similar to the sound waves and can travel through solids and fluids. Their motion is parallel to the direction they travel through. S-waves on the other hand, are known as secondary, shear or transverse waves, which causes shearing deformation. S-waves direction of movement can be divided into two components, SV (vertical plane movement) and SH (horizontal plane movement). Since geological materials are stiff in compression, p-waves travel faster than the seismic waves. Fluids on the other hand, have no shearing stiffness, and thereby, they cannot sustain s-waves. Surface waves produces because of the interaction between body waves, surface, and the surficial layers of the earth. "They travel along the earth's surface with amplitudes that decreases roughly exponentially with depth". Rayleigh and Love waves are the most important surface waves for the engineering purposes. Rayleigh waves are produced by the interaction of p- and SV-waves with the earth surface, it contains both vertical and horizontal particle motions. Love waves are produced from the interaction of SH-waves with a soft surficial layer, this does not contain vertical component.
(Kramer, 1996)

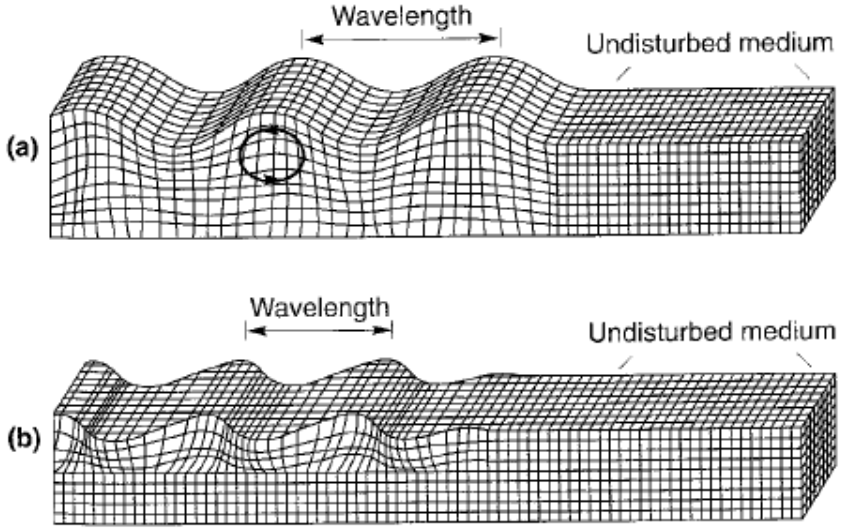

Figure 2: Deformations produced by surface waves: (a) Rayleigh wave, (b) Love wave, (Kramer, 1996)

2.3 Free Vibration

Free vibration response term refers to the response of a mechanical system where no external force causing the motion, but the system is excited by an initial disturbance alone. The equation of motion for a SDOF system when damping is viscous, can be written as:

$$m\ddot{u}(t) + c\dot{u} + ku = p \tag{2.1}$$

Provided that m, c, and k do not vary with time. Equation (2.1) is a linear second-order differential equation. The solution of the equation depends on the nature of the applied force and the initial conditions from which the motion is started. Even if p (external load) is zero, and system has given initial displacement, initial velocity, or both, the system will still undergo vibrations. Solving equation (2.1) and dividing it by mass m:

$$\ddot{u} + 2\xi\omega_n\dot{u} + \omega_n^2 u = 0 \tag{2.2}$$

Where

$$\omega_n = \sqrt{\frac{k}{m}} \tag{2.3}$$

$$\xi = \frac{c}{2m\omega_n} = \frac{c}{c_{cr}} \tag{2.4}$$

$$c_{cr} = 2m\omega_n = 2\sqrt{km} = \frac{2k}{\omega_n} \tag{2.5}$$

ω_n is natural angular frequency
ξ is damping ratio or fraction of critical damping
c_{cr} is critical damping coefficient
c is damping constant and is a measure of energy dissipated in a cycle of free vibration

"If $c < c_{cr}$ or $\xi < 1$ the system oscillates about its equilibrium position with a progressively decreasing amplitude. (underdamped system)

If $c = c_{cr}$ or $\xi = 1$ the system will return to its equilibrium position without oscillating. (critically damped system)

If $c > c_{cr}$ or $\xi > 1$ the system does not oscillate and returns to its equilibrium position. (overdamped system)" (K.Chopra, 2012)

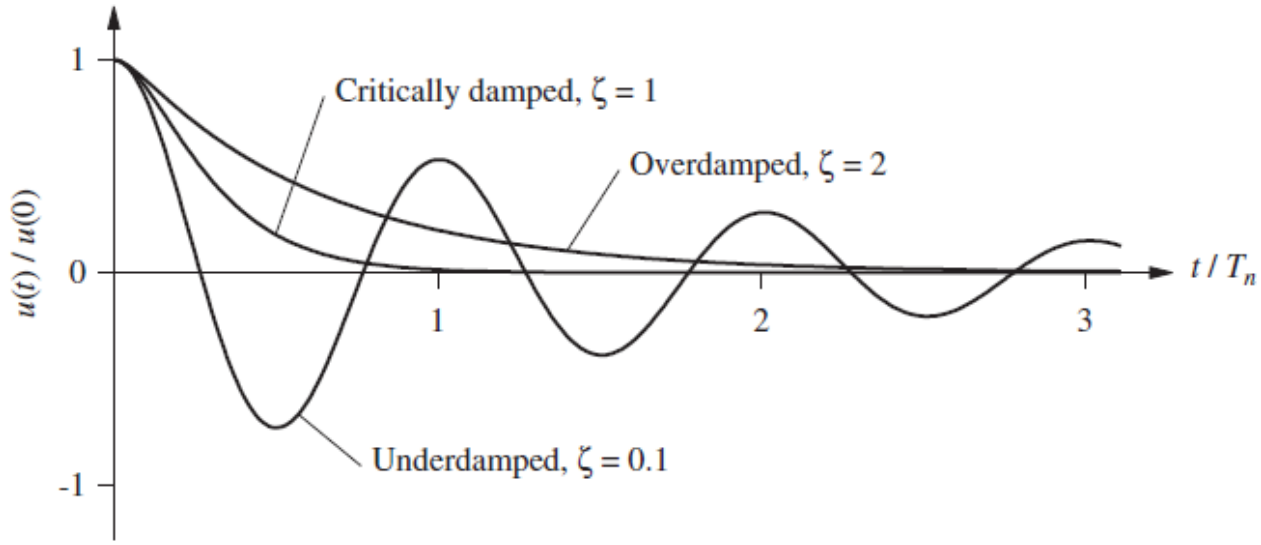

Figure 3: Free vibration of underdamped, critically damped, and overdamped systems, (K.Chopra, 2012)

It is important to study the response of free vibration of a system. The objective in this report is to find overlying structure's natural frequency and compare it with the maximum amplification of the ground motion. If the frequency at which maximum amplification of the ground is close to the natural frequency of the overlying structure, the structure and ground motions are in resonance, this means that the system will oscillate with very high amplitude and can cause damage to the structure.

2.4 Ground Response Analysis

Ground response analysis is used to predict ground surface motions for the design response spectra, and to determine earthquake induced forces that may lead to the instability of the structures. Most used methods are one-, two-, and three-dimensional ground response analysis. EERA and DEEPSOIL will be used as one-dimensional, whereas, PLAXIS 2D will be used as two-dimensional ground response analysis. This will be discussed further in section 3 METHODOLOGY and results will be shown in section 4.1 Part 1.

"One-dimensional ground response analysis is based on assumption that all boundaries are horizontal and that the response of a soil deposit is predominantly caused by SH-waves propagating vertically from the underlying rock". (Kramer, 1996)

The motion at the base of the soil deposit is called bedrock motion, and if the bedrock is exposed at the ground surface, it is called rock outcropping motion. Figure 4

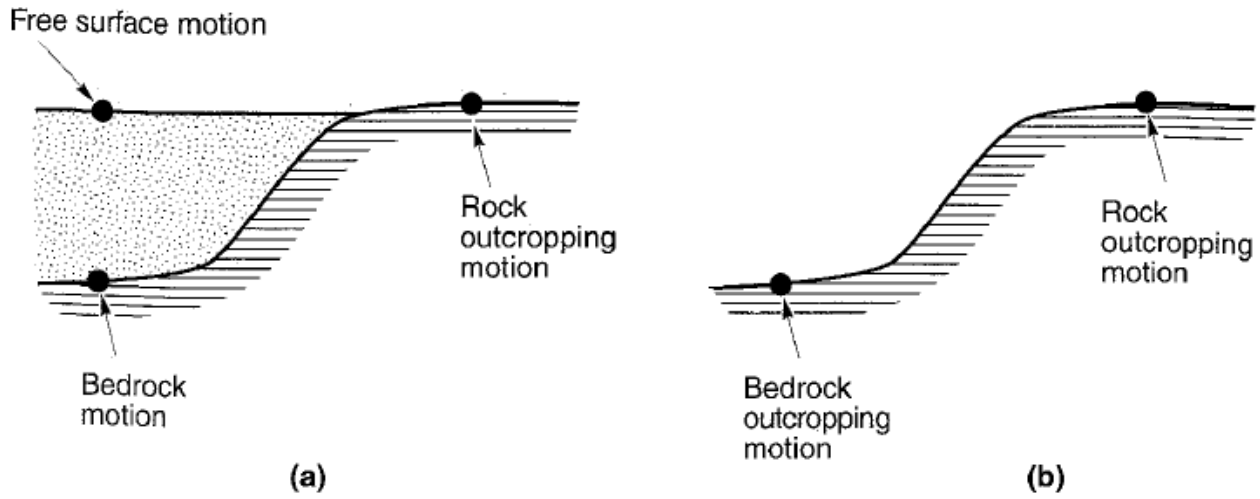

Figure 4: Ground response nomenclature: (a) soil overlying bedrock, (b) no soil overlying bedrock, (Kramer, 1996)

One-dimensional ground response analysis can be used for most cases, however, sloping, or irregular ground surfaces, embedded structures, tunnels, and the presence of heavy or stiff structures, requires two-dimensional ground response analysis. Figure 5

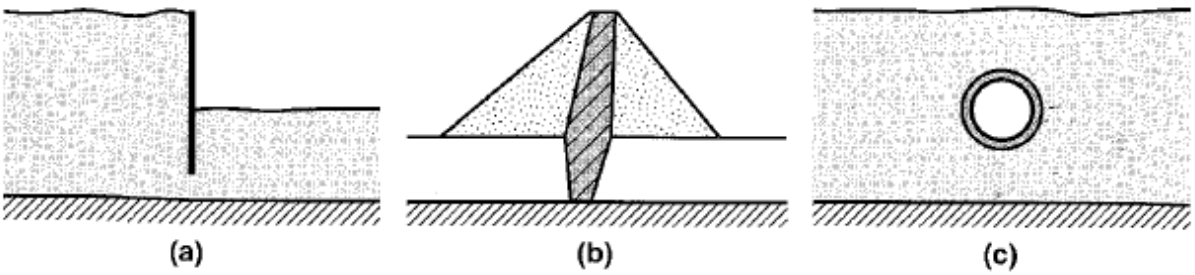

Figure 5: Examples of common problems typically analyzed by two-dimensional plane strain dynamic response analysis: (a) cantilever retaining wall, (b) earth dam, (c) tunnel, (Kramer, 1996)

In the following sections, two different ground response approach will be discussed, the equivalent linear and the nonlinear approach. Furthermore, the most common soil stiffness module, shear modulus G will be also discussed.

2.4.1 Equivalent Linear Analysis

The Equivalent Linear (EL) model is an iterative procedure and is based on Kelvin-Voigt model, it presents the soil stress-strain response and accounts for some types of the soil nonlinearities. Soil exhibits nonlinear and shows inelastic behavior under the cyclic loading conditions, and this can be approximated by the equivalent linear soil properties.

$$\tau = G * \gamma + \eta * \dot{\gamma} \tag{2.6}$$

G is shear modulus

τ is shear stress

γ is shear strain

$\dot{\gamma}$ shear strain rate

η is viscosity

The shear strain and its rate are defined as follow for a one-dimensional shear beam column, at depth z, time t and the horizontal displacement $u\,(z,t)$:

$$\gamma = \frac{\partial_u(z,t)}{\partial_z} \quad and \quad \dot{\gamma} = \frac{\partial_\gamma(z,t)}{\partial_t} = \frac{\partial_u^2(z,t)}{\partial_z * \partial_t} \tag{2.7}$$

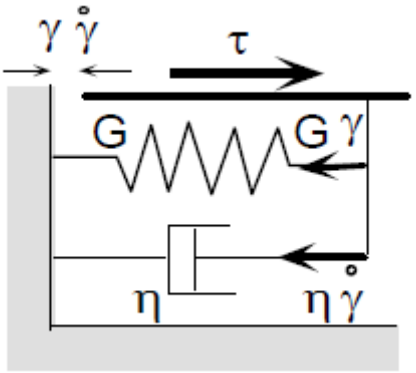

Figure 6: Schematic representation of stress-strain model used in EL model, (EERA Manual)

Figure 7 shows the nonlinear and the hysteretic stress-strain behavior of the soils, approximated during the cyclic loading. The secant modulus G_s depends on the shear strain amplitude γ.

$$G_s = \frac{\tau_c}{\gamma_c} \tag{2.8}$$

Where

τ_c is shear stress

γ_c is strain amplitude

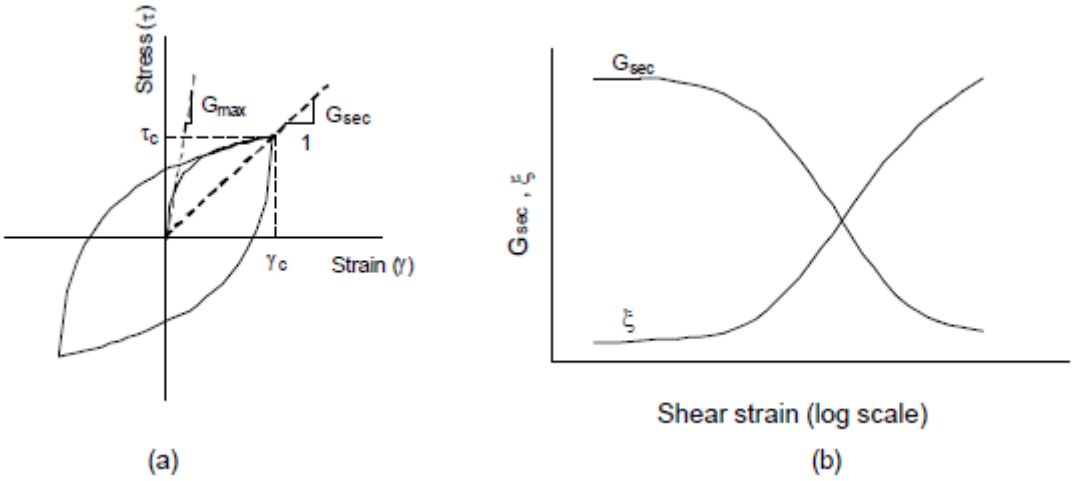

Figure 7: Equivalent-Linear Model, (a) Hysteresis stress-strain curve, (b) Variation of secant shear modulus and damping ration with shear strain amplitude (EERA Manual)

Figure 7(b) shows that as cyclic strain amplitude γ increases, stiffness G decreases and the damping ξ increases. Two important characteristics of the hysteresis loop are its breadth and its inclination. The secant shear modulus G_{sec} describes the general inclination of the hysteresis loop, and its inclination depends on the stiffness of the soil. The secant shear modulus G_{sec} value over the entire loop can be found by the equation (2.6). The breadth of the hysteresis loop is related to the area, it is a measure of the energy dissipation and it can be described as the damping ratio ξ.

$$\xi = \frac{W_D}{4 * \pi * W_s} = \frac{A_{loop}}{2 * \pi * G_{sec} * \gamma_c^2} \tag{2.9}$$

Where
W_D is dissipated energy
W_s is maximum strain energy
A_{loop} is area of the hysteresis loop

In the equivalent linear model, two parameters are well known, secant shear modulus G_{sec} and the damping ratio ξ , these are used to describe the soil. The EL approach works in frequency domain, and computation can be performed rapidly. Most of the ground response analysis programs are based on the equivalent linear model. In this report, two one-dimensional programs, DEEPSOIL and EERA will be used to perform ground response analysis. The disadvantage of the equivalent linear model is it cannot predict the permanent deformation or failure since this model implies that strain will always return to zero after the cyclic loading.

2.4.2 Non-Linear Analysis

The nonlinear model in contrast to the equivalent linear approach provides actual nonlinear response of the soil deposit using the direct numerical integration in the time domain. This model is also capable of computing pore pressure, permanent strain and thereby permanent deformations, stiffness degradation and dilation.

This method gives more accurate results than EL. However, it requires accurate nonlinear model parameters or a substantial field and laboratory testing. Results from the nonlinear analysis match EL when the strains are small, it is preferred to use the nonlinear analysis when strains are high, for instance for soft soils or for strong shaking. The disadvantages of the nonlinear analysis are, it is difficult to calibrate constitutive parameters, and in large models, program may crash. PLAXIS 2D which is based on Finite Element Method and uses the nonlinear analysis will be used in this report. A comparison of EL and the nonlinear analysis results from ground response analysis will be demonstrated in section 4.1 Part 1.

2.4.3 Shear Modulus

The shear modulus G presents the ratio between incremental shear stress and shear strain, in other words, it measures soil resistance to the shear deformation.

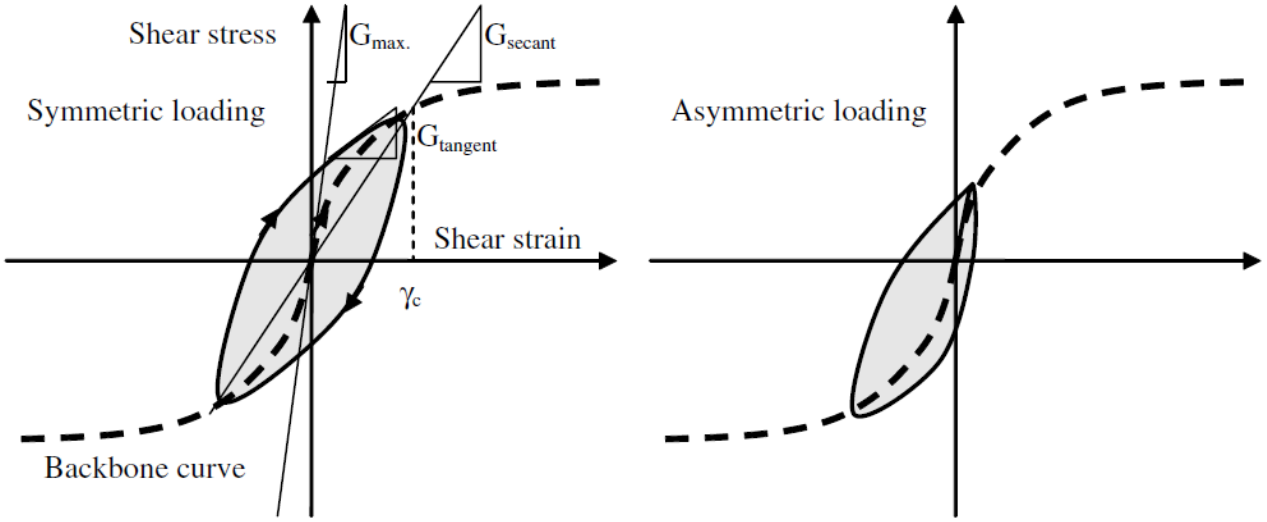

Figure 8: A hysteretic loop in one cycle of soil shearing, (SRBULOV, 2008)

Figure 7 and Figure 8 are the same, increasing of the shear strain will cause slippage between the grains and the weakening of the soil structure, hence shear strength and stiffness of the soil will be decreased. "This process results in rotation of the hysteretic loop towards the horizontal axis. The locus of points corresponding to the tips of the hysteretic loops of various cyclic strain amplitudes is called a backbone curve". (SRBULOV, 2008)

Laboratory tests have shown that soil stiffness is influenced by the cyclic strain amplitude, density, void ratio, mean principal effective stress, plasticity index, over consolidation ratio, and number of loading cycles (e.g. Seed and Idriss (1970), Hardin and Drnevich (1972), Vucetic and Dobry (1991), Ishibashi (1992), and Kramer (1996). (SRBULOV, 2008)

The maximum shear modulus can be computed by:

$$G_{max} = \rho * V_s^2 \tag{2.10}$$

In the equation (2.10) the most reliable means is the measured shear wave velocity V_s, since this will give the proper maximum shear modulus G_{max}. In section 3 METHODOLOGY, the relation between the maximum shear modulus and other material parameters will be shown.

2.5 Analyzing Method

In this section, two analyzing methods will be discussed for the calculation of Base Shear Force. The PLAXIS 2D program will be used as a FEM analysis method and simplified approach according to the methods proposed by the EC8. For generating time series, SeismoMatch application will be used. The generated time series from SeismoMatch will be used as input signal motion for the DEEPSOIL, EERA and PLAXIS 2D. DEEPSOIL and EERA will be used for the Site Response analysis, where results will be then compared with the PLAXIS 2D.

2.5.1 Finite Element Method

PLAXIS 2D is based on Finite Element Method analysis, and it will be used in this Thesis for the dynamic analysis part.

Dynamic Analysis

PLAXIS 2D has developed one module for the Dynamic Analysis. This module can analyze the dynamic loads such as vibration from machines, impact and blast loads, moving vehicle loads and the earthquake loads. The dynamic analysis can be done as drained, undrained, or Dynamics with consolidation.

The input dynamic load can be displacement multiplier or load multiplier and can be defined as harmonic or input table. Two special factors should be considered when performing dynamic analysis in the PLAXIS 2D, special boundary type should be selected and define correct dynamic time interval, Max steps and Number of sub-steps to obtain accurate results. Input signal motions can be also scaled into the desired value, user can select drift correction in the Multipliers menu for correction of the displacement drift, it will enhance and gives a smooth curve.

Although, PLAXIS 2D has different boundary conditions both for the base and lateral boundaries, these should be chosen with great care when it comes to the dynamic analysis. Selection of boundary condition will affect output results.

User can plot different curves, such as acceleration, displacement, and velocity. To determine the predominant period, PSA spectrum graph can be plotted. From PSA graph, maximum shear stress at the base of the structure can be calculated according to the following equation:

$$F_{max} = m * PSA = \frac{PSA}{g} * w \tag{2.11}$$

Where m is mass of the structure [kg], and g is gravity acceleration [m/s^2].

In the PLAXIS, the response spectrum is calculated as the response of the SDOF systems in terms of accelerations, characterized by different stiffness k, but with same damping ratio ξ. Stiffness of the structure k is incorporated in the natural period T equation. (A. Laera, 2017)

$$T = 2\pi\sqrt{\frac{m}{k}} \tag{2.12}$$

Material Model

PLAXIS program has several material models, the one which is recommended by the PLAXIS for the dynamic analysis and is used in this report is the Hardening Soil model with small-strain stiffness, known as Hardening Soil Small (HSsmall). This model can simulate strain dependency of stiffness and the hysteretic damping. PLAXIS has published a manual for the material model, *Material Models Manual*. It is recommended to read the manual to understand capability and limitations of each material model.

Hardening Soil Model with Small Strain Stiffness (HSsmall)

The Hardening Soil model with small-strain stiffness is an advanced model and is based on the Hardening Soil model. In this model, increased stiffness of the soil at small strain is considered, which makes this model unique for the dynamic analysis. The HSsmall model uses the same material parameters like Hardening Soil model, extended by introducing two additional parameters which describe the variation of the stiffness with strain.

1. Small-strain shear modulus G_0
2. Shear strain level $\gamma_{0,7}$ at which the secant shear modulus G_s is reduced to about 70% of G_0

Following equations are used for HSsmall model:

$$E_{50} = E_{50}^{ref} * \left(\frac{\sigma_3' + a}{p_{ref} + a}\right)^m \tag{2.13}$$

$$E_{ur} = E_{ur}^{ref} * \left(\frac{\sigma_3' + a}{p_{ref} + a}\right)^m \tag{2.14}$$

$$E_{oed} = E_{oed}^{ref} * \left(\frac{\sigma_1' + a}{p_{ref} + a}\right)^m \tag{2.15}$$

$$G_0 = G_0^{ref} \left(\frac{\mathrm{c} * \cos(\varphi) - \sigma_3' * \sin(\varphi)}{\mathrm{c} * \cos(\varphi) + p^{ref} * sin(\varphi)}\right)^m \tag{2.16}$$

$$G_0^{ref} = \frac{E_0^{ref}}{2 * (1 + \upsilon_{ur})} \tag{2.17}$$

Where

m is Power for stress-level dependency of stiffness, varies normally between 0,5 and 1,0

E_{50}^{ref} is Secant stiffness in standard drained triaxial test

E_{oed}^{ref} is Tangent stiffness for primary oedometer loading

E_{ur}^{ref} is Unloading/reloading stiffness from drained triaxial test

ν_{ur} is Poisson's ratio

p_{ref} is Atmospheric pressure, $p_{ref} = 100\ kpa$

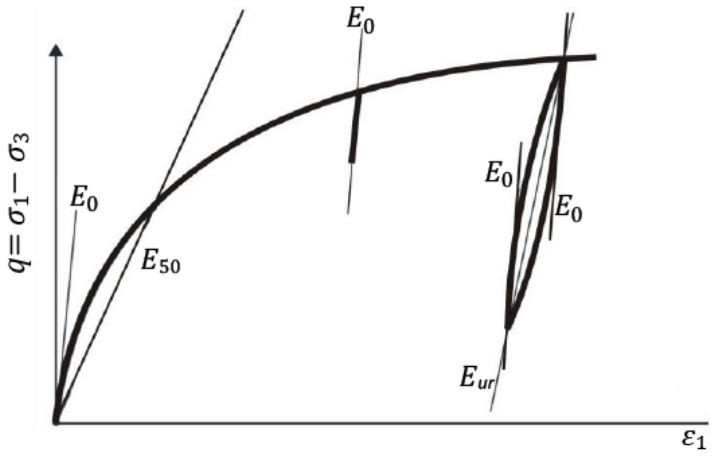

Figure 9: Stiffness parameters of Hardening Soil model with small-strain stiffness in a triaxial test, (Bentley-12, 2021)

The original Hardening Soil model assumes elastic material behavior during unloading and reloading. However, the strain range in which the soil can be considered truly elastic, i.e. where they recover from the applied straining almost completely, is very small. With increasing strain amplitude, the soil stiffness decays nonlinearly. Figure 10 (Bentley-12, 2021)

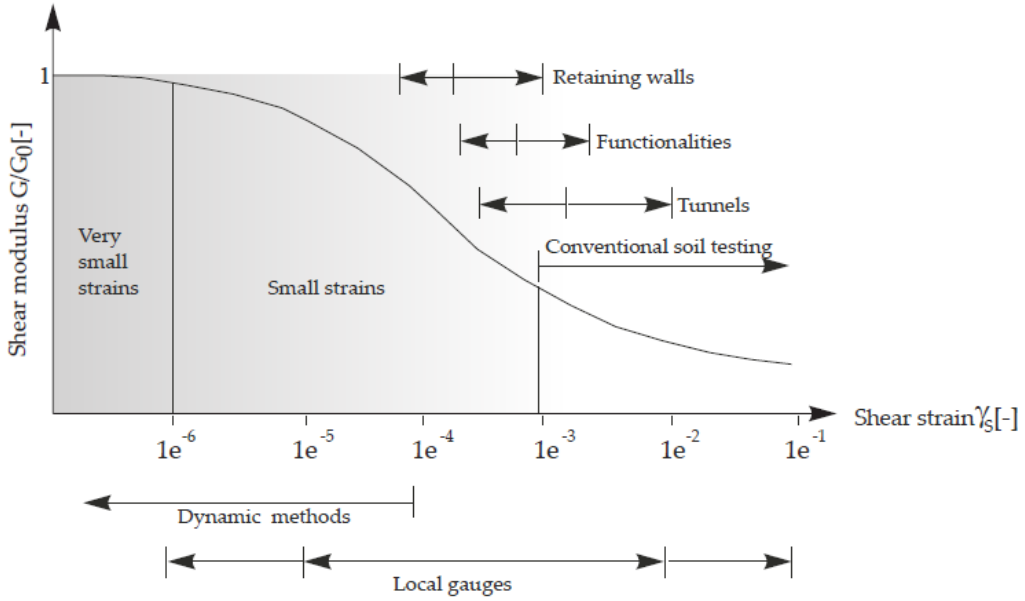

Figure 10: Characteristic stiffness-strain behavior of soil, (Bentley-12, 2021)

The Hardin-Drnevich relationship is perhaps the most frequently used model in the soil dynamics and following equation was proposed for the stress-strain curve for small strain:

$$\frac{G_s}{G_0} = \frac{1}{1 + \left|\frac{\gamma}{\gamma_r}\right|} \tag{2.18}$$

Where

$$\gamma_r = \frac{\tau_{max}}{G_0} \tag{2.19}$$

τ_{max} is the shear stress at failure
G_0 is initial shear stiffness

Equation (2.18) and (2.19) was later simplified by Santos and Correia (2001), and suggested to use $\gamma_r = \gamma_{0,7}$ at which the secant shear modulus G_s is reduced to 70%

$$\frac{G_s}{G_0} = \frac{1}{1 + a\left|\frac{\gamma}{\gamma_{0,7}}\right|} \tag{2.20}$$

Where a=0,385

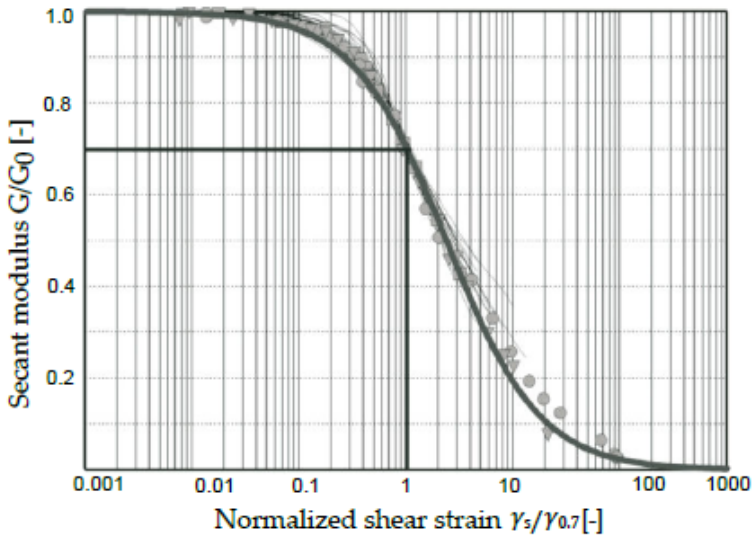

Figure 11: Results from the Hardin-Drnevich relationship compare to test data by Santos & Correia (2001), (Bentley-12, 2021)

HSsmall model is the most apparent in working load condition and demonstrates more reliable displacement than HS model, hence more suitable for the dynamic analysis. Another feature of HSsmall when applied in the dynamics analysis is, this leads to hysteretic damping, which means the nonlinear stress-strain characteristics of the material. Figure 12 shows typical hysteretic behavior. The amount of the hysteretic damping depends on the applied load and the corresponding strain amplitude. Moreover, it can be seen from the Figure 12 that the initial tangent and G_s of the initial loading coincides with the maximum shear stiffness G_0. Stiffness decays by increasing the shear strain. When the load is reversed, the stiffness starts from the same G_0 and decreases until next load reversal. (A. Laera, 2017)

Following equation shows the stress-strain relationship.

$$\tau = G_s * \gamma \tag{2.21}$$

G_s is secant shear stiffness

The local hysteretic damping ratio is described by the following equation, same as the equation (2.9):

$$\xi = \frac{E_D}{4\pi E_s} \tag{2.22}$$

ξ damping ratio

E_D is dissipated energy, given by the area of the closed loop (yellow and green areas) Figure 12

E_s is the energy accumulated at the maximum shear strain γ_C (green and blue areas), Figure 12

The green curve in Figure 12 shows the ratio of G_s/G_0.

The orange curve in Figure 12 shows the ratio of G_t/G_0.

G_t is tangent shear stiffness

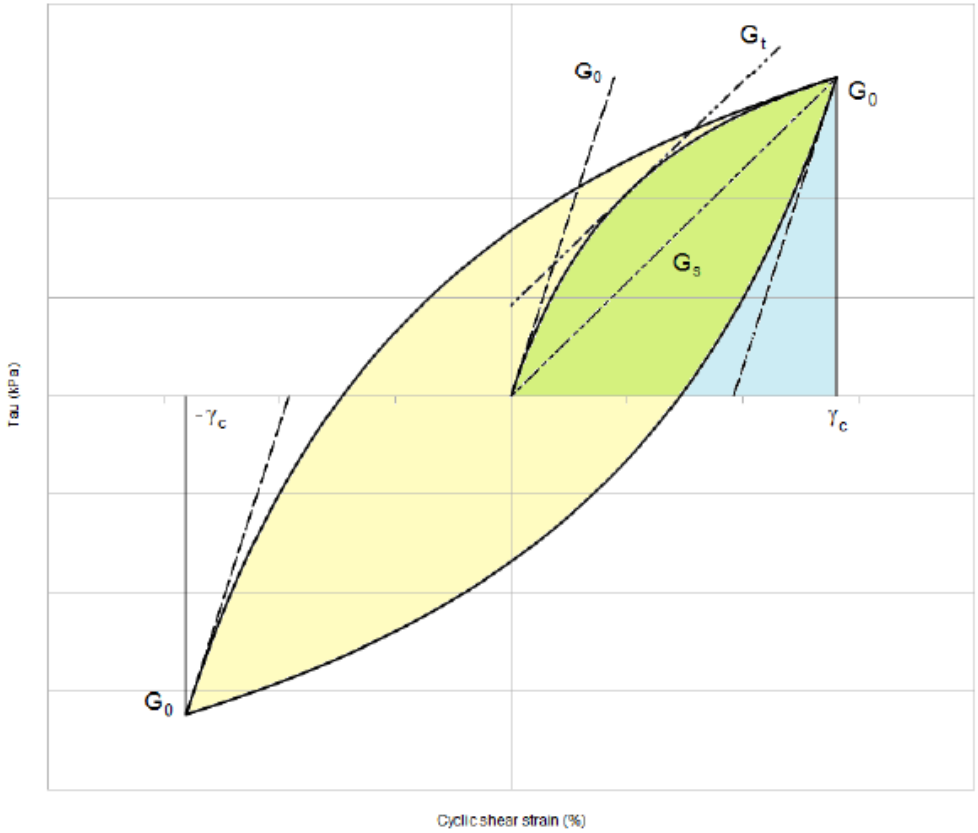

Figure 12: Hysteretic behavior in the HSsmall model, (A. Laera, 2017)

Vucetic & Dorby (1991) described different values of the plasticity index, for clay layer, they have proposed PI=50%, presented with blue line curve in Figure 13.

Figure 14 presents cut-off shear strain for the clay PI=50%, where the limit above the damping ratio ξ cannot increase further.

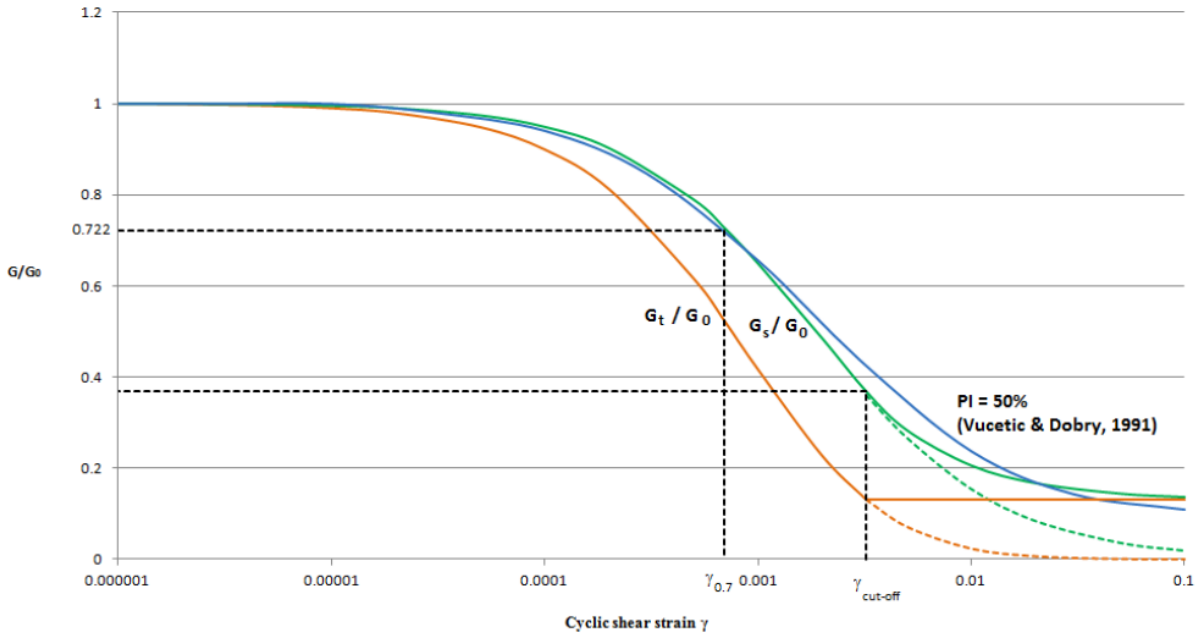

Figure 13: Modulus reduction curves, (A. Laera, 2017)

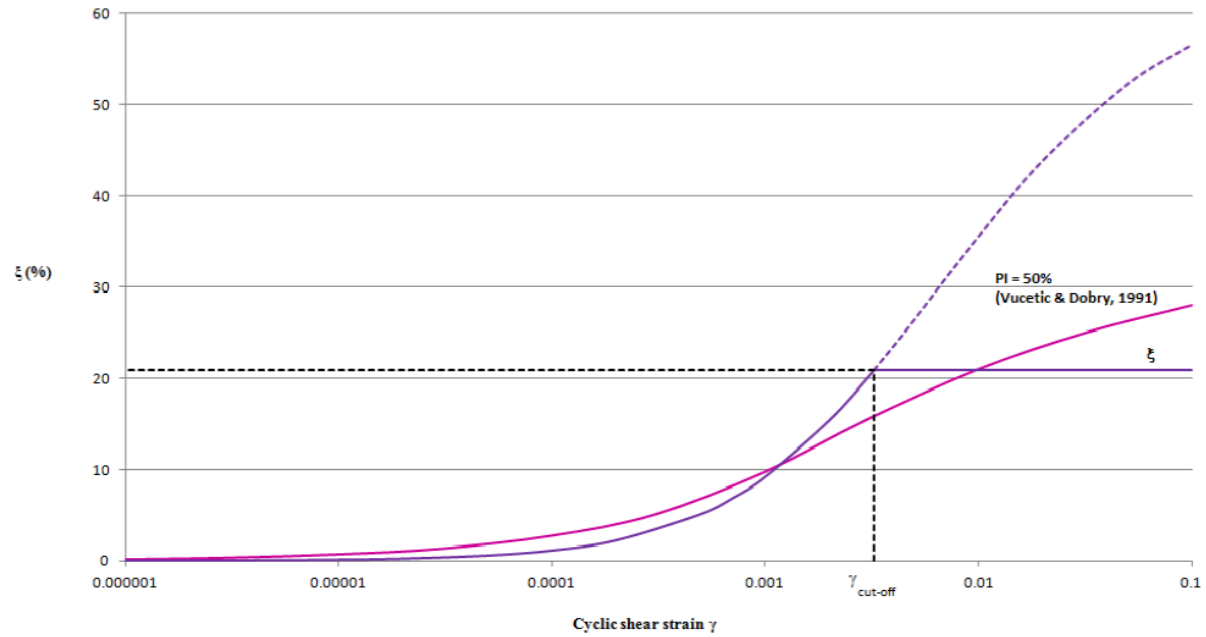

Figure 14: Damping curve, (A. Laera, 2017)

Damping

Damping is the mechanism that has the effect of reducing or absorbing the energy, in structures, damping dissipates the energy stored in an oscillatory system.

"Material damping in the dynamics calculations is caused by the viscous properties of soil, friction, and the development of irreversible strains. All plasticity models in PLAXIS 2D can generate irreversible (plastic) strains and may cause material damping. However, this damping is generally not enough to model the damping characteristics of real soils. For example, most soil models show pure elastic behavior upon unloading and reloading which does not lead to damping at all". Reference Manual (Bentley-10, 2020)

Among soil models in the PLAXIS, Soft Soil Creep model includes viscous behavior. This model may lead to viscous damping, but hardly shows creep strain in the load/reload cycles. The Hardening Soil model with small-strain stiffness is the model where hysteretic behavior in the loading/reload cycles is included. When using the HSsmall model in the dynamic analysis, in very small vibrations, this model does not show material and numerical damping. Therefore, additional damping is needed to model the realistic damping characteristics of the soil. This can be done by defining the Rayleigh damping.

PLAXIS offers hysteretic, viscous material damping, and numerical damping. Rayleigh damping is a numerical feature, and it simulates viscous material damping. The Rayleigh damping can be applied to each material and is composed by adding mass M and stiffness K matrices along with α and β (Rayleigh coefficients).

$$[C] = \alpha[M] + \beta[K] \tag{2.23}$$

Where M is mass matrix and K is stiffness matrix, α and β are the Rayleigh coefficients

$$\alpha + \beta\omega^2 = 2\omega\xi \tag{2.24}$$

$$\omega = 2\pi f \tag{2.25}$$

$$\alpha = 2\omega_1 * \omega_2 * \frac{\omega_1 * \xi_2 - \omega_2 * \xi_1}{\omega_1^2 - \omega_2^2} \tag{2.26}$$

$$\beta = 2 * \frac{\omega_1 * \xi_1 - \omega_2 * \xi_2}{\omega_1^2 - \omega_2^2} \tag{2.27}$$

ω is angular frequency in rad/s

ξ is damping ratio, $\xi = 1$ for critical damping, the amount of damping needed to let a SDOF system which is released from an initial excitation u_0 smoothly stop without rebouncing.

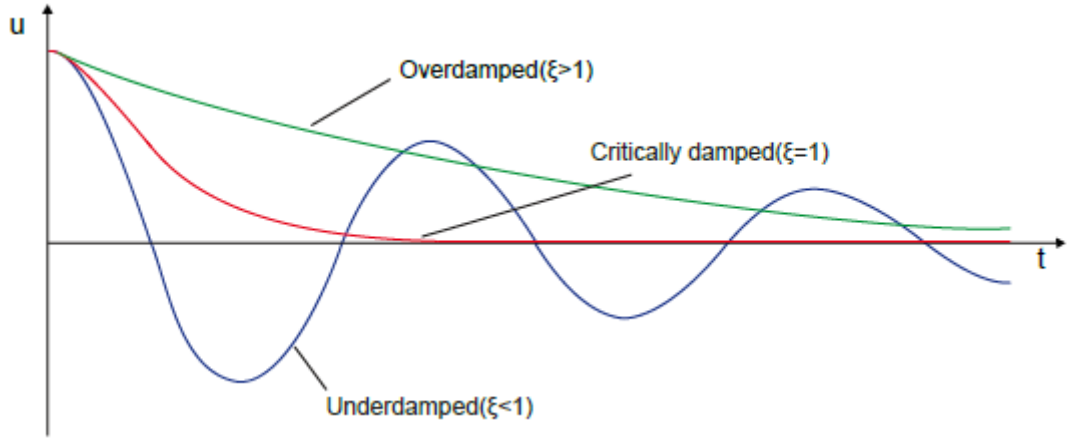

Figure 15: Role of damping ratio ξ in free vibration of a SDOF system, (Bentley-12, 2021)

PLAXIS suggests keeping ξ value for Target 1 and Target 2, between 0,5 and 2%. According to Hudson, Idriss & Beirkae (1994), and Hashash & Park (2002), set first target frequency equal to the fundamental frequency of the whole soil layer, and second frequency as the closest odd number given by the ratio of the fundamental frequency of input signal at the bedrock and the fundament frequency of the whole soil layer. (A. Laera, 2017)

$$f_1 = \frac{V_s}{4H} \tag{2.28}$$

Boundary conditions

The selection of boundary condition should be problem dependent, boundaries should be selected accordingly. PLAXIS 2D offers several types of boundary conditions, each boundary type will be studied below.

I. Viscous Boundaries

Viscous boundaries are not appropriate for the seismic ground response analysis, and they are best suited when the dynamic source is within the mesh. This type of boundary can be used for seismic analysis. However, boundaries should be placed at sufficient distance to minimize wave reflections to the model and to achieve free-field conditions. In other words, this will require rather larger model width and sufficient damping in the soil.

II. Tied Degrees of Freedom

This type of boundary is optimum for the seismic ground response analysis, are only available for the lateral boundaries (x_min and x_max). This type of boundary is perfect for one dimensional soil column to perform site response analysis. Tied degree of freedom boundaries tie the nodes on the same elevation at left and right boundaries, so that they will undergo exact same displacement.

III. Free Field Boundaries

This type of boundary is also only available for the lateral boundaries (x_min and x_max) and made up of a combination of a load history and a viscous boundary. These boundaries should be placed at a distance for which the free-field conditions are reached, they are in general preferred for the earthquake analysis. This type of boundary conditions imposes free-field motion at the sides and absorbs the reflected secondary waves.

IV. Compliant Base Boundaries

This type of boundary is only available for the base of the model (y_min). These boundaries are made up of a combination of line prescribed displacement and viscous boundary. This type of boundary condition is also preferred for the earthquake analysis. "The compliant base boundary condition for the bottom boundary ensures that reflected waves from the layers above are absorbed and allows direct application of an input (upward propagating) accelerogram". Reference Manual (Bentley-10, 2020)

As stated, there are different options for boundary conditions. There is also option for choosing "Non" fixities, and when this type of boundary is applied, no special dynamic boundary conditions are used. To define *Fixed base*, "*None*" option can be selected combined with a line prescribed displacement. The *Fixed base* is a fully reflective boundary. User can specify input motion as displacement, velocity, or acceleration history via the line prescribed displacement. The input motion can be derived through equivalent linear program such as SHAKE, DEEPSOIL or SeismoMatch.

When using free field and/or compliant base, user should create node pairs along the base of the boundary, a dummy plate should be created at the base of the model, hence viscous damper is created between these two nodes. (Figure 16)
This will allow transfer of the input motion and absorbing of the incoming waves.

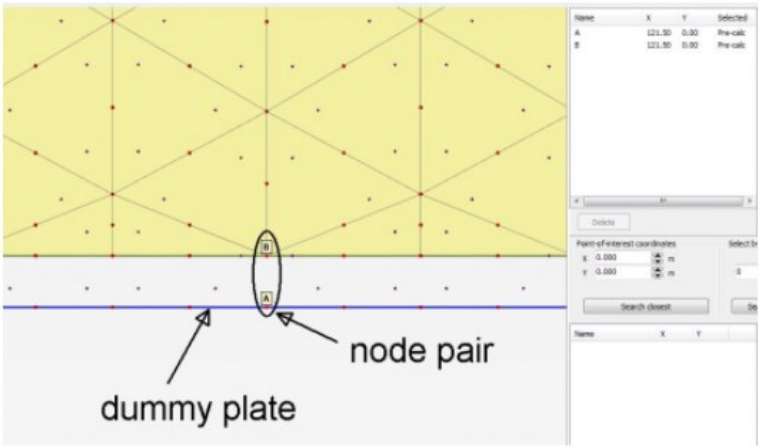

Figure 16: Node selection for input signal on dummy plate, (Bentley-05, 2014)

Regardless of which type of the dynamic boundaries user select, a good practice is to check signal output at the base of the model and compare the results with input signal motion. This will be demonstrated in 4.1 Part 1.

Interfaces

Interfaces are designed to model the Soil-Structure interaction and should be applied at all regions where Soil-Structure contact exist in the model. In the PLAXIS 2D, there are "+", and "-" interfaces, they have no physical meaning. Interfaces require an "R_{inter}" values, this is basically a reduction factor, and changes stiffness and strength of the soil at the structure contact. It is important to select proper value for the R_{inter}, because it can influence result.

Meshing

When a model is constructed in any finite element program, before performing finite element calculations, structural elements must be divided into small elements. This composition of finite element is called mesh. Mesh should be refined in areas where large strain gradients are expected. The mesh size should be suitably fine to obtain accurate results, but not very fine meshes, since very fine mesh leads to unnecessary extra calculation time.

Time Step

In the dynamics analysis, critical time step and element length are related. The effective element length and corresponding time step must represent complete wave travel precisely.

Dynamic elementary time step:

$$\delta t = \frac{\Delta t}{n * m} \tag{2.29}$$

Δt is time interval (for full calculation phase)

n is Max steps

m is number of sub-steps

According to the equation (2.29), it is advised to use Δt, m and n in such a way that sub step time interval (δt) is equal to the input signal time interval. When input signal time interval corresponds with the sub step time interval, the result looks like as shown in figure below.

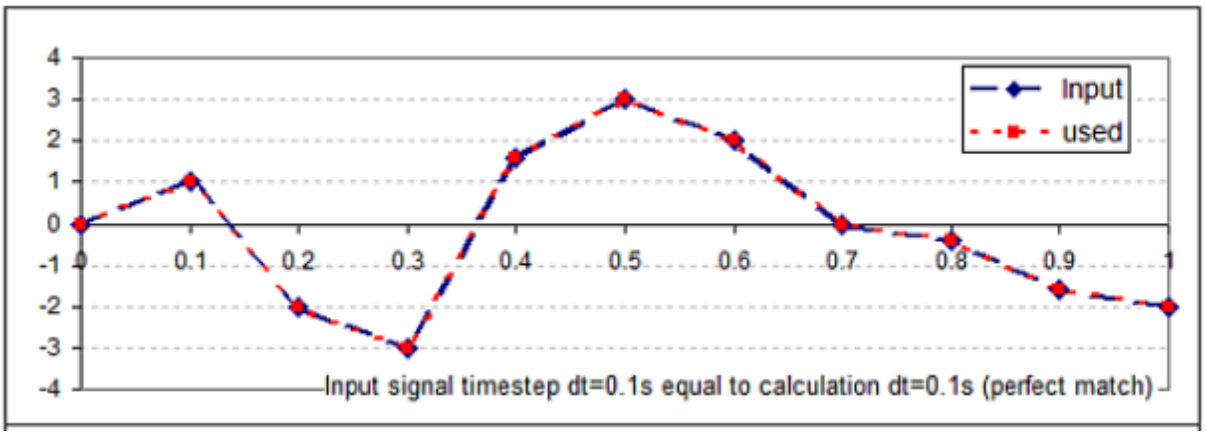

Figure 17: Dynamic steps and the input signal, (Bentley-02, 2012)

However, if the sub step time interval does not correspond with the input signal time interval, the result will look like as shown in Figure 18.

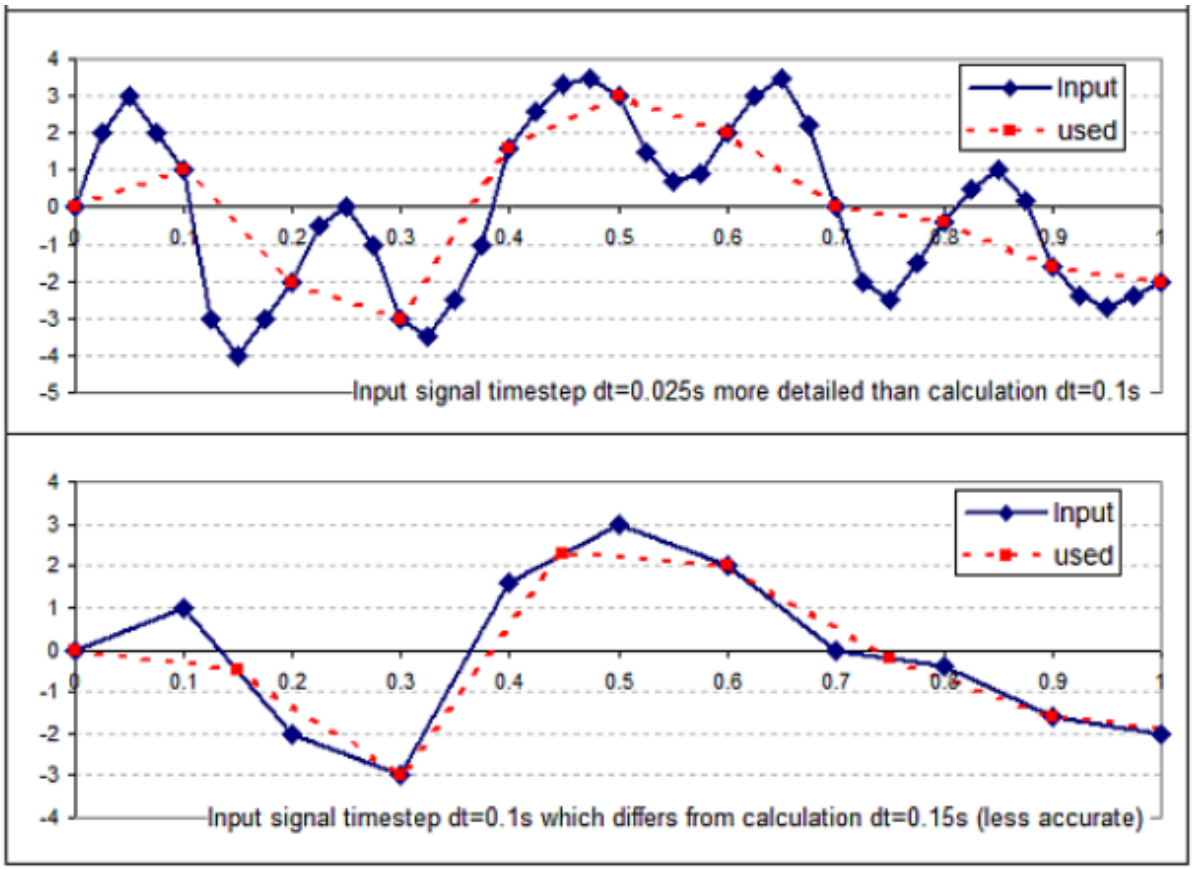

Figure 18: Dynamic steps and the input signal, (Bentley-02, 2012)

During a dynamic load, forces and displacement will vary with time. To generate envelope forces, user should select points for the curves. It is important to distinguish between Pre-calculation and Post-calculation points. Pre-calculation points generates information related to the stresses and strains at the selected points. Whereases, plotting structural forces curves

can only be generated by selecting the Post-calculation points. When selecting Pre-calculation points, user should select points before running the analysis. However, Post-calculation points can be selected after the calculation is performed and model is saved. In the PLAXIS 2D in the Phase panel, by default the Max number of steps stored is set to 1.0. This means that the only last calculation step of the phase is saved. (Bentley-10, 2020) Figure 19

Since force envelope distribution can occur at any calculation step of the phase and not necessarily at the last calculation step of the phase, it is therefore recommended to select higher Max number of steps stored.

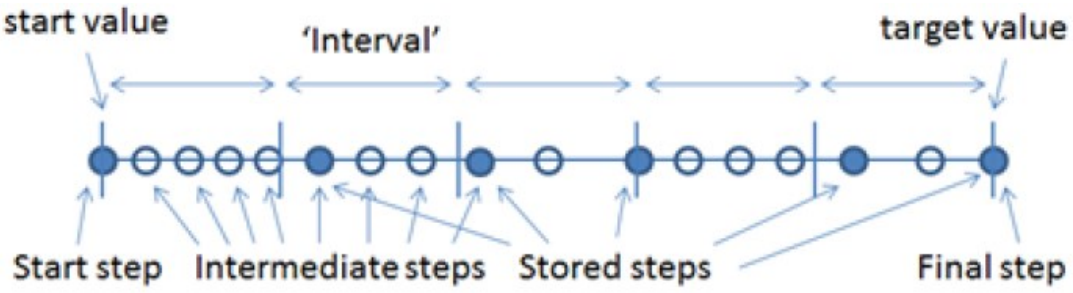

Figure 19: Max number of steps stored, Reference Manual (Bentley-10, 2020)

PLAXIS 2D allows user to choose between automatic time stepping, semi-automatic or manual option. "Selecting Automatic time stepping option will ensure accurately model wave propagation and will reduce numerical error due to the integration of time history function". Reference Manual (Bentley-10, 2020)

Element Size

The element size should be selected in accordance with the target frequency range and following two criteria should be fulfilled to obtain correct results.

Length of shear wave

$$\lambda s = \frac{V_s}{f_{max}} \tag{2.30}$$

Element size should be less than:

$$\frac{\lambda s}{8} \tag{2.31}$$

2.5.2 One-Dimensional Analysis

For this Thesis, SeismoMatch is used to generate input signal motion (Time Series). Generated signal motion is then used as input for DEEPSOIL, EERA and PLAXIS 2D.

SeismoMatch

SeismoMatch is a user-friendly application and requires few input parameters to generate Time Series and Response Spectra graphs. In the SeismoMatch application, accelerogram can be scaled to match a desired target response spectrum. This application uses wavelets algorithm proposed by Abrahamson [1992] and Hancock et al. [2006], or the algorithm proposed by Al Atik and Abrahamson [2010]. (SEiSMOSOFT, 2021)

User can load either single or multiple pre-defined accelerogram examples, and after few input parameters for the desired spectral, spectral matching is then executed. User can select matched spectrum that fulfils user's requirement, and all output results can be copied to Excel file.

DEEPSOIL

DEEPSOIL is a unified one-dimensional site response analysis and can carry out shear wave propagation analysis in linear, equivalent linear and nonlinear analysis, analysis can be performed in the time and frequency domain. DEEPSOIL has some pre-calculated examples, which are quite convenient to use, user can either input their own time series or chose from the pre-defined list. Pre-defined reference curves are useful, user can either chose the one which fits the material layer or input values for the modulus reduction curve. PLAXIS suggests using Vucetic and Dobry (1991) modulus reduction curve and plasticity index 50% for clay, which is selected for this report. DEEPSOIL recommends choosing *Frequency Independent* for calculation of the *complex shear modulus*:

$$G^* = G(1 + i2\xi) \tag{2.32}$$

Alternatively, user can select the simplified formulation:

$$G^* = G(1 - \xi^2 + i2\xi) \tag{2.33}$$

All output results can be simply exported to Excel and plots can be generated.

EERA

EERA is basically a Microsoft Excel sheet, and was previously implemented in the original version of SHAKE (Schnabel et al., 1972). The analysis approach in this program is equivalent linear (EL), this assumes that shear modulus and the damping ratio are function of the shear strain amplitude, and these values are determined by the iteration process so they become consistent with the level of strain induced in each layer. (EERA Manual)

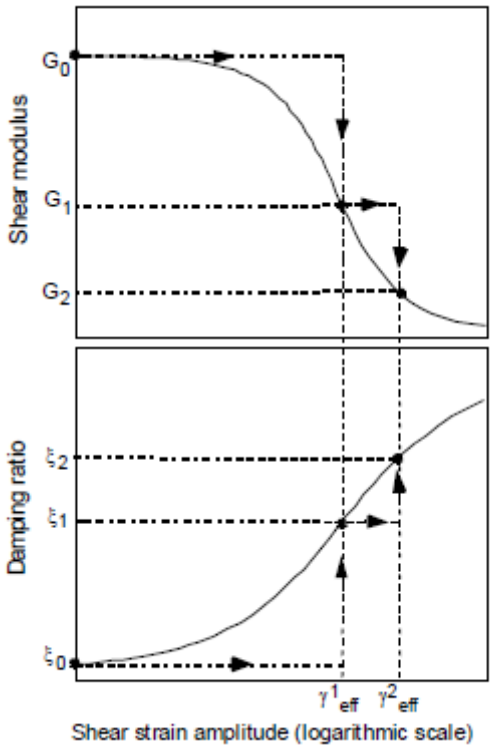

Figure 20: Iteration of shear modulus and damping ratio with shear strain in equivalent linear analysis, (EERA Manual)

EERA proposes two different analysis models. Model 1 assumes that ξ is constant and independent of ω, this means that G^* is also independent of ω. The dissipated energy during the cyclic loading can be computed by:

$$W_d = 4\pi W_s \xi = 2\pi \xi G \gamma_c^2 \omega \tag{2.34}$$

The dissipated energy increases linearly with ξ, is independent of ω, this implies that area of stress-strain loop is frequency independent. The amplitude of complex shear modulus $|G^*|$ increases with ξ, and its relationship with the real shear modulus is as follows:

$$|G^*| = G\sqrt{1 + 4\xi^2} \tag{2.35}$$

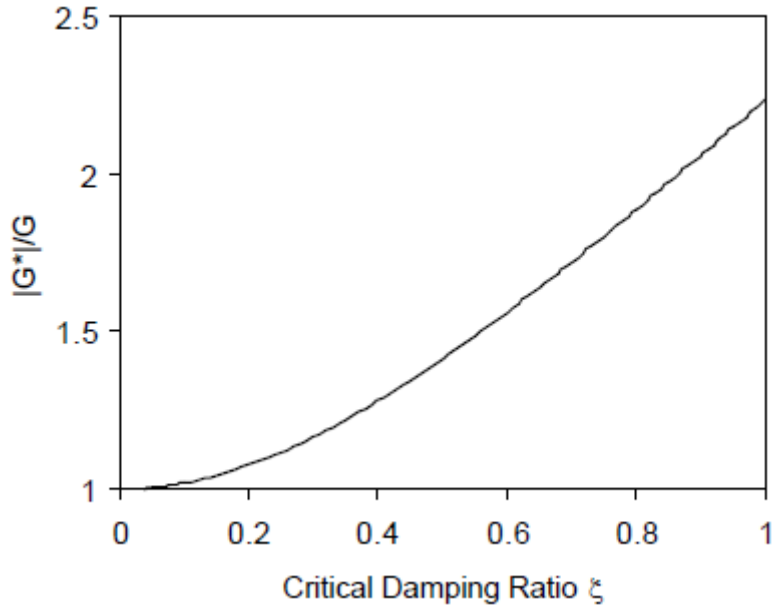

Figure 21: Normalized variation of complex shear modulus amplitude with critical damping ratio (Model 1), (EERA manual)

Model 2 is used in SHAKE 91 (Idriss and Sun, 1992) and assumes that complex shear modulus is a function of ξ.

$$G^* = G\left\{(1-2\xi^2) + 2\xi_j\sqrt{1-\xi^2}\right\} \tag{2.36}$$

Equation (2.36) describes the material behavior, and it implies that complex and shear modulus have same amplitude:

$$G^* = G\{(1-2\xi^2) + 4\xi^2(1-\xi^2)\} = G \tag{2.37}$$

Energy dissipated during cyclic loading:

$$W_d = \frac{1}{2}\omega\gamma_c^2\int_t^{t+\frac{2\pi}{\omega}} 2G\xi\sqrt{1-\xi^2 dt} = 2\pi G\xi\sqrt{1-\xi^2}\gamma_c^2 \tag{2.38}$$

For practical purposes, ξ is usually less than 25%, this will imply that energy dissipated by Model 1 and Model 2 are similar.

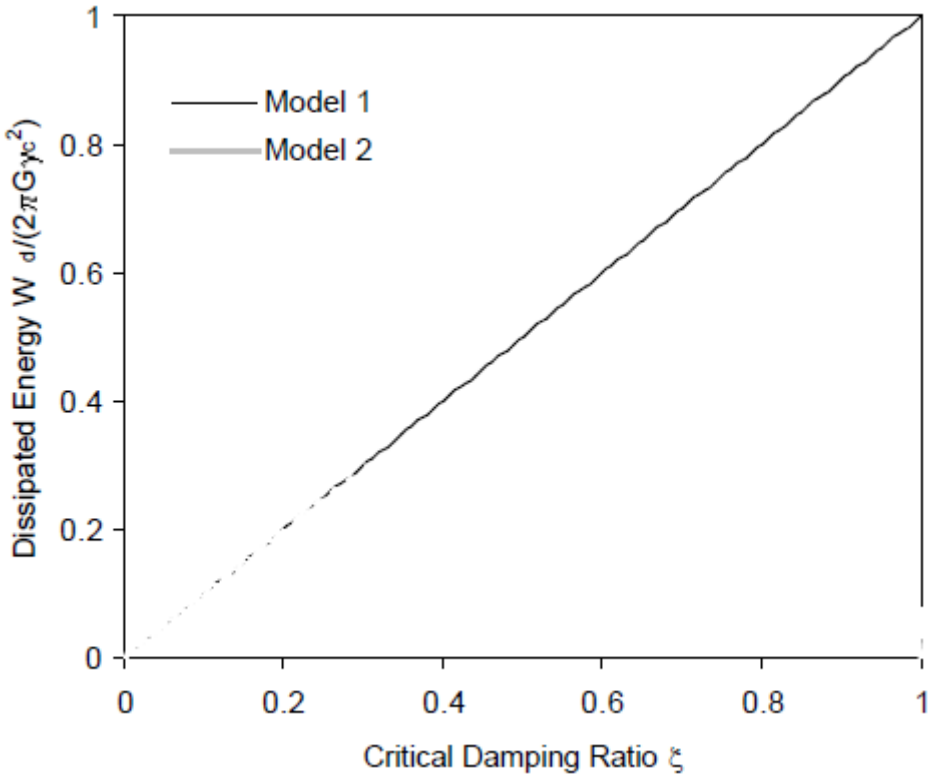

Figure 22: Normalized variation of energy dissipated per loading cycle as a function of critical damping ratio for model 1 and 2, (EERA manual)

The iteration procedure for equivalent linear approach in each layer:

1. Initialize the value of $G^i$and ξ^i
2. Compute the ground response and get maximum shear strain γ_{max}
3. Determine the effective shear strain γ_{eff} from γ_{max}
$$\gamma_{eff} = R_\gamma * \gamma_{max} \tag{2.39}$$
Where R_γ is the ratio of the effective shear strain to maximum shear strain.
4. Calculate the new equivalent linear values G_{i+1} and ξ_{i+1} corresponding to the effective shear strain γ_{eff}.
5. Repeat steps 2 to 4 until differences between the computed values of shear modulus and the damping ratio fall between some predetermined value in all layers, generally 8 iterations are sufficient.

2.5.3 Eurocode 8

Technical Committee CEN/TC 250 "Structural Eurocodes" has prepared the European Standard EN 1998-1, Eurocode 8: Design of structures for earthquake resistance. This applies to design and construction of buildings and civil engineering works in the seismic regions, and its purpose is to ensure that in the event of earthquakes, human lives are protected, damage is limited and structures important for the civil protection remain operational.

Calculations according to the part 1 of Eurocode 8 is a central part of this Thesis. The Norwegian National Annex values, tables and figures are used in this report. Relevant parts of EC8-1 which are scope of this Thesis, are presented here.

Ground types

The Eurocode 8 has classified ground types based on their description of the stratigraphic profiles and parameters to seven different types, A-E, S_1 and S_2. Appendix F

Determining of the ground type should be based on the local conditions, site should be classified according to the values of average shear wave velocity (V_s) given in EC8 table NA.3.1, if data is available, otherwise the values of N_{SPT} should be used.

The average shear wave velocity at small strain level ($V_{s,30}$) should be computed using following equation:

$$V_{s,30} = \frac{30}{\Sigma_{i=1,N} \frac{h_i}{v_i}} \tag{2.40}$$

Where h_i and v_i are the thickness (in meters) and shear wave velocity (at a shear strain level of 10^{-5} or less) of the corresponding $i-th$ layer, in a total of N, existing in the top 30m. Special studies should be executed if the site condition matches S_1 or S_2 ground type, this is due to soil failure under the seismic action, has low V_s, low internal damping, and abnormally extended range of the linear behavior.

Seismic zones

National Authorities in each country divides the territory into several seismic zones according to the hazard level of the seismic. Based on this, the reference peak ground acceleration for each zone, corresponds to the reference return period T_{NCR}, or equivalency the reference probability of exceedance in 50 years P_{NCR} chosen by the National Authorities. According to the EC8, the reference peak ground acceleration is given on the ground type A. An importance factor (γ_I) is assigned to the reference return period and is different for each seismic importance class.

Table 1: Values of importance factor (NS-EN 1998-1, table NA.4(091))

Importance class	γ_I
I	0,7
II	1,0
III	1,4
IV	2,0

The design ground acceleration on type ground A is then:

$$a_g = \gamma_I * a_{gR} \tag{2.41}$$

Followed by a_{gR}

$$a_{gR} = 0{,}8 * a_{g40\,Hz} \tag{2.42}$$

Where $a_{g40\,Hz}$ denotes the ground acceleration at frequency $f = 40\,Hz$ ($T = 0{,}025\,s$).

Horizontal elastic response spectrum

According to the EC8, the elastic response spectrum Se (T)is defined by the following equations.

$$0 \le T \le T_B: S_e(T) = a_g * S * \left[1 + \frac{T}{T_B}(\eta * 2{,}5 - 1)\right] \tag{2.43}$$

$$T_B \le T \le T_C: S_e(T) = a_g * S * \eta * 2{,}5 \tag{2.44}$$

$$T_C \le T \le T_D: S_e(T) = a_g * S * \eta * 2{,}5\left[\frac{T_C}{T}\right] \tag{2.45}$$

$$T_D \le T \le 4s: S_e(T) = a_g * S * \eta * 2{,}5\left[\frac{T_C * T_D}{T^2}\right] \tag{2.46}$$

Where

Se(T) is the elastic response spectrum

T is the vibration of a linear SDOF system

a_g is the design ground acceleration on type A ground

T_B is the lower limit of the period of the constant spectral acceleration branch

T_C is the upper limit of the period of the constant spectral acceleration branch

T_D is the value defining the beginning of constant displacement response range of the spectrum

S is the soil factor

η is the damping correction factor with a reference value of $\eta = 1$ for 5% viscous damping, and can be determined by following equation:

$$\eta = \sqrt{\frac{10}{(5+\xi)}} \geq 0{,}55 \tag{2.47}$$

ξ is the viscous damping ratio of the structure and expressed as percentage.

The values of period T_B, T_C, T_D, and S (soil factor) depend on the ground type. Table 2

Table 2: Values of the parameters describing the recommended elastic response spectra (NS-EN 1998-1, Tabell NA.3.3)

Ground type	S	T_B (s)	T_C (s)	T_D (s)
A	1,0	0,10	0,20	1,7
B	1,3	0,10	0,25	1,5
C	1,4	0,10	0,30	1,5
D	1,55	0,15	0,40	1,6
E	1,65	0,15	0,30	1,4

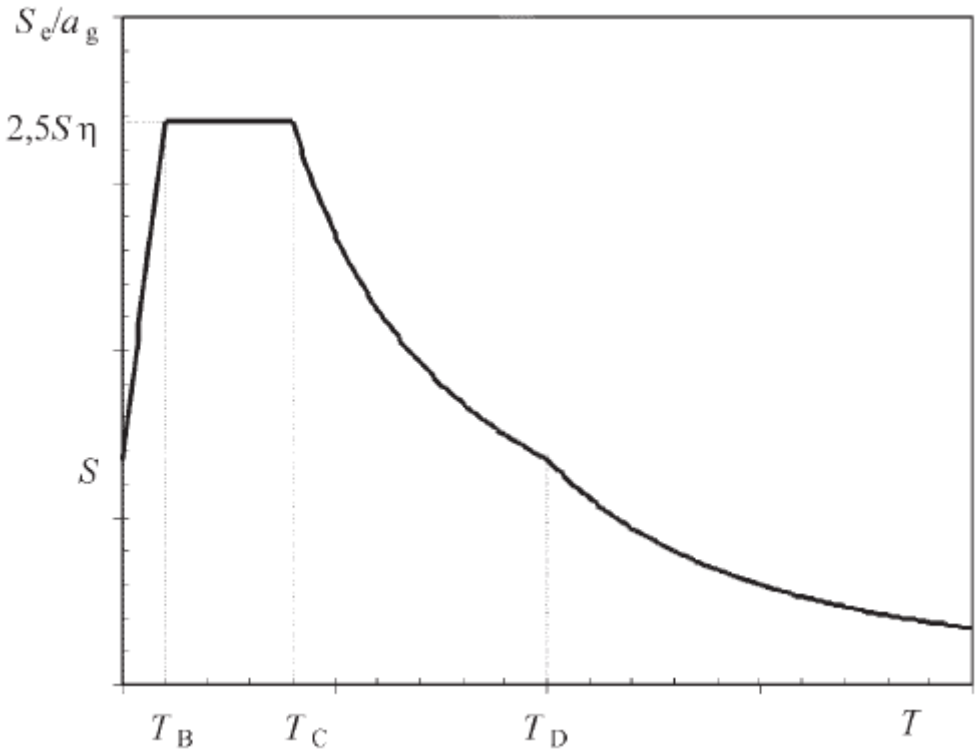

Figure 23: Shape of the elastic response spectrum (NS-EN 1998-1, figure 3.1)

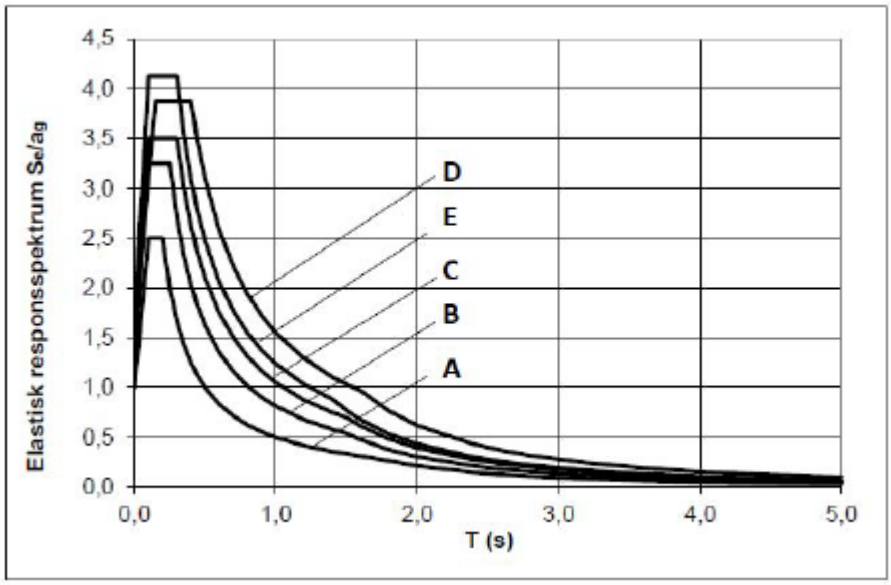

Figure 24: Horizontal elastic response spectra for use in Norway for ground type A to E (NS-EN 1998-1, figure NA.3(903))

Vertical elastic response spectrum

The vertical component of the seismic action (S_{ve}) can be derived by using following equations, and shall be represented by an elastic spectrum:

$$0 \leq T \leq T_B: S_{ve}(T) = a_{vg} * \left[1 + \frac{T}{T_B}(\eta * 3{,}0 - 1)\right] \quad (2.48)$$

$$T_B \leq T \leq T_C: S_{ve}(T) = a_{vg} * \eta * 3{,}0 \quad (2.49)$$

$$T_C \leq T \leq T_D: S_{ve}(T) = a_{vg} * \eta * 3{,}0 \left[\frac{T_C}{T}\right] \quad (2.50)$$

$$T_D \leq T \leq 4s: S_{ve}(T) = a_{vg} * \eta * 3{,}0 \left[\frac{T_C * T_D}{T^2}\right] \quad (2.51)$$

The values of T, T_B, T_C, and η as already described.

a_{vg} is design ground acceleration in the vertical direction

Table 3: Values of parameters describing the vertical elastic response spectrum (CEN, 2004), Table NA.3.4

Description	a_{vg} / a_g	T_B (s)	T_C (s)	T_D (s)
Vertical response spectrum	0,6	0,05	0,20	1,2

Design spectrum for elastic analysis

The structural system has higher capacity to absorb the energy or resist seismic actions in a non-linear range than those corresponding to a linear elastic range. The energy absorption capacity is mainly due to the structural elements and/or other mechanism's ductile behavior, called the "behavior factor, q". To avoid complicated inelastic structural analysis in design, ductility behavior of the structure is considered, and an elastic analysis based on a response spectrum is performed, this is called "design spectrum".

The behavior factor q is the capacity of the structure to dissipate energy, their values are different for ductility classes (low, medium, high). "The value of the behavior factor "q" may be different in different horizontal directions, although the ductility classification shall be the same in all directions". (CEN, 2004)

The behavior factor q is a factor, an approximation of the ratio of the seismic forces that the structure would experience if its response was completely elastic with 5% viscous damping, to the seismic forces that may be used in the design, with a conventional elastic model, still ensuring a satisfactory response of the structure. (CEN, 2004)

In Norway, low or medium ductility classes can be used, and most structures are designed for $q \leq 1{,}5$. High ductility class should be used for the structures located in high bedrock ground acceleration, according to this class, a factor of $q > 4{,}0$ can be used. However, in Norway DCH it is not used and thereby, highest behavior factor is $q = 4{,}0$.

The design spectrum values for elastic analysis can be derived from following equations:

$$0 \leq T \leq T_B: S_d(T) = a_g * S * \left[\frac{2}{3} + \frac{T}{T_B}\left(\frac{2{,}5}{q} - \frac{2}{3}\right)\right] \tag{2.52}$$

$$T_B \leq T \leq T_C: S_d(T) = a_g * S * \frac{2{,}5}{q} \tag{2.53}$$

$$T_C \leq T \leq T_D: S_d(T) = \begin{Bmatrix} = a_g * S * \frac{2{,}5}{q} * \left[\frac{T_C}{T}\right] \\ \geq \beta * a_g \end{Bmatrix} \tag{2.54}$$

$$T_D \leq T: S_d(T) = \begin{Bmatrix} = a_g * S * \frac{2{,}5}{q} * \left[\frac{T_C * T_D}{T^2}\right] \\ \geq \beta * a_g \end{Bmatrix} \tag{2.55}$$

The values of T, T_B, T_C, η and S as already described.

q is the behaviour factor

β is the lower bound factor for the horizontal design spectrum, can be found in National Annex and is equal to 0,2

Base Shear Force

Base shear force (F_b) calculation according to the EC8 is one of the main topics of this Thesis, and to use *Lateral force method of analysis*, following conditions must be fulfilled:

$$T_1 \leq \begin{Bmatrix} 4 * T_C \\ 2{,}0\ s \end{Bmatrix} \tag{2.56}$$

The second criteria which is for regularity in elevation, described in 4.2.3.3 in EC8, all three models in this report satisfies this criterion.

The seismic base shear force can be calculated by using following equation:

$$F_b = S_d\,(T_1) * m * \lambda \tag{2.57}$$

Where $S_d\ (T_1)$ is the ordinate of the design spectrum at period T_1
T_1 is the fundamental period of vibration of the building for lateral motion
m is the total mass of the building, either above of the foundation or above the top of a rigid basement
λ is the correction factor, if $T1 \leq 2$ T_C and building has more than two stories, $\lambda = 0{,}85$, or $\lambda = 1{,}0$ otherwise.

As the EC8 suggest in section 4.3.3.2.2(2) and (3), determination of the fundamental period of vibration period T_1, expressions based on methods of the structural dynamics (for example the Rayleigh method) may be used. For buildings with heights of up to 40 m the value of T_1 may be approximated by the following expression: (CEN, 2004)

$$T_1 = C_t * H^{\frac{3}{4}} \tag{2.58}$$

Where, C_t is $0{,}085$ for moment resistant steel frames and $0{,}075$ for moment resistant concrete frames, $0{,}050$ for other structures
H is the height of the building either from foundation or from the top of a rigid basement
C_t can be also calculated by the following equation:

$$C_t = \frac{0{,}075}{\sqrt{A_c}} \tag{2.59}$$

Because of the limit scope of this Thesis, suggested values by EC8 for concrete frame is used, hence equation (2.59) is not used in this report.
Alternative 2, T_1 can be calculated according to the paragraph 4.3.3.2.2 (5) in EC8.

$$T_1 = 2\sqrt{d} \tag{2.60}$$

Where d is lateral displacement of the top of the building.
Alternative 3, (Rayleigh method), T_1 can be calculated according to the section 4.3.3.2.2 (2) in EC8.

$$T_1 = 2\pi \sqrt{\frac{\sum m_i * u_i^2}{\sum F_i * u_i}} \tag{2.61}$$

Where m_i is mass at floor "i" , u_i is deformation of floor "i" because of force F_i at floor "i".

Here it will be shown how equation (2.57) is computed for a SDOF system. Objective of this demonstration is discussing *Lateral force method analysis* in section 5 CONCLUSION. It is to be mentioned that deriving equation (2.67) is not scope of this report.

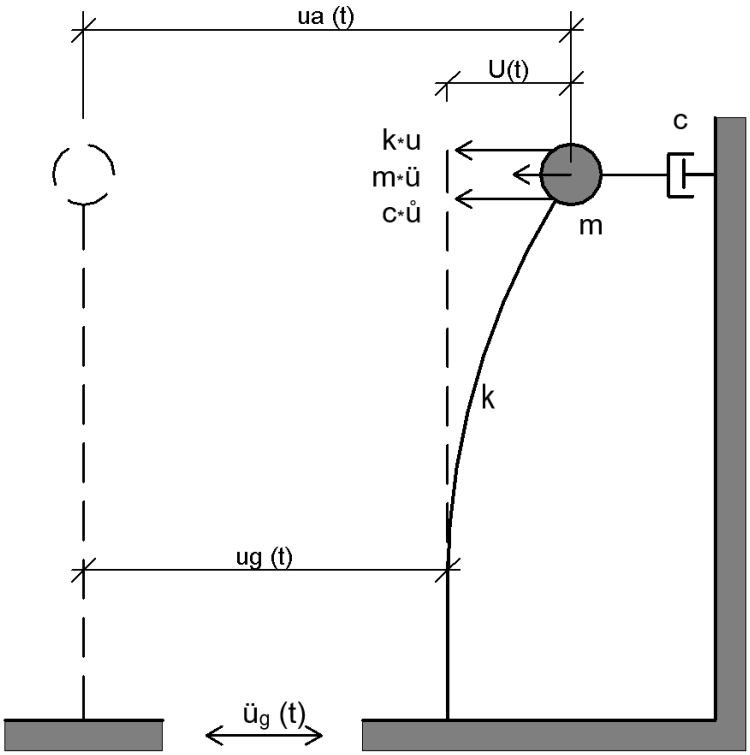

Figure 25: SDOF system with ground excitation, illustration by Hijratullah Niazi, after Dimensjonering for JORDSKJELV (Øystein Løset, et al 2010)

Using basic dynamic equilibrium, solving for maximum shear force for biggest mode shape.

$$m * \ddot{u}\,(t) + c * \dot{u}(t) + k * u(t) = 0 \tag{2.62}$$

$$m * \ddot{u}\,(t) + c * \dot{u}(t) + k * u(t) = -\,m * \ddot{u}_{\,g} = p_{eff}(t) \tag{2.63}$$

$$u(t) = \frac{1}{\omega} V(t) \tag{2.64}$$

$$V(t) = \int_0^t \ddot{u}_g\,(t) * sin\omega(t-\tau) e^{-\xi\omega(t-\tau)} \tag{2.65}$$

Velocity

$$S_v(\xi, \omega) \;=\; |V(t, \xi, \omega|_{max} \tag{2.66}$$

Solving velocity with maximum pseudo-acceleration, maximum shear force for the biggest mode shape can be found.

The maximum shear force for the biggest mode shape is:

$$F_{max} = \; k * u_{max} = k\frac{1}{\omega} S_v(\xi, \omega) = \frac{k}{\omega^2} S_d(\xi, \omega) \; = m * S_d(\xi, \omega) \tag{2.67}$$

3 METHODOLOGY

In this chapter methodology of how analysis is carry out in SeismoMatch, DEEPSOIL, EERA and PLAXIS 2D will be discussed. The procedure how models are constructed in the PLAXIS 2D and how various graphs are plotted will be also demonstrated in this chapter.

SeismoMatch

Upon opening SeismoMatch, user can load single or multiple predefined accelerogram files. For this Thesis, several attempts have been performed for the Multiple accelerogram files. However, the one which its Response Spectra is representative to EC8 is used in this report. The Kobe acceleration file provide a good match with EC8 Response Spectra. There are only two steps to input parameters and plot the graphs.
From the input file parameter menu in step 1, *Time and Acceleration* is chosen.

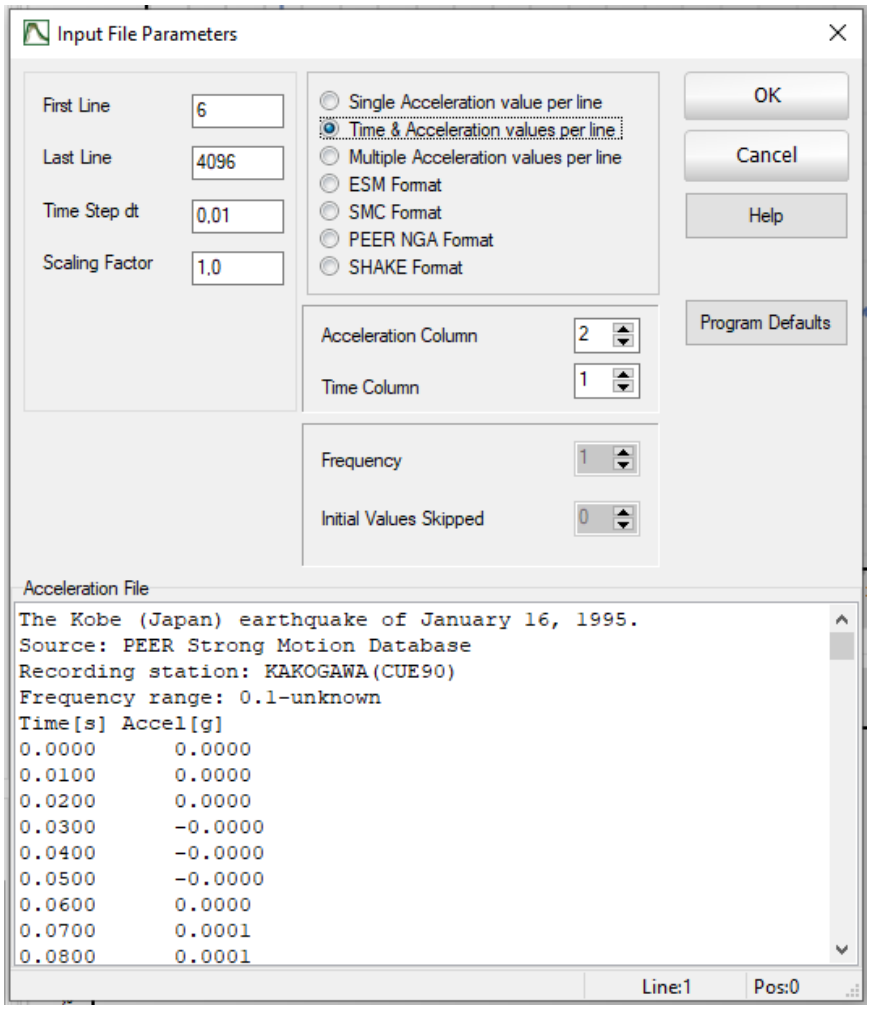

Figure 26: Input File Parameters, SeismoMatch

Four different accelerogram file are selected.

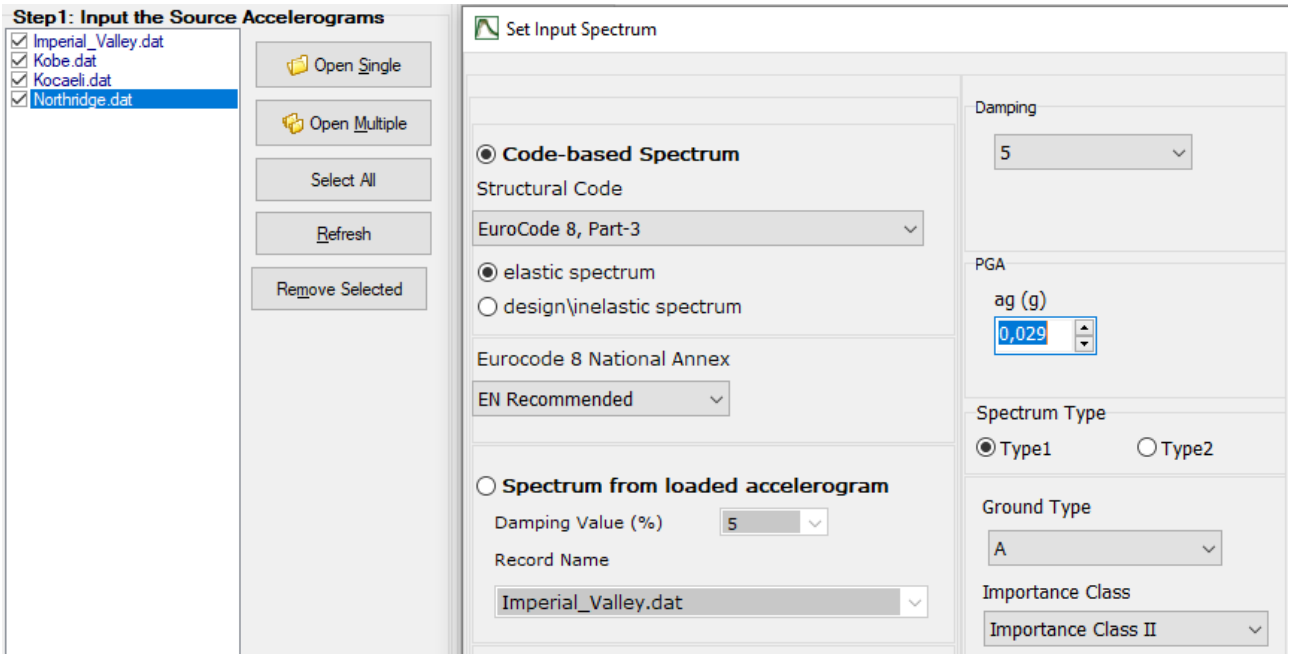

Figure 27: Input multiple source accelerogram, SeismoMatch

After defining the target spectrum, Time Series and Response Spectra graphs can be generated. Figure 28, Kobe Accelerogram provides a good match with Target Spectrum. All graphs can be easily plotted in the Excel program.

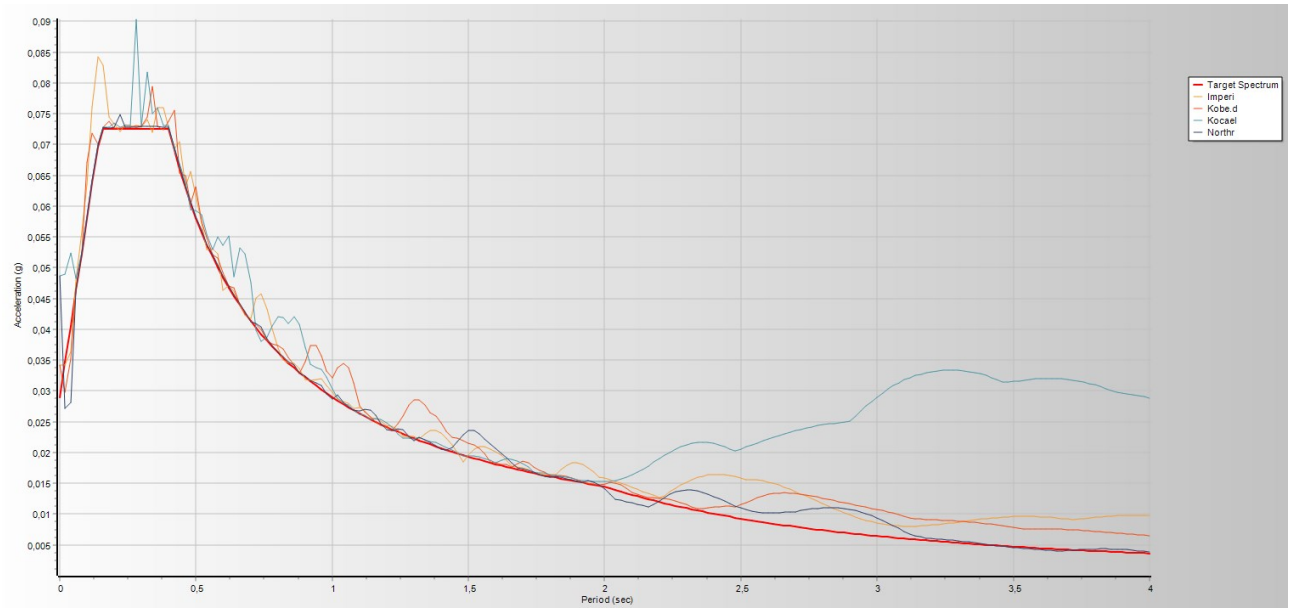

Figure 28: Different Accelerogram files, SeismoMatch

To control output results, Time Series from SeismoMatch is plotted and peak values is compared with input value. Result output from SeismoMatch are attached in Appendix C.

DEEPSOIL

DEEPSOIL program has also pre-defined examples and user can choose among them. Each pre-defined example is different based on the Analysis Method and Solution Type. Alternatively, user can make their own file. For this Thesis, *Equivalent Linear* analysis method is selected, and *Frequency Domain* is selected for the *Solution Type*.

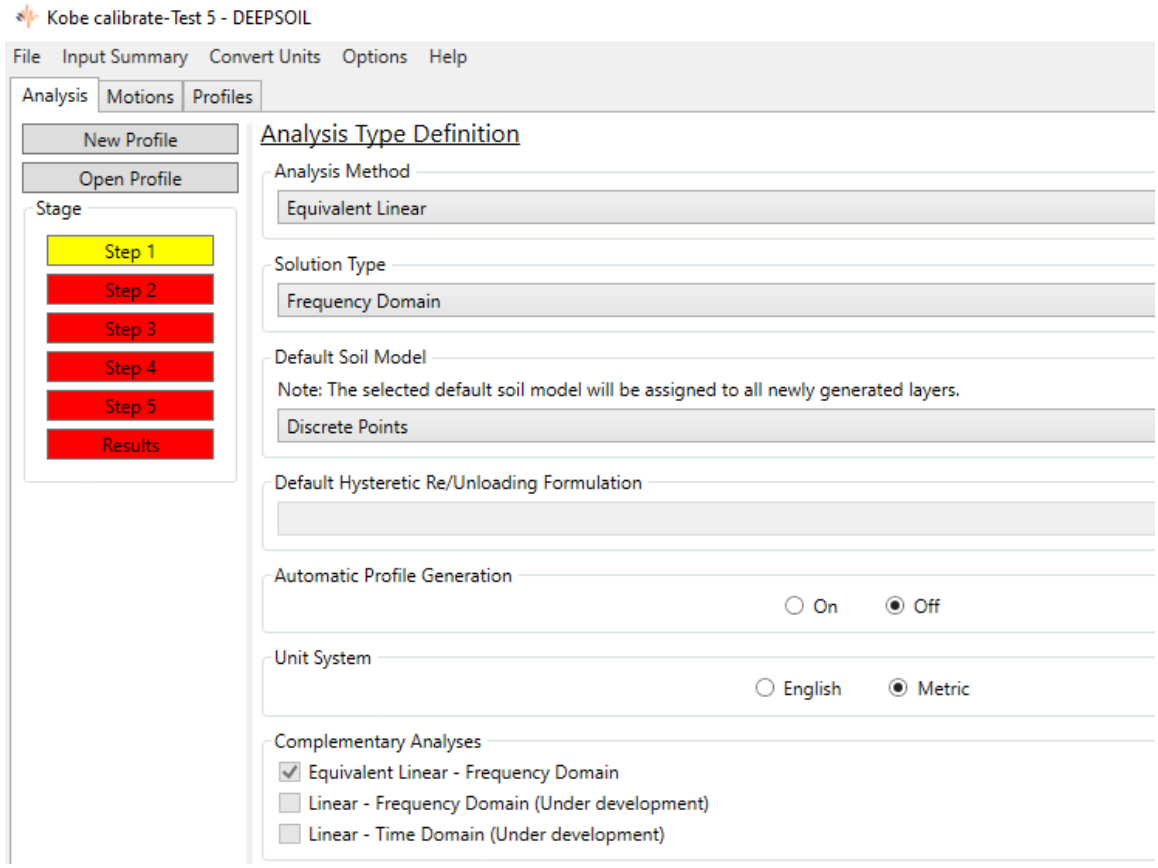

Figure 29: Analysis Control Definition-1, DEEPSOIL

After defining soil profile, Vucetic and Dobry (1991) modulus reduction curve is selected, soil type is clay and plasticity index is defined to be **50%**.

In the Step 3, output time series obtained from the SeismoMatch is used as input motion in the DEEPSOIL. One thing to be noticed, output results from SeismoMatch has unit "g". Output results from SeismoMatch is converted to m/s^2 and then used as input signal motion in the DEEPSOIL and PLAXIS 2D. This will make the process easier in the later stage since units for acceleration in the PLAXIS 2D is m/s^2.

In Step 5, default setting is used, and output results are chosen for the surface of the soil, shown in Figure 30.

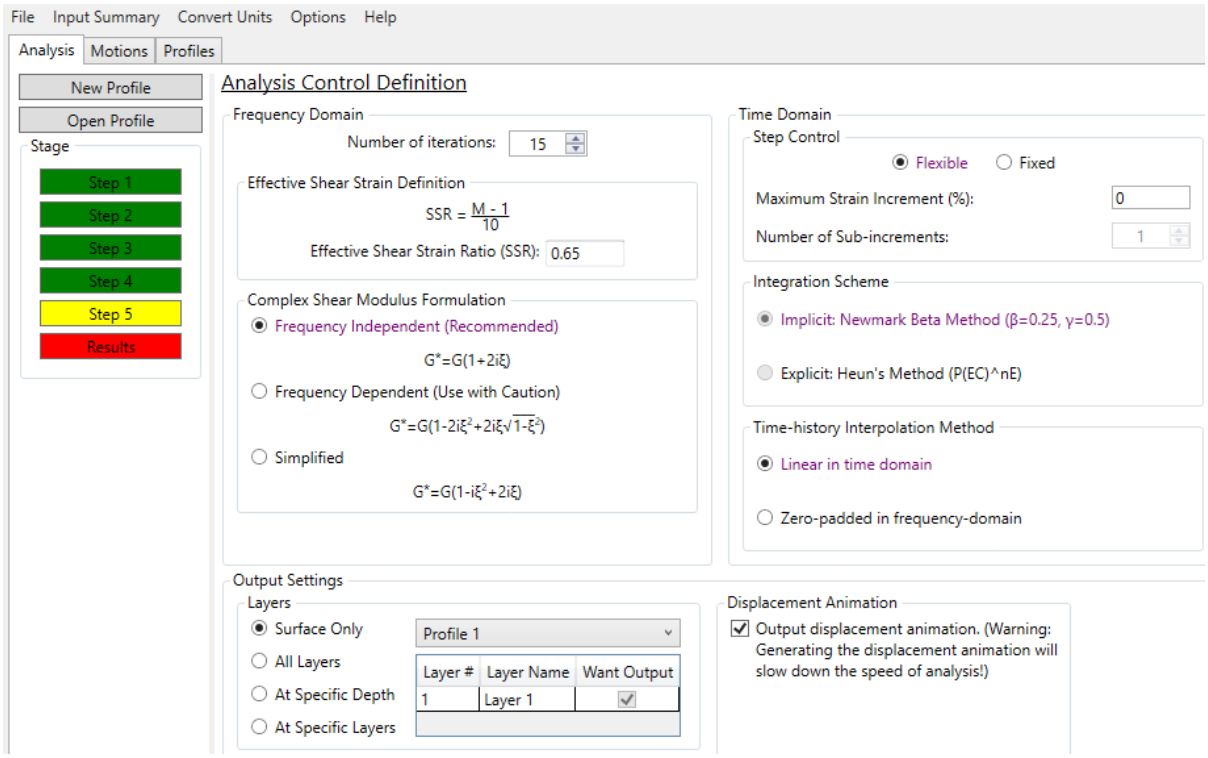

Figure 30: Analysis Control Definition-2, DEEPSOIL

At the final step, results are shown. Results can be easily exported to Excel, Time History Plot and Spectral Plot is used for this report, and these are attached in Appendix D.

EERA

Using EERA is challenging, since system requirement is 32-bit Excel program, it will not work in 64-bit. It is convenient to generate necessary plots. The time series generated in the SeismoMatch is copied in EERA Excel program at *Earthquake* tab sheet. In the *Profile* tab sheet, layers and the shear velocity of each layer is inserted. Shear velocity calculation are shown in Table 26. Necessary plots are then generated, output results from EERA sheet are attached in the Appendix E.

Eurocode 8

Calculations according to the EC8 method is not complicated, and all relevant equations which are discussed in section 2.5.3 Eurocode 8 are used for calculations of the base shear force. All detailed calculations are attached in the Appendix F.

PLAXIS 2D

This section will cover the procedure of constructing of the FEM models in PLAXIS 2D. In section 4.1 Part 1, a representative model without structure is created for ground response analysis. PLAXIS 2D has developed a simple approach (*Site response*) for generating soil column from a PLAXIS model. Steps how this can be generated is shown in the Appendix G.

This approach will allow user to save time for the ground analysis, and is very convenient to use, especially when there are several layers of soil present in the model. Alternative option is to make a 1,0 m or 1,5 width soil column. However, the first approach is even better, since PLAXIS 2D selects proper meshing, dynamic boundary conditions and time stepping, and selects nodes for generating curves for the output result.

The height of soil layer is 15m and is located on top of the bedrock, water level is at 5,0m from top of the soil.

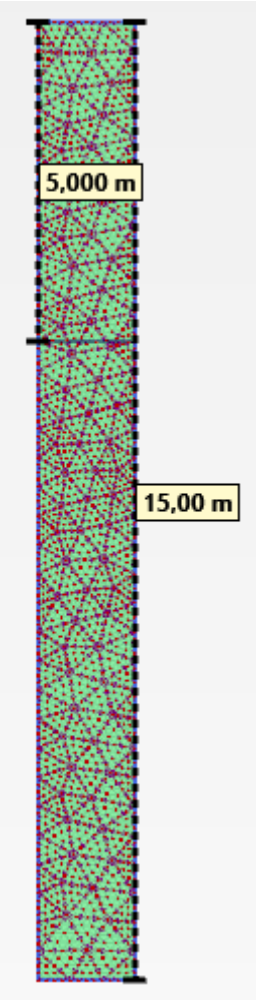

Figure 31: Soil column, PLAXIS 2D

Since there is only one soil layer present in the analysis of this report, a 1,5m width soil column is modelled for Part 1.

Following material parameters are defined in the PLAXIS 2D.

Table 4: Soil material parameter

Parameter	Symbol	Value/Layer	Unit
Material model	-	HS Small	-
Drainage type	-	Drained	-
Soil unit weight, saturate	γ_{sat}	20	kN/m^3
Soil unit weight, unsaturated	γ_{unsat}	*20*	kN/m^3
Secant stiffness in standard drained triaxial test	E_{50}^{ref}	*6815*	kN/m^2
Tangent stiffness for primary oedometer loading	E_{oed}^{ref}	*6815*	kN/m^2
Unloading / reloading stiffness from drained triaxial test	E_{ur}^{ref}	*20446*	kN/m^2
Stress-level dependency power	m	*0,8*	-
Cohesion (Effective)	c'_{ref}	*10*	kN/m^2
Friction angle	$\varphi'(phi)$	*18*	°
Dilatancy angle	$\psi(psi)$	-	°
Threshold Shear Strain at which Gs = 0.722G0	$\gamma_{0,7}$	*0,700E-3*	-
Reference Shear Modulus at very small strains	G_0^{ref}	*66450*	kN/m^2
Poisson's Ratio	ν	*0,2*	-
K0-for normally consolidated soil	-	*0,6910*	-
Interface	R_{inter}	*0,8*	-

The detailed calculation of Table 4 is shown in Table 26 in Appendix A.

Ground Response Analysis example performed by the PLAXIS has been used as a benchmark for recommendations on stiffness parameters, and all parameters are calculated based on the recommendations from PLAXIS. (A. Laera, 2017)

Following recommendations on stiffness parameters have been gathered from various manuals, documents, training manuals, PLAXIS webinars, and examples performed by PLAXIS. As an example, ratio between G_0^{ref} and G_{ur}^{ref} is given in the *Ground response analysis* example performed by PLAXIS (A. Laera, 2017).

Steps to calculate stiffness parameters:

- Compute $G_0^{ref} = G_0 = G_{max}$ at the base of the model which gives desired V_s, use equation (2.10)
- Solve for G_{ur}^{ref} using ratio $\frac{G_0^{ref}}{G_{ur}^{ref}} = (2{,}5\ to\ 10) going\ from\ hard\ to\ soft\ soils$
- Solve for E_{ur}^{ref} using

$$G_{ur}^{ref} = \frac{E_{ur}^{ref}}{2 * (1 + \upsilon_{ur})} \tag{3.1}$$

- Solve for E_{oed}^{ref} using $E_{ur}^{ref} = 3 * E_{oed}^{ref}$

Boundary conditions are shown in Table 5. This also corresponds with the boundary type chosen in the *Ground Response Analysis* performed by PLAXIS.

Table 5: Boundary conditions

Boundary	Type
X min	Tied degrees of freedom
X max	Tied degrees of freedom
Y min	None
Y max	None

Input signal motion in the PLAXIS 2D is generated in SeismoMatch and is defined as dynamic line displacement at the bottom of the model. Signal motion can be displacement, velocity, or acceleration. Input signal motion in this report is chosen to be acceleration. The location of the building is in the Trondheim area and according to the EC8, the peak acceleration is ag=0,288 g. Detailed calculation is shown in the Appendix F.

For the stage construction, since it is a simple soil column, only three phases are defined as shown in Table 6.

Table 6: Stage construction for Part 1

Phase	Calculation type	Description
Initial phase	K0 procedure	-
Phase_1	Plastic	-
Phase_2	Dynamic	Dynamic time interval 52,78 s

The dynamic time interval is chosen for 52,78 s. This value is chosen based on the number of rows in the input signal motion, consequently, the number of Max step in Phase settings for the dynamic phase is the same as the number of rows in the input signal motion. The ratio of the *dynamic time interval* and *Max step* gives 0,01 which is the same time interval as the input signal motion. Detailed calculation is attached in the Appendix A, Figure 57.

After the geometry and soil parameters are defined, mesh is generated. Thereafter, stage construction is defined, and before running calculation analysis, two nodes at the bottom and top of the soil are selected. Graphs are generated after calculation is finished, results are shown in 4.1 Part 1. Output signal at the bottom of the soil is plotted and compared with the input signal motion, this is also demonstrated in section 4.1 Part 1.

For Part 2, the same soil material property, input signal motion and boundary conditions are used, and three different models are constructed in the PLAXIS 2D.

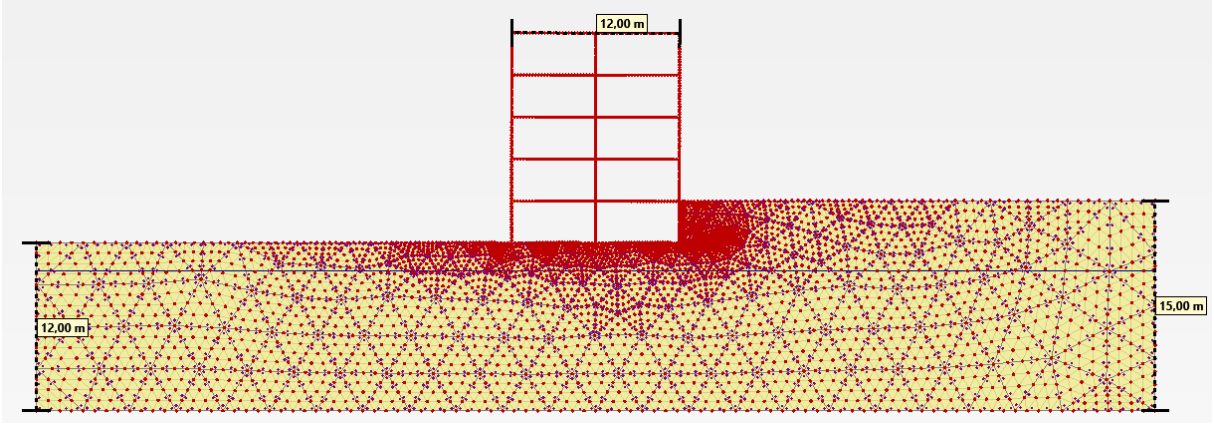

Figure 32: Model 1

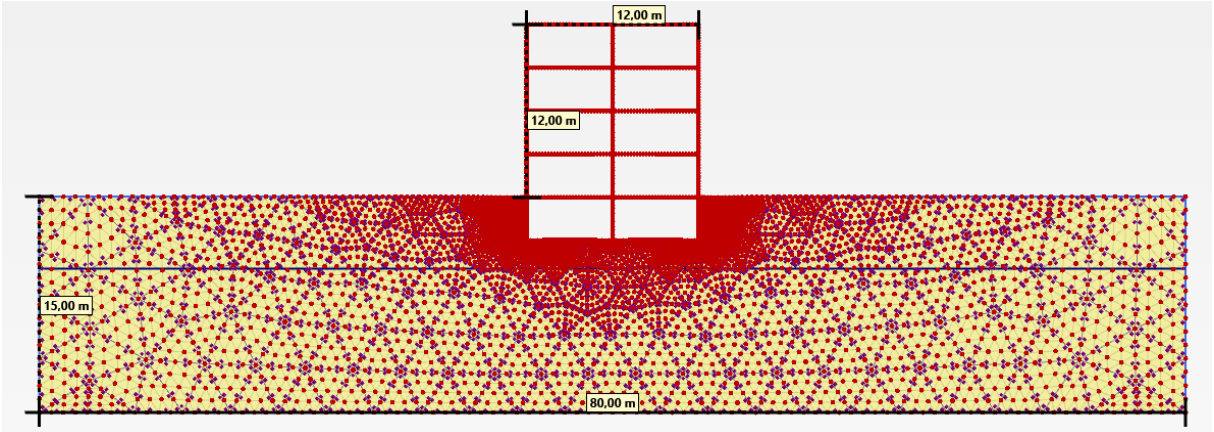

Figure 33: Model 2

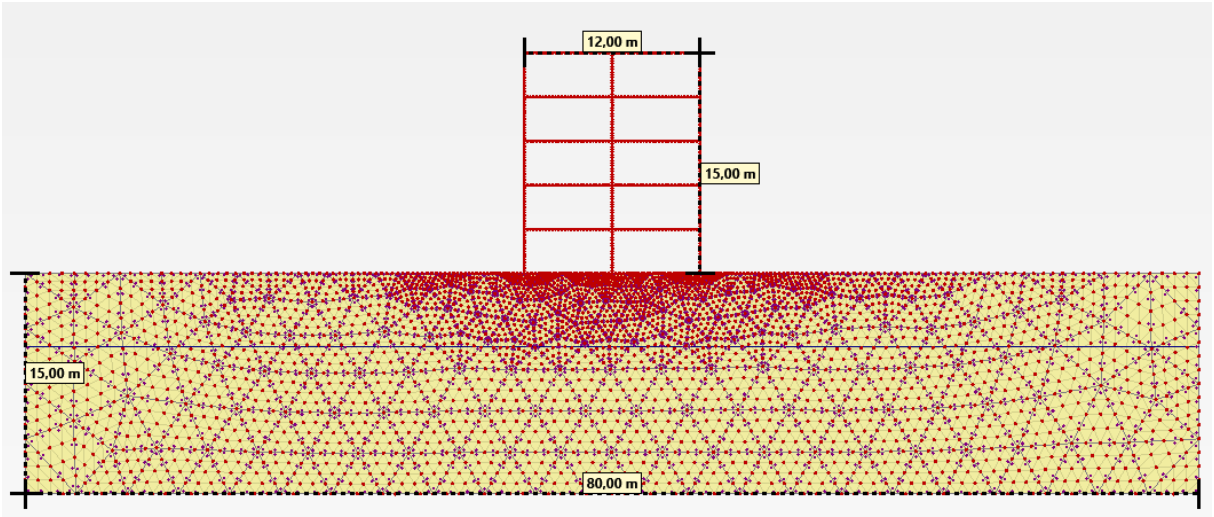

Figure 34: Model 3

Since in Part 2, the soil will be excavated and the construction phase will be included, stage construction will be different than Part 1.

Table 7: Stage construction for Part 2-Model 1 and Model 2

Phase	Calculation type	Description
Initial phase	K0 procedure	-
Excavation	Plastic	Excavation of basement
Construction I	Plastic	Concrete casting of ground floor
Backfilling	Plastic	Backfilling behind basement wall
Construction II	Plastic	Concrete casting of structure, 1^{st}-4^{th} floor
Horizontal load	Plastic	Horizontal load at the top of the structure
Dynamic 5s	Dynamic	For free vibration analysis
Dynamic	Dynamic	Dynamic time interval 52,78 s

Table 8: Stage construction for Part 2-Model 3

Phase	Calculation type	Description
Initial phase	K0 procedure	-
Construction	Plastic	Concrete casting of structure
Horizontal load	Plastic	Horizontal load at the top of the structure
Dynamic 5s	Dynamic	For free vibration analysis
Dynamic	Dynamic	Dynamic time interval 52,78 s

Table 9: Material properties of concrete

Element	Thickness [mm]	EA [kN/m]	EI [kN m²/m]	w [kN/m/m]
Wall 200	200	7,00E+06	1,47E+04	4,80
Floor 300	300	1,05E+07	4,96E+04	7,20
Base slab	350	1,23E+07	7,87E+04	12,60

Results output PLAXIS 2D

For Part 1, accelerogram plots at the bottom and top of the soil are generated. Results of the PSA and accelerogram plots are then compared with the DEEPSOIL and EERA results.

To verify boundary conditions, dynamic time stepping and element size, output signal at the bottom of the soil is plotted and compared with the input signal motion. If these plots give a good match, this implies that the chosen boundary, dynamic time stepping, and the element size has been chosen correctly. This plot is demonstrated in section 4.1 Part 1 and 4.3 Part 2. Steps how to check dynamic time interval is demonstrated in the Appendix G, Figure 91.

In section 4.4 Part 2, two extra plots are generated, horizontal displacement and frequency representation (spectrum). A Pre-calculation point is selected at the top of the wall 2, and two plots are generated from the *Dynamic 5s* phase. This is a free vibration analysis, and the objective is to observe the horizontal displacement of the structure with time. Whilst, the second graph presents natural frequency of the structure. Steps how to plot Frequency representation (Spectrum) is shown in Appendix G, Figure 92.

For section 4.5.2 PLAXIS 2D, Post-calculation points have been selected for the base of the walls, and Shear Force “Q” is plotted against Step for each wall. Time step for the maximum shear force is chosen and two other walls shear forces are plotted for the same time step. Plots are shown in Appendix B.

4 ANALYSIS AND RESULTS

This section will be studied in two parts. In Part 1, the results from the PLAXIS 2D will be compared with the one-dimensional programs, DEEPSOIL and EERA. The objective is to calibrate PLAXIS 2D material properties with DEEPSOIL and EERA, ensuring that material input in PLAXIS 2D provides close result as DEEPSOIL and EERA.

In Part 2, the calibrated material properties obtained from the Part 1 will be used. Three different models are created in PLAXIS 2D, and results between the EC8 method and the PLAXIS 2D will be compared.

4.1 Part 1

In this part, a response analysis model is executed in the PLAXIS 2D, results obtained from the top of the model from PLAXIS 2D will be compared with the results obtained from the DEEPSOIL and EERA.

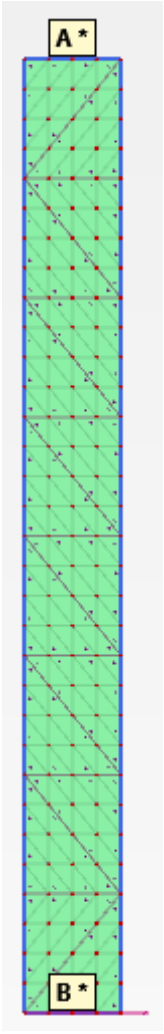

Figure 35: Points selected for output result-Part 1

From PLAXIS 2D, two plots are generated from point A (surface of the model), Accelerogram and PSA.

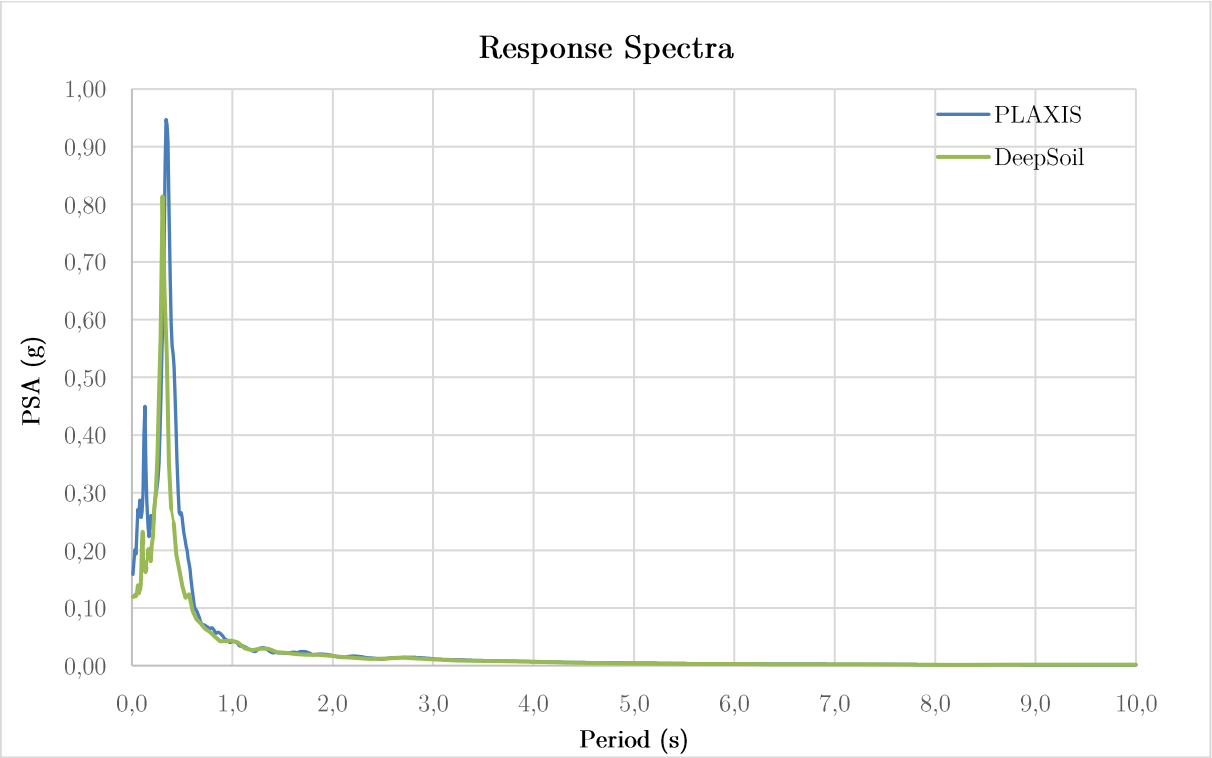

Figure 36: PSA response spectra at point A

From Figure 36 it can be seen that peak PSA and their period (s) both in PLAXIS 2D and DEEPSOIL are close enough. The pattern of both graphs shows relatively good match.

Table 10: Comparison PSA in PLAXIS 2D and DEEPSOIL

Software	PSA (g)	Period (s)
PLAXIS	0,947	0,340
DEEPSOIL	0,814	0,305

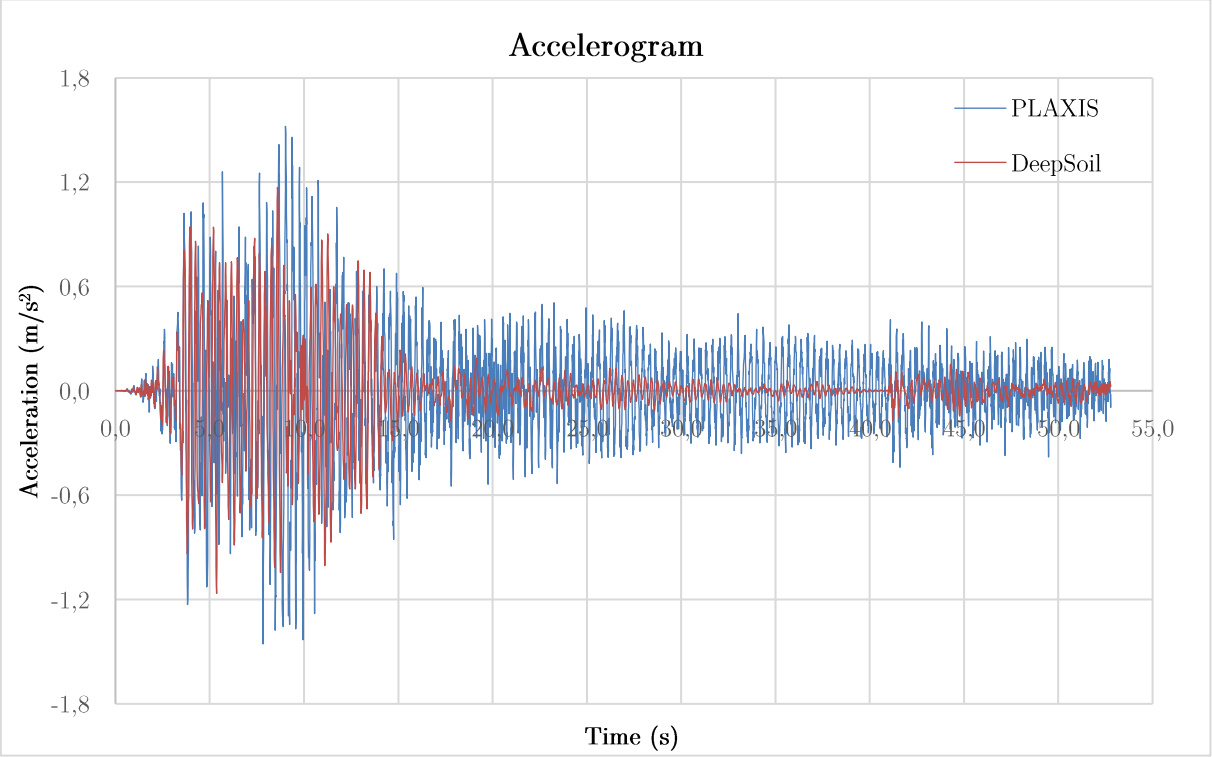

Figure 37: Acceleration at point A, without Rayleigh damping

Figure 37 shows that DEEPSOIL has more damping than the PLAXIS 2D, peak acceleration and their peak time are not very close. In this example, no Rayleigh damping coefficients are used in PLAXIS 2D.

Table 11: Comparison Accelerogram in PLAXIS 2D and DEEPSOIL

Software	Acceleration (m/s²)	Period (s)
PLAXIS 2D	1,52	9,02
DEEPSOIL	1,17	8,60

To make a comparison if defining Rayleigh damping coefficients in PLAXIS 2D will provide better match with the DEEPSOIL, another simulation is done with the Rayleigh damping coefficients. Figure 38

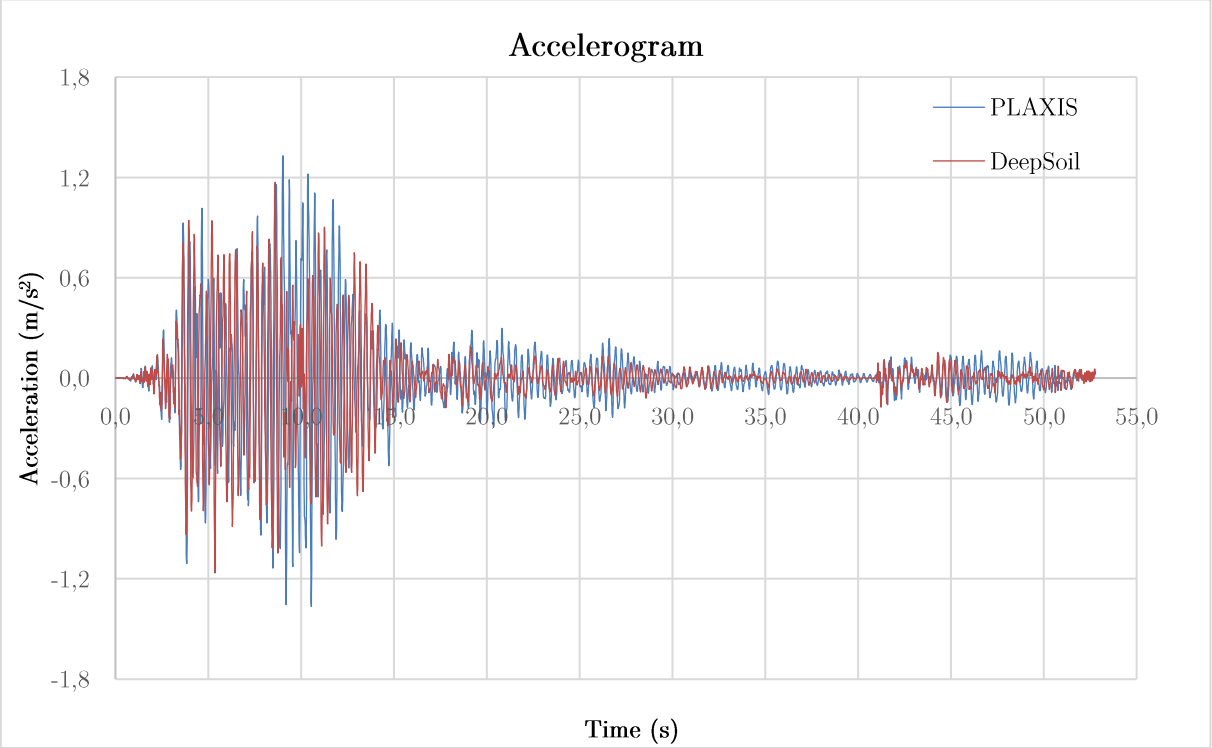

Figure 38: Acceleration at point A with Rayleigh damping coefficients

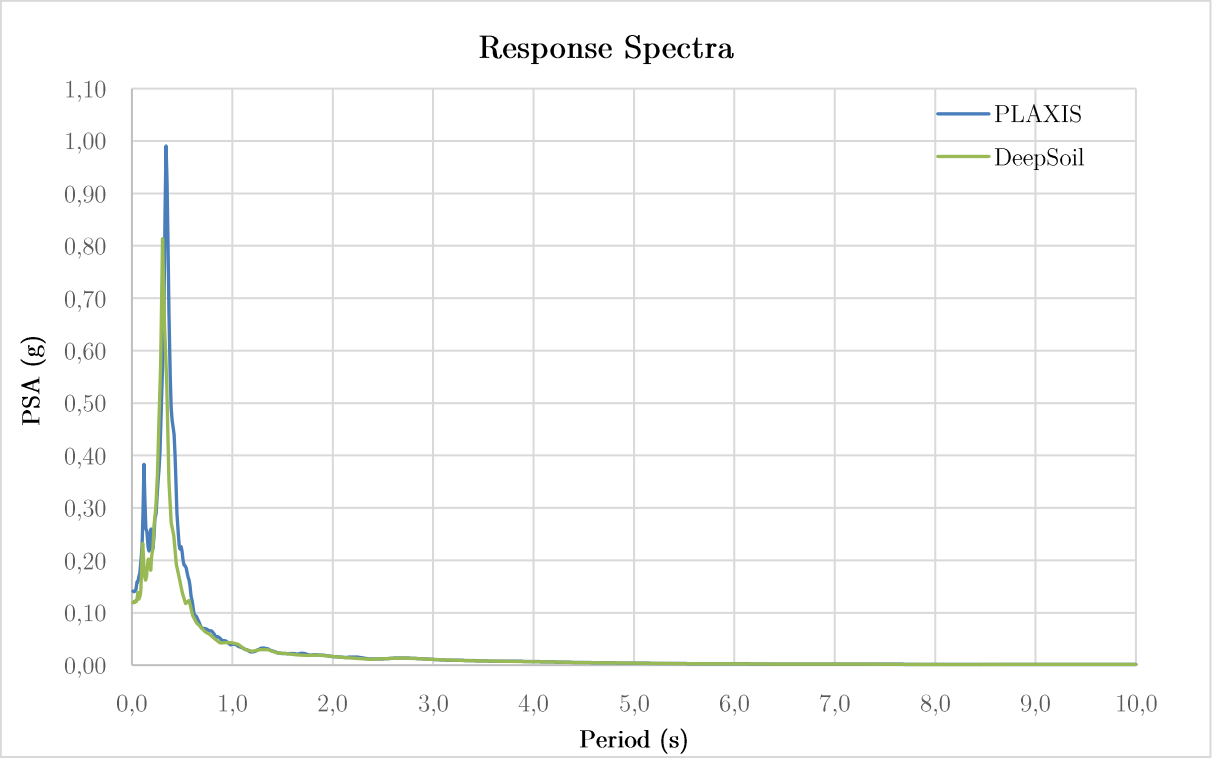

Figure 39: PSA response spectra at point A (with Rayleigh damping)

Results from the PLAXIS 2D with the Rayleigh damping coefficients show relatively better match with the DEEPSOIL.

Table 12: Comparison Accelerogram in PLAXIS 2D (with Rayleigh damping) and DEEPSOIL

Software	Acceleration (m/s^2)	Period (s)
PLAXIS 2D	1,33	9,02
DEEPSOIL	1,17	8,60

Table 13: Comparison PSA in PLAXIS 2D (with Rayleigh damping) and DEEPSOIL

Software	PSA (g)	Period (s)
PLAXIS 2D	0,990	0,340
DEEPSOIL	0,814	0,305

Another comparison is carried out between the PLAXIS 2D and EERA both for the PSA and Accelerogram, the objective is to compare if EERA provides better match than the results obtained from the DEEPSOIL.

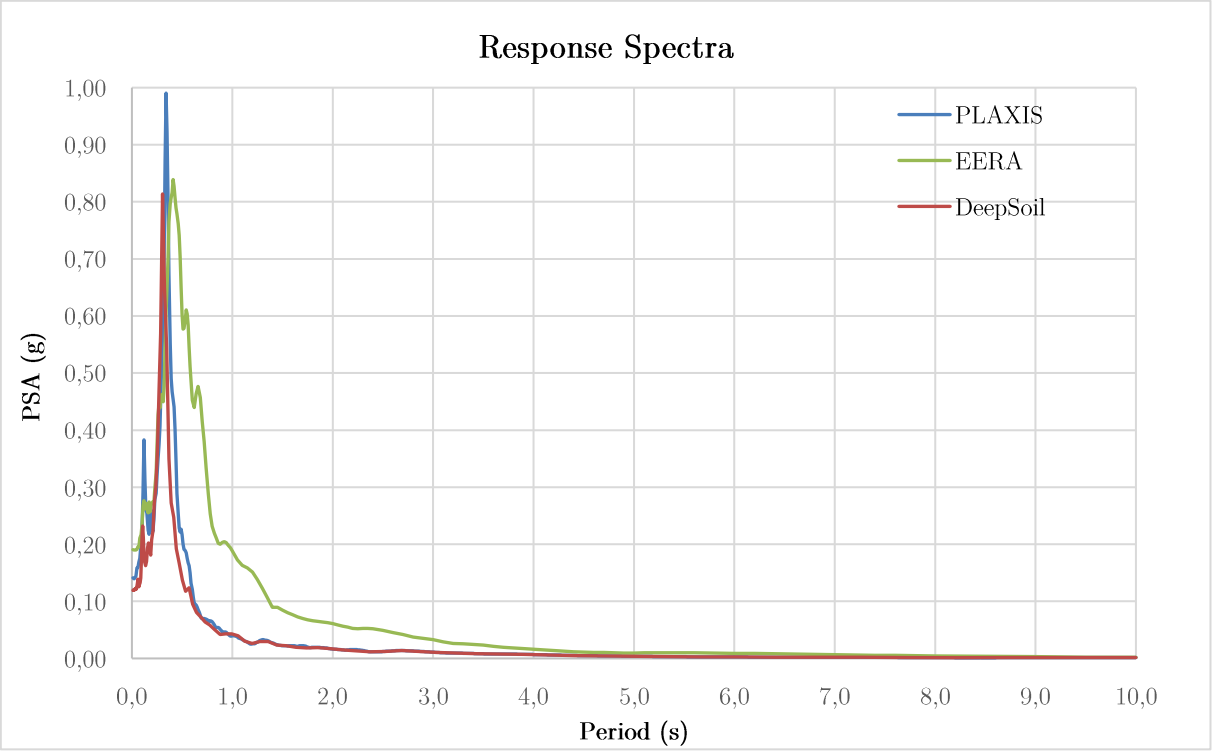

Figure 40: PSA response at point A, PLAXIS, DEEPSOIL and EERA

The results of the PSA shows good agreement between EERA and the DEEPSOIL, peak PSA is somewhat close, whereas, PLAXIS 2D shows slightly higher PSA than the EERA and the DEEPSOIL.

Table 14: Summary PSA, PLAXIS, DEEPSOIL and EERA

Software	PSA (g)	Period (s)
PLAXIS 2D	0,990	0,340
EERA	0,839	0,410
DEEPSOIL	0,814	0,305

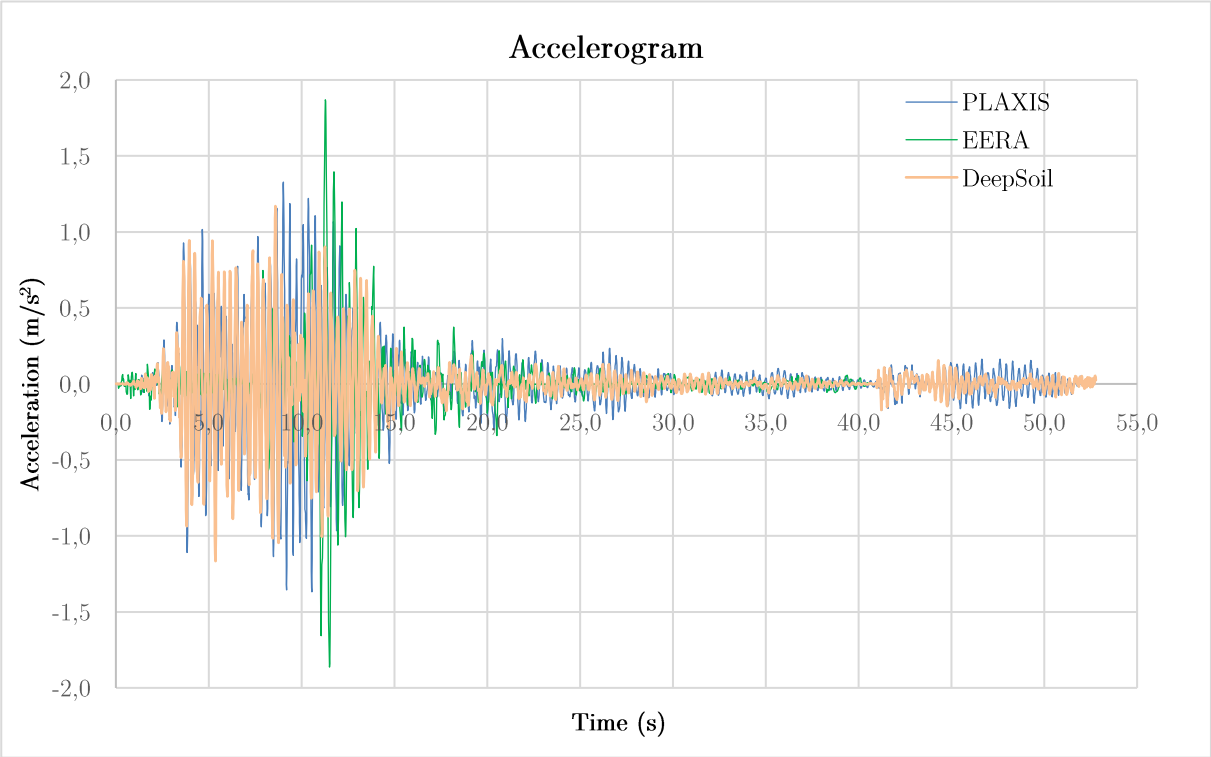

Figure 41: Acceleration at point A, PLAXIS, DEEPSOIL and EERA

Figure above shows pretty good match, only remarkable difference is EERA gives higher peak acceleration (positive and negative) than PLAXIS 2D and DEEPSOIL.

Table 15: Summary comparison Accelerogram PLAXIS 2D, DEEPSOIL and EERA

Software	Acceleration (m/s^2)	Period (s)
PLAXIS 2D	1,33	9,02
EERA	1,87	11,28
DEEPSOIL	1,170	8,600

The To verify if appropriate boundary conditions and time interval is selected in the PLAXIS 2D, output signal at the bottom of the model is plotted and compared with the input signal motion, this is shown in Figure 42.

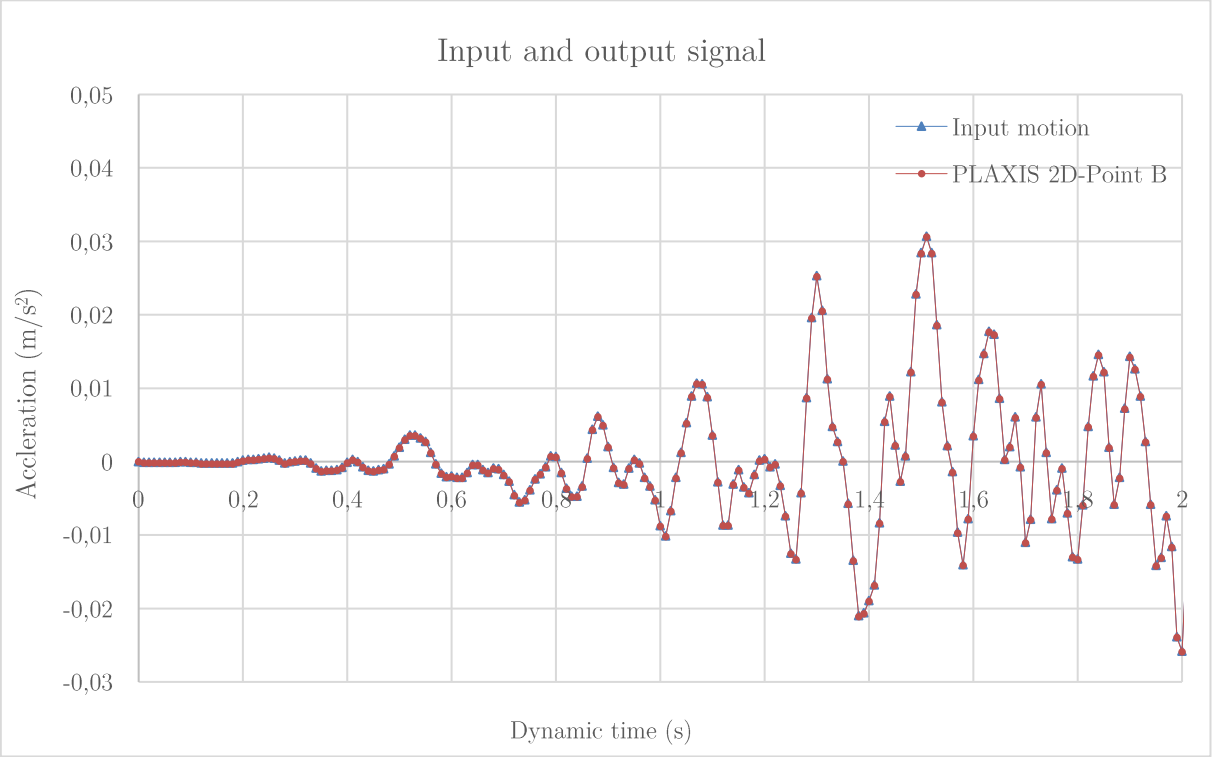

Figure 42: Input and output signal at point B

The graph shows perfect match. Dynamic duration time is chosen for a short time to visualize the graph better. Complete graph is attached in Appendix B, Figure 64.

To illustrate how graphs of input and output signal might be, if incorrect time interval is chosen, another simulation is carried out and the time interval is changed in the model, all other settings and parameter remain the same. Result is illustrated in Figure 43.

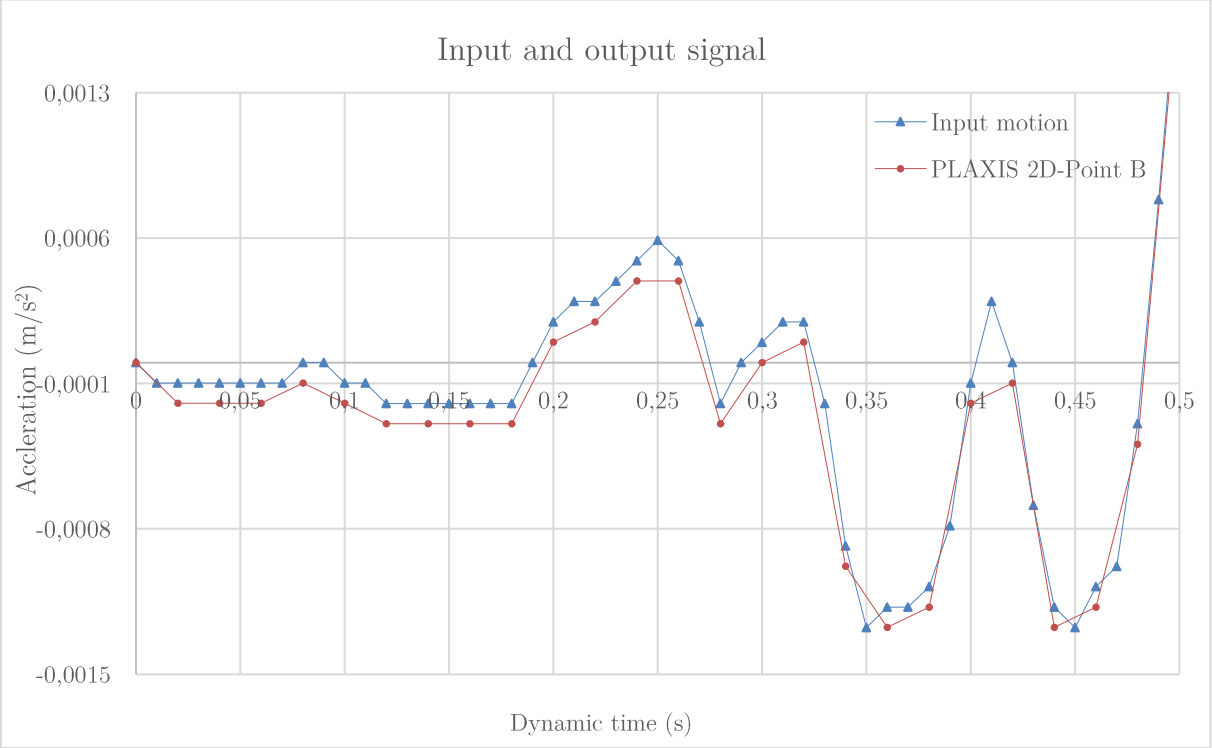

Figure 43: Input and output signal at point B for $\delta_t = 0{,}02$

The graph does not show good match between the input and output signal. The difference between each point does not seems to be very high, however, this difference might be bigger as it is shown in Figure 18. The objective of this graph is to visualize difference in input and output signal motion if incorrect dynamic time interval and the corresponding Max step is chosen.

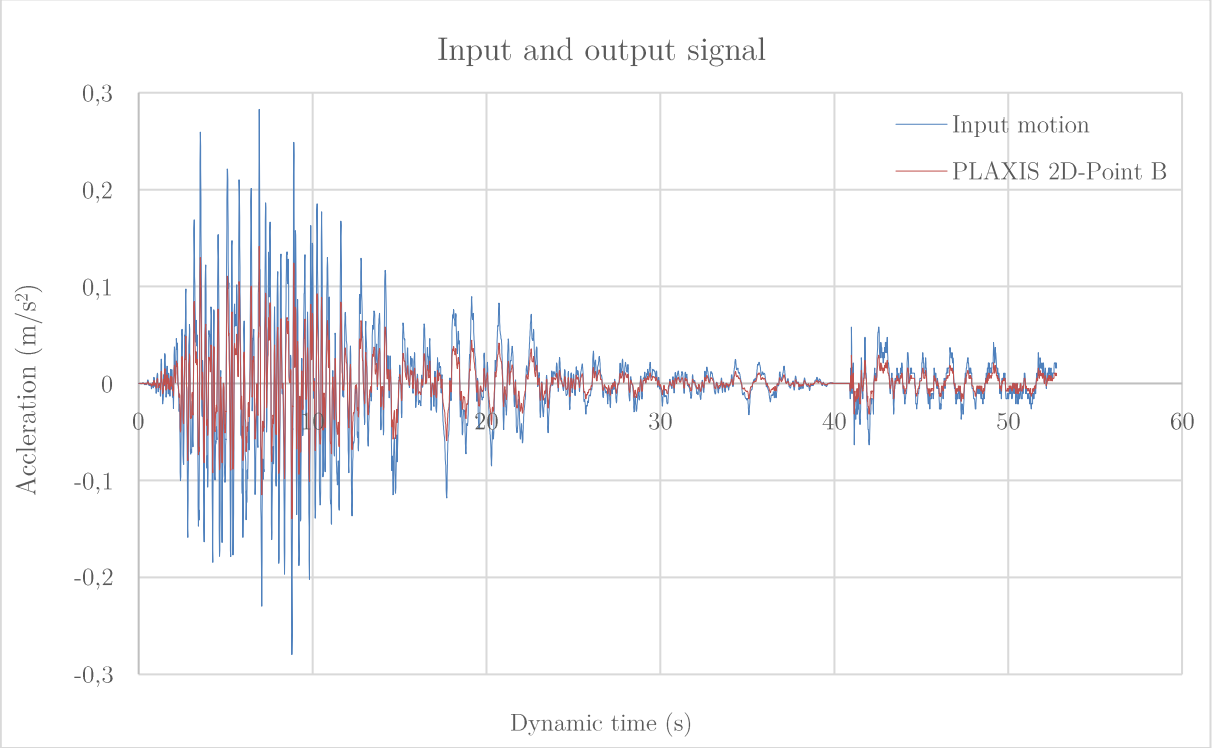

Figure 44: Input and output signal at point B for Compliant base boundary

Another ground response analysis is carried out for *Compliant base* boundary, all other parameters remain unchanged. The objective of this is to assess if *Compliant base* boundary provides same output as input signal motion at the bottom of the model. No further analysis is provided since there is considerable deviation between input and the output signal motion.

4.2 Summary and Discussion

The key part in this section is to choose proper material property, boundary conditions and the dynamic time interval to obtain close results between PLAXIS 2D and one-dimensional program, DEEPSOIL or EERA. The objective is to calibrate PLAXIS 2D model with DEEPSOIL or EERA.

Figure 36 and Figure 37 show good match between the PLAXIS 2D and DEEPSOIL. The results from DEEPSOIL shows more damping than the PALXI 2D. After defining the Rayleigh damping coefficients in the PLAXIS 2D, the accelerogram results become closer to the DEEPSOIL, and provide better match than the model without Rayleigh damping coefficients. However, the peak value of PSA increased slightly, Figure 38 and Figure 39.

EERA is another one-dimensional program like DEEPSOIL. Another comparison is carried out between the PLAXIS 2D, DEEPSOIL and EERA. The objective here is to study if EERA provides approximate results as the DEEPSOIL. Results from EERA show that PSA graph gives good match with the DEEPSOIL, however peak acceleration is quite higher than the PLAXIS 2D and DEEPSOIL, Figure 40 and Figure 41 respectively.

Verification of the boundary conditions and the dynamic time interval is important in the PLAXIS 2D for the dynamic analysis. To verify if correct dynamic boundary conditions and dynamic time interval are chosen, the accelerogram at the bottom of the model is plotted where output signal is compared with the input signal motion. The result suggests in Figure 42 that the chosen boundary condition provides same result as input signal motion, this implies that correct boundary condition is chosen. Computing the dynamic time interval is discussed in section 2.5.1 Finite Element Method and according to the PLAXIS, equation (2.29) should be used. Defined the dynamic time interval should correspond with the input signal motion time interval. This is also shown in Figure 42 that computed dynamic time interval corresponds with the input signal motion time interval.

Because the input signal motion and the dynamic boundary conditions are defined at the base of the model, therefore verifications for the boundary conditions and the dynamic time interval is carried out at the base of the model. It is also possible to select several points from base of the model to the top of the soil and study how accelerogram varies with the height.

To study if choosing different dynamic time interval gives different result, only dynamic time interval is changed in the model and accelerogram is plotted at the base of the model. Result in Figure 43 implies that the output signal do not match if incorrect dynamic time interval is defined in the PLAXIS 2D, hence it does not correspond with the input signal motion.

Because of the difference in the input signal motion and the output signal at the base of the model, this may lead to incorrect results at the top of the model. Therefore, no further analysis is done in this report for the incorrect dynamic time interval.

PLAXIS 2D has carried out *Free Vibration and Earthquake Analysis of a Building* (Bentley-13, 2021), where in this example PLAXIS has used *Compliant base* boundary conditions at the base of the model. This example is not calibrated with one-dimensional program. Although PLAXIS recommends using the *Compliant base* boundary condition for the dynamic analysis, it did not provide good match with DEEPSOIL for the calculations in this report. Figure 44

When it comes to the selection of the material model and boundary conditions, PLAXIS has carried out different examples for the different material models and boundary conditions. After studying different material models behavior under dynamic actions, the HSsmall material model is chosen based on its characteristics and behavior under the dynamic actions. All material stiffness parameters are calculated based on the recommendations from the PLAXIS, this also apply for choosing of the boundary conditions. PLAXIS has carried out Ground Response Analysis and compared the results with EERA. (A. Laera, 2017)

In this example, PLAXIS used the HSsmall model and same boundary condition as selected for this report, shown in Table 5. Comparison of the Accelerogram and PSA results between PLAXIS and EERA are shown in Figure 45 and Figure 46. These two graphs do not match perfectly, and graphs deviates somewhat, yet good match. In this example, PLAXIS defined the Rayleigh damping coefficients, yet EERA result shows more damping than the PLAXIS 2D, and Peak acceleration (negative) is higher in EERA compare to the PLAXIS 2D.

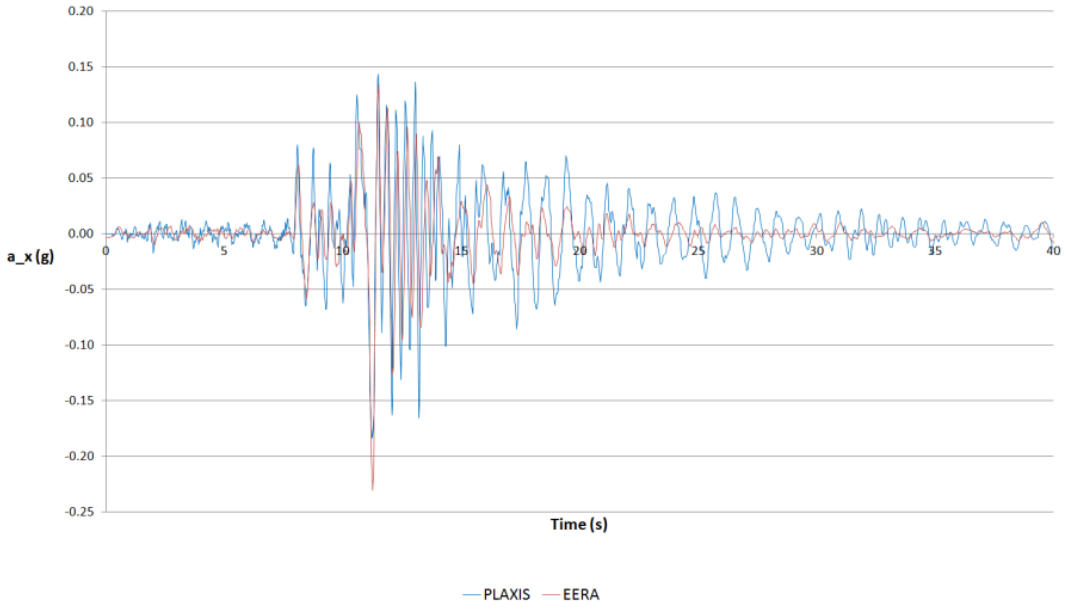

Figure 45: Accelerogram at 3,6m from the surface level, (A. Laera, 2017)

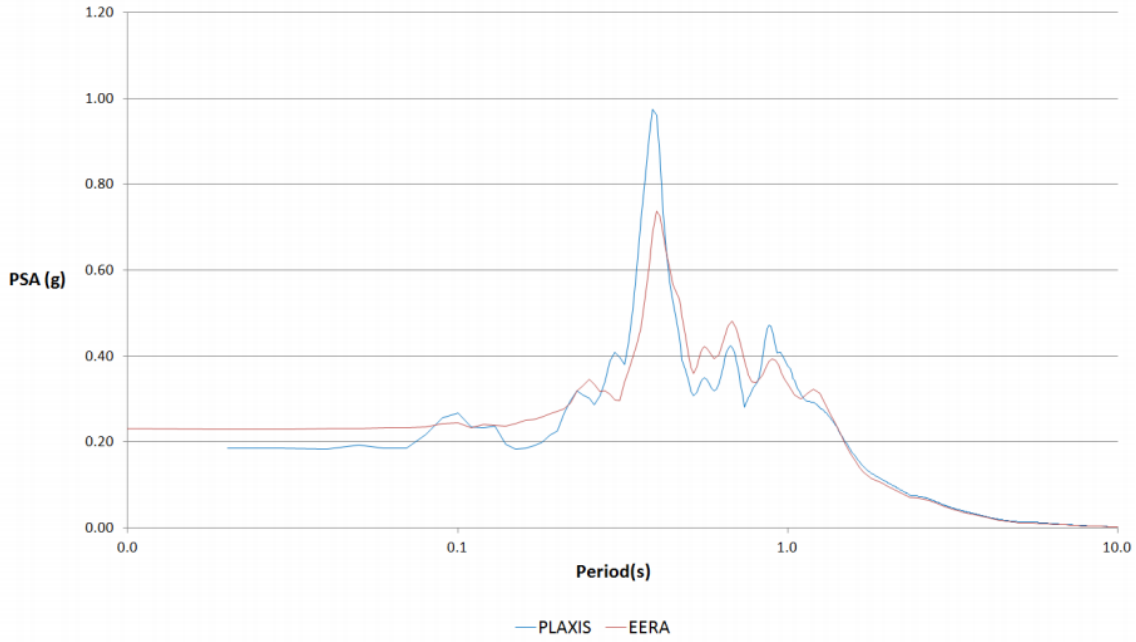

Figure 46: PSA spectrum at 3.6 m from the surface level, (A. Laera, 2017)

For this report several tests have been carried out for different types of boundaries, the one which provided better results is chosen and all relevant results based on chosen boundaries are included in this report. This conclusion was based on the comparison of the input signal motion and output result at the base of the model, where both boundary conditions and the dynamic time interval are compared. Additionally, obtained results from the surface of the model were compared with the one-dimensional program. The selected boundary conditions in this report provided better match with DEEPSOIL and EERA. Ground Response Analysis (A. Laera, 2017) is used as a benchmark in this Thesis, and all necessary calculations for computing the material stiffness parameters are done according to this example and generally according to the recommendations from PLAXIS.

The results of this report obtained from the PLAXIS 2D, DEEPSOIL and EERA deviates somewhat, and the same applies to the results for *Ground Response Analysis* example performed by PLAXIS. Defining Rayleigh damping coefficient suggest that the accelerogram graph deviation became smaller to an extent, but peak PSA value increased slightly.

4.3 Part 2

In this section, seismic analysis will be performed in the PLAXIS 2D and the base shear force results will be compared with the EC8 method.

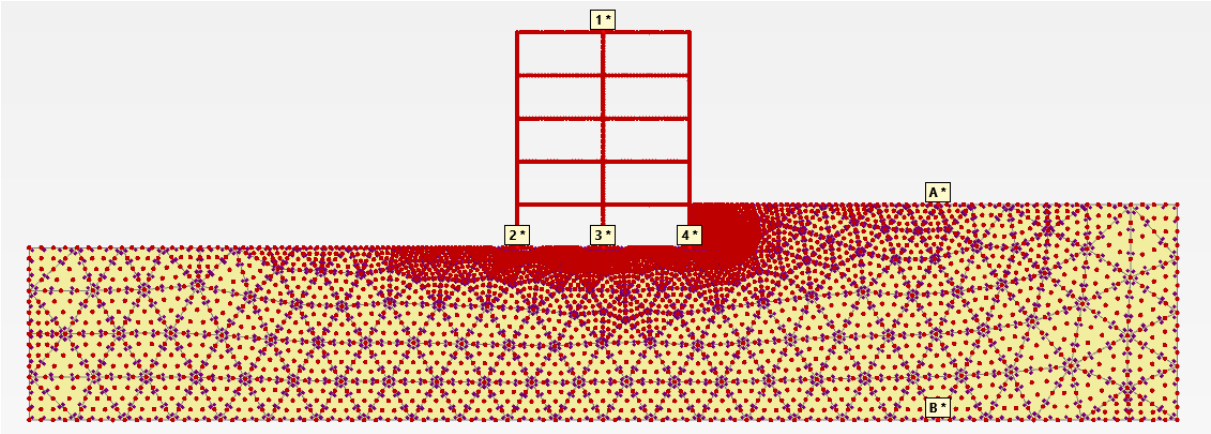

Figure 47: Generated mesh with selected nodes-Model 1

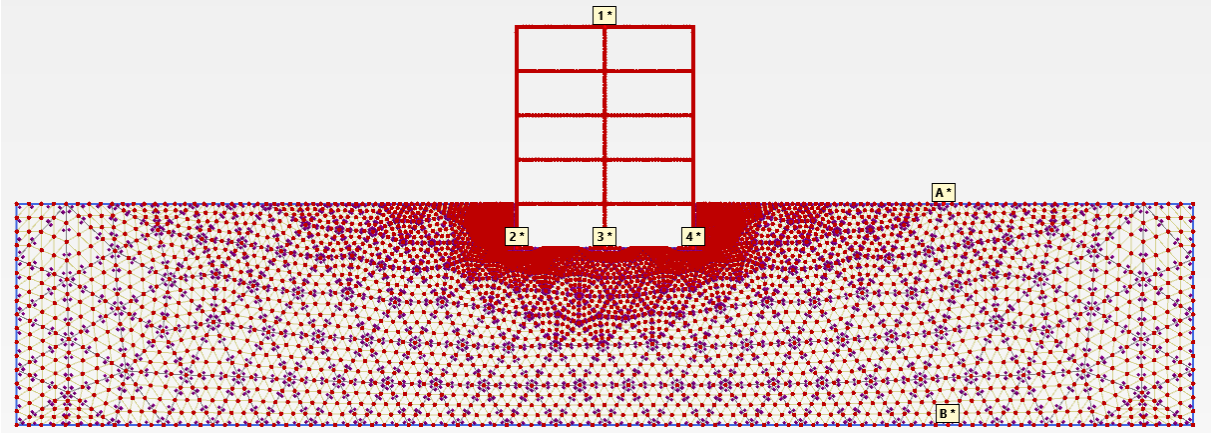

Figure 48: Generated mesh with selected nodes-Model 2

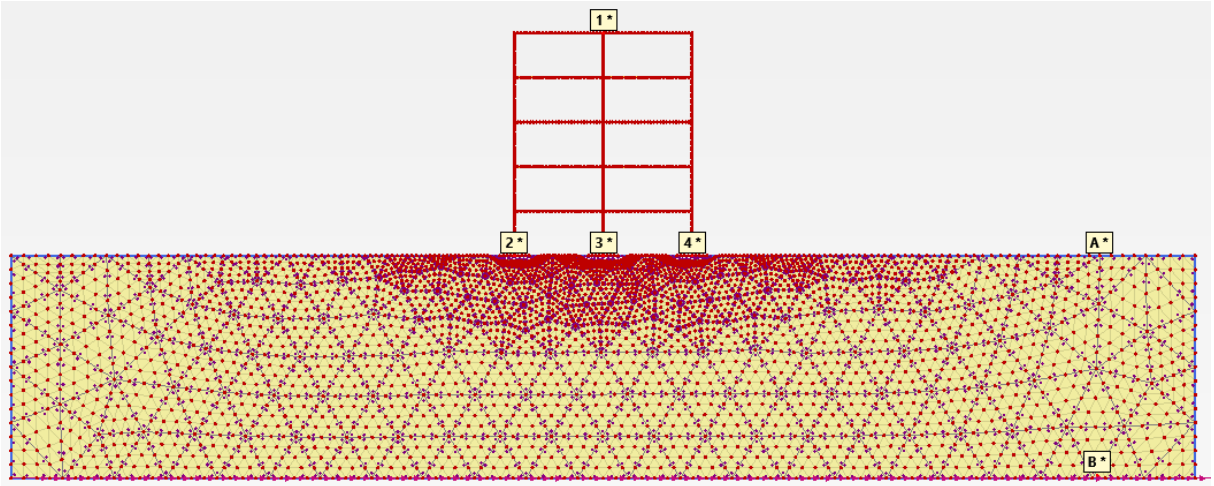

Figure 49: Generated mesh with selected nodes-Model 3

4.4 Free Vibration Analysis

Two plots will be generated for each model, horizontal displacement, and frequency of the structure.

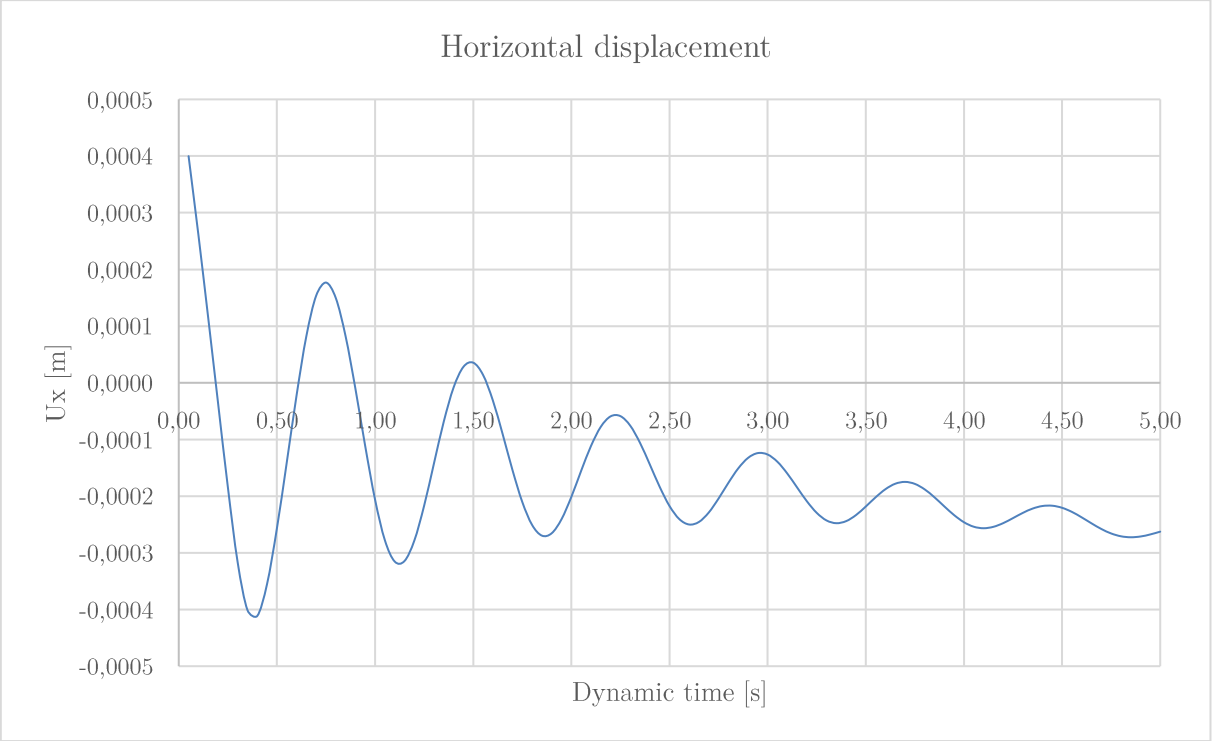

Figure 50: Time history of displacement at point 1-Model 1

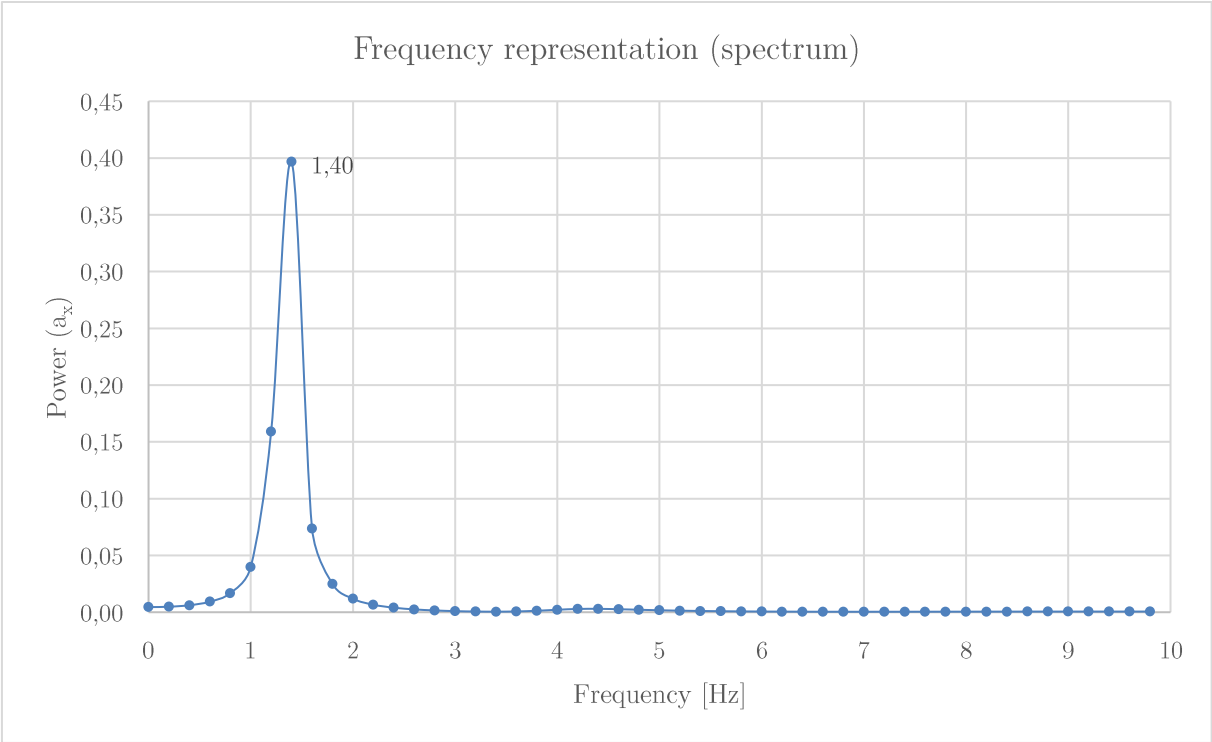

Figure 51: Frequency representation (spectrum)-Model 1

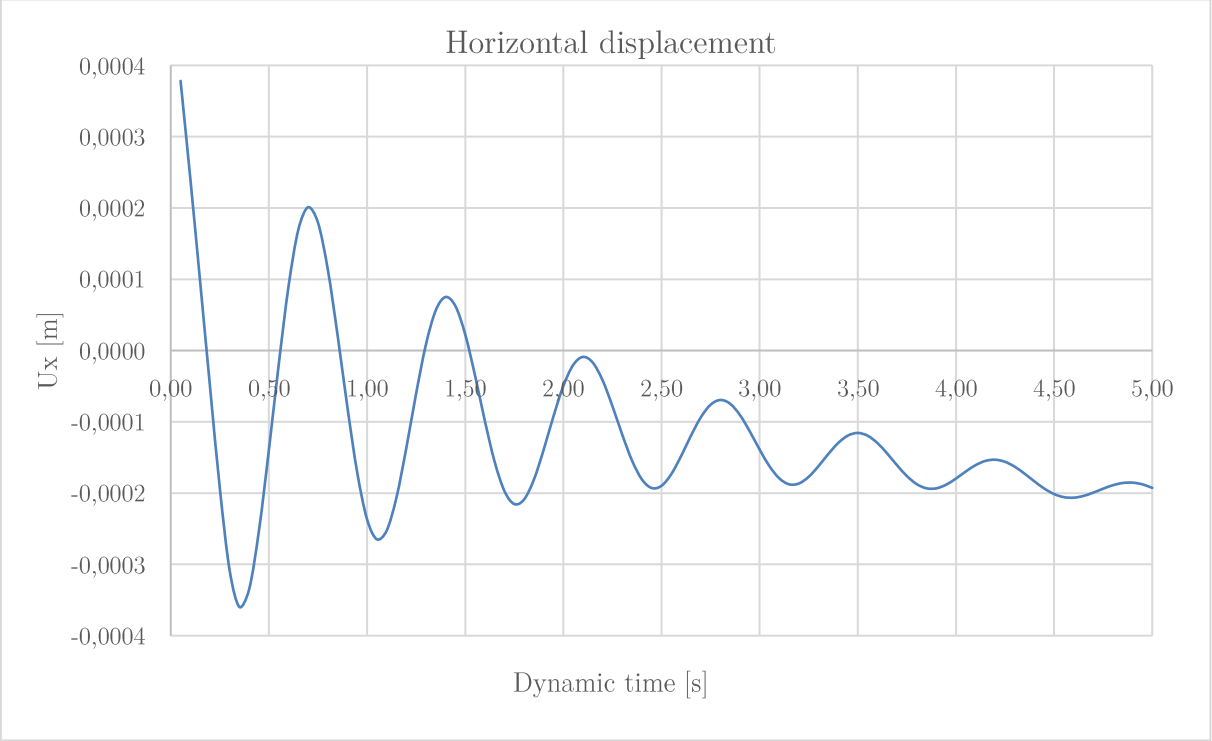

Figure 52: Time history of displacement at point 1-Model 2

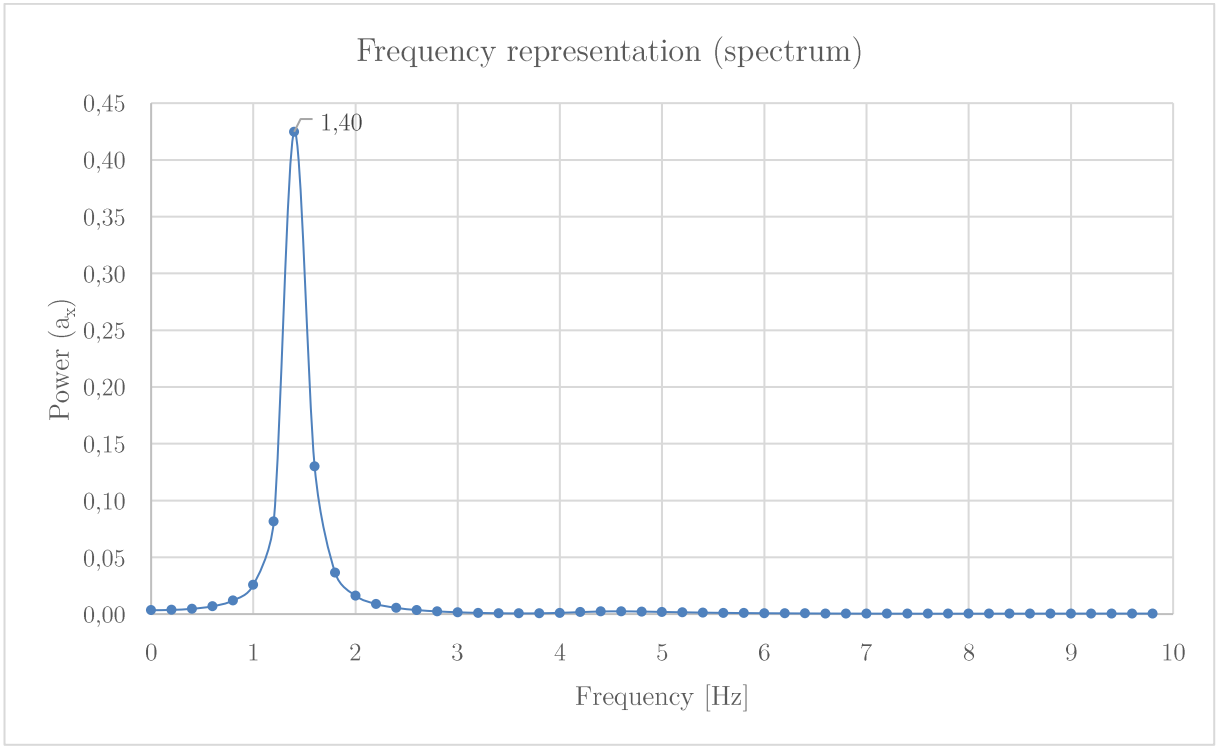

Figure 53: Frequency representation (spectrum)-Model 2

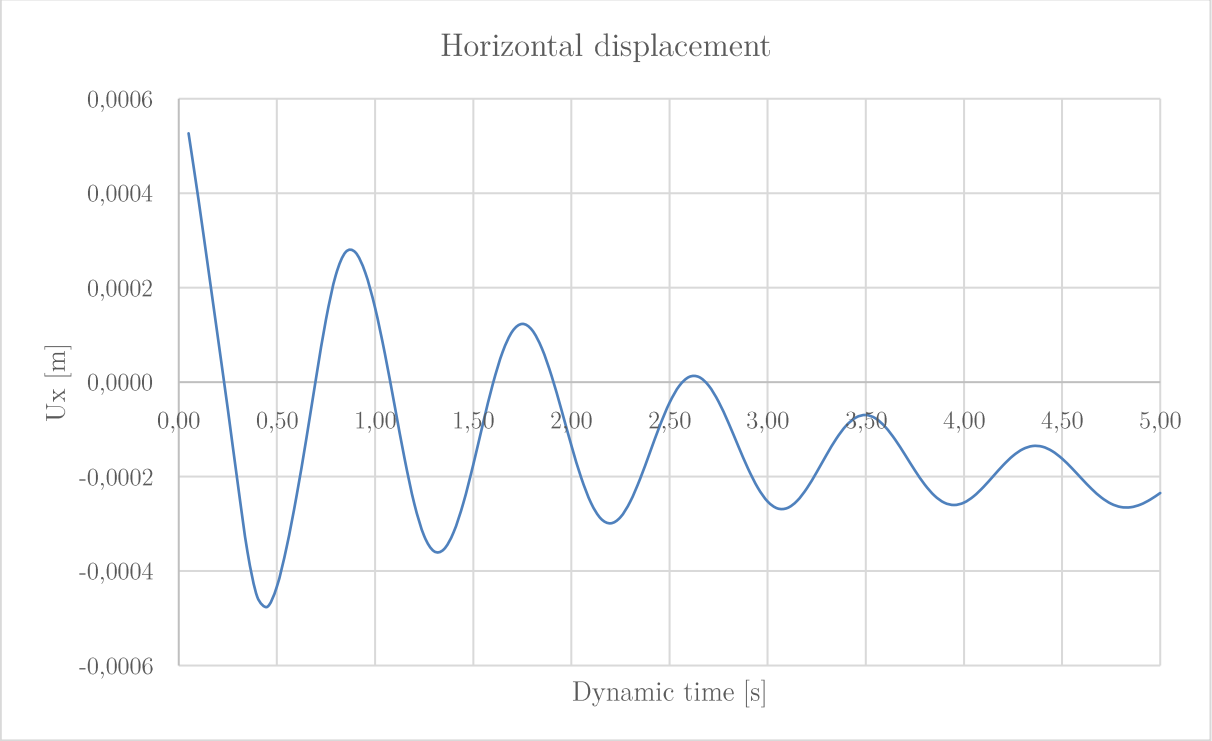

Figure 54: Time history of displacement at point 1-Model 3

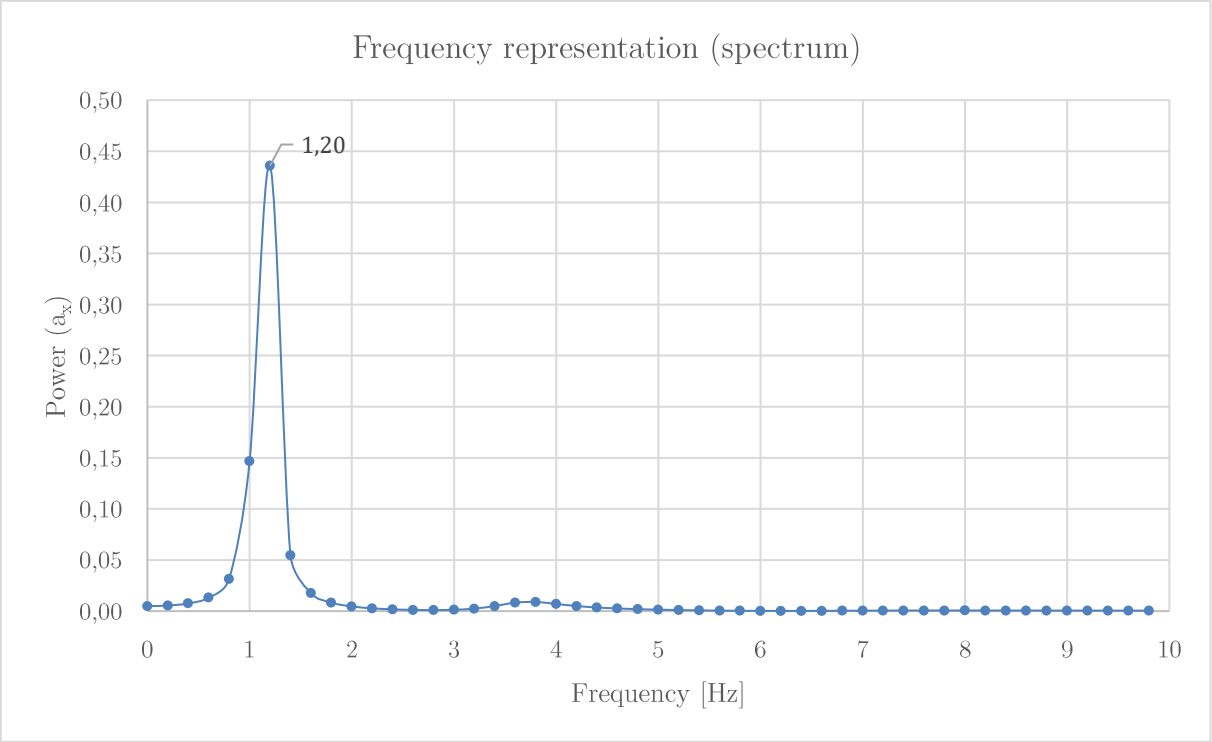

Figure 55: Frequency representation (spectrum)-Model 3

The objective of plotting above plots are to observe behavior of the structure under free vibration. It is clear from Figure 50, Figure 52, and Figure 54 that horizontal displacement decays with time, and all three models have very small horizontal displacement.

Figure 51, Figure 53, and Figure 55 represents frequency representation. Graphs give information about the natural frequency of the building. The objective here is to compare the natural frequency of the building with the predominant period of the peak value in the PSA spectrum. If the natural frequency of the overlying structure occurs at the same period, this indicates that the system is in resonance and this will cause damages to the structure. Plotting of frequency representation (spectrum) can also be plotted for `Power (Ux)`, procedure is the same as for the `Power (ax)` and both graphs will provide same peak frequency. Tips how to generate this plot is given in Appendix G.

Table 16: Summary building natural frequency

Model	1	2	3
Max PSA period [s]	0,32	0,34	0,34
Building natural frequency, T=1/f [s]	0,83	0,71	0,83

For simplicity, bottom of the one wall is selected in each model and PSA graphs are generated for all three models. Graphs are shown in Appendix B. Based on the findings in Table 16, none of the buildings are in the resonance.

4.5 Calculation of Base Shear Force

This section will cover the Base Shear Force calculation according to the EC8 method and based on the results obtained from the PLAXIS 2D. Results from both methods will be then compared.

4.5.1 Eurocode 8

All relevant equations for calculation of the Base Shear Force according to the EC8 are presented in 2.5.3 Eurocode 8, and detailed calculations are shown in Appendix F.

$a_g = 0{,}288\ g$

$S = 1{,}65$

$q = 1{,}5$

$H = 15\ m$

$C_t = 0{,}075$

$Ground\ type -\ E$

$T_B\ = 0{,}10\ s$

$T_C = 0{,}30\ s$

$T_D\ = 1{,}40\ s$

Above values, except H are the same for all three models.

<u>Model 1 and Model 3</u>

$m = 72360\ kg$

$\lambda = 0{,}85$

$T_1\ = 0{,}572\ s$

$S_d =\ 0{,}416\ m/s^2$

$F_b =\ 25{,}6\ kN$

Since the building frequency form the PLAXIS 2D is different than the one calculated with the EC8 method, the obtained building frequency from the PLAXIS 2D will be used in the EC8 method to compare difference:

<u>Model 1</u>

$T_1\ = 0{,}714\ s$

$S_d =\ 0{,}333\ m/s^2$

$F_b =\ 24{,}1kN$

Model 3

$T_1 = 0{,}833\ s$

$S_d = 0{,}285\ m/s^2$

$F_b = 20{,}6\ kN$

As described in section 2.5.3 Eurocode 8, the total mass of the building can be computed either above the foundation level or above the top of a rigid basement. For model 1 and model 3, the total mass (m) of the structure is assumed to be above the foundation level. Whereas, for the model 2 the mass of the structure is assumed to be above the top of the basement floor since basement is rigid. Detail mass calculation for each model is attached in Appendix F.

Model 2

$H = 12\ m$

$m = 60480\ kg$

$T_1 = 0{,}484\ s$

$S_d = 0{,}491\ m/s^2$

$F_b = 25{,}3\ kN$

Using building frequency obtained from PLAXIS 2D:

$T_1 = 0{,}714\ s$

$S_d = 0{,}333\ m/s^2$

$F_b = 20{,}1\ kN$

Another simulation is done in FEM-Design program. This program is mostly used by Structural Design Engineers and is based on Finite Element Method. The objective here is to perform a comparison of the structure mass and base shear force with EC8 method. Input for the FEM-Design program, ground type, concrete type, building geometry and member thickness assumptions are all the same.

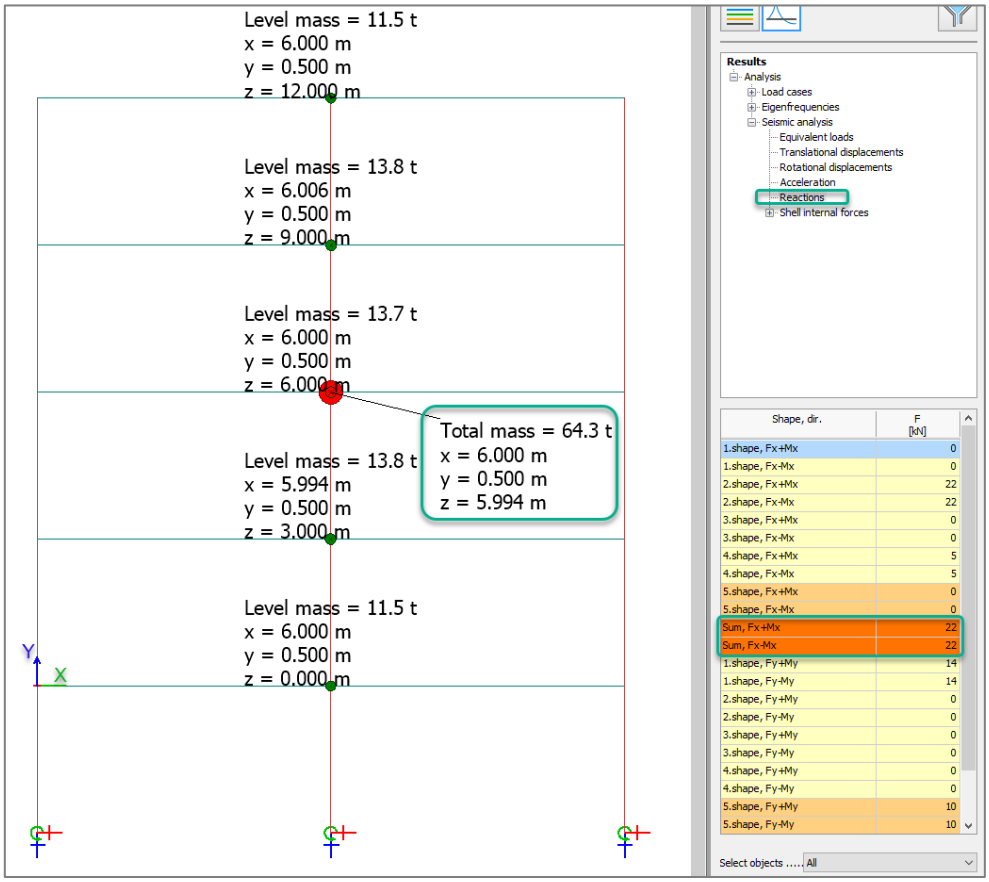

Figure 56: Shear Base Force obtained from FEM-Design

In the Figure 56 mass of the base plates is not included, which is $75{,}6\ kN$. This will give a total mass of $64{,}3 * 10 + 75{,}6 = 718{,}6\ kN$, which is quite close to the one calculated manually $723{,}6\ kN$. For the simplicity of the conversion between ton and kN, unit of 10 is used instead of $9{,}8$. The base shear force obtained from FEM-Design $(22\ kN/m)$ is also very close with the one obtained from the EC8 method $(25{,}6\ kN/m)$.

4.5.2 PLAXIS 2D

In this section, summary of the base shear force results obtained from the PLAXIS 2D will be presented. Additionally, the results from three extra simulations carried out in the PLAXIS 2D are also presented, where in these models, different variables are used. Objective is to study effect of using different parameters on the base shear force. All detailed graphs are shown in Appendix B. Walls are numbered from left to the right. Figure 66

Table 17: Base shear force-Model 1

Wall	Wall 1	Wall 2	Wall 3
Shear Force [kN/m]	22,3	20,0	13,3
Step	896	896	896
Total:	55,6 kN/m		

Table 18: Base shear force -Model 2

Wall	Wall 1	Wall 2	Wall 3
Shear Force [kN/m]	-8,2	5,4	18,1
Step	501	501	501
Total:	15,4 kN/m		

Table 19: Base shear force -Model 3

Wall	Wall 1	Wall 2	Wall 3
Shear Force [kN/m]	5,6	8,4	8,9
Step	2373	2373	2373
Total:	23,0 kN/m		

Another simulation is done for different interface (R_{int}), this is done only for Model 3 as an example. The objective is to study if interface affects base shear force. Summary of shear base force is shown in Table 20.

Table 20: Base shear force, Model 3 for Interface R=0,6

Wall	Wall 1	Wall 2	Wall 3
Shear Force [kN/m]	5,9	8,8	9,3
Step	2085	2085	2085
Total:	24,0 kN/m		

To study if defining Rayleigh damping coefficients affects base shear force, another simulation was done without the Rayleigh damping for Model 1. Table 21

Table 21: Base Shear Force, Model 1 without Rayleigh damping coefficient

Wall	Wall 1	Wall 2	Wall 3
Shear Force [kN/m]	24,4	21,7	11,8
Step	890	890	890
Total:	57,9 kN/m		

PLAXIS suggests choosing a higher value for *Max number of steps stored* in the phase settings. This is discussed in section 2.5.1 Finite Element Method, Figure 19. In PLAXIS 2D, in default this number is set to 1,0. To illustrate if choosing lower number affect base shear force, simulation is carried out for model 3, where *Max number of steps stored* is decreased from 200 to 50. This number should be applied only for the dynamic phase. Results are shown in Table 22.

Table 22: Base Shear Force-Model 3 for Max number of steps stored=50

Wall	Wall 1	Wall 2	Wall 3
Shear Force [kN/m]	3,9	6,2	6,8
Step	1475	1475	1475
Total:	16,9 kN/m		

4.6 Discussion

In this section two topics will be discussed, features in PLAXIS 2D which may influence base shear force and a comparison of base shear force results using PLAXIS 2D and the EC8 method, respectively.

The PLAXIS 2D program offers many features. In order to obtain better results, all settings and parameters which may affect results should be studied and verified. To confirm if the value of interface affects the base shear force, simulation is undertaken for another different (R_{int}) value. The summary of results obtained for $R_{int} = 0{,}6$ shown in Table 20, provides $1\ kN/m$ higher base shear force than the results obtained for $R_{int} = 0{,}8$. Although this difference is not high, this is still a factor which affects base shear force result.

Another simulation is carried out for a model without Rayleigh damping coefficient. Results show $2{,}3\ kN/m$ higher base shear force than those found in the model with Rayleigh damping coefficients. Results are shown in Table 21.

The results from Table 22 are lower values than those found in Table 19. As already discussed in section 2.5.1 Finite Element Method, it is important to choose a higher value for the *Max number of steps stored* for the dynamic phase to include all mode shapes.

The summary of the base shear force presented in Table 23 suggests that model 1 has the highest base shear force, whilst model 2 has the lowest. The best match between EC8 and PLAXIS 2D calculations is for model 3, where the difference between the two methods is only $2{,}6\ kN/m$ compared to model 1, where difference is $30\ kN/m$.

Table 23: Summary Base Shear Force

Model	Model 1	Model 2	Model 3
PLAXIS 2D [kN/m]	55,6	15,4	23,0
EC8 using T1 from PLAXIS [kN/m]	24,1	20,1	20,6
EC 8 [kN/m]	25,6	25,3	25,6

In the EC8 method, the building's natural frequency obtained from PLAXIS 2D is also used in a separate calculation. This has been done due to the fact that the natural frequency T_1 calculated in EC8 was different from that calculated in PLAXIS 2D. The objective is to assess whether building's natural frequency obtained from PLAXIS 2D provides a good match with EC8 method. Table 23

The base shear force for models 1 and 2 obtained from PLAXIS 2D is not close to the one calculated according to the EC8 method, and the difference is relatively high. Especially for model 1, PLAXIS 2D provides two times higher base shear force than EC8 method. For model 2, EC8 results in an approximately 70% higher value than PLAXIS 2D. As demonstrated, EC8 uses a simplified method, assumes the structure is fixed at its base, does not account for rigidity of the structure, or the presence of a basement. Hence, results from EC8 are either over or underestimate.

The difference in results between model 1 and model 2 are quite high in PLAXIS 2D. This could be due to different possible reasons. The overburden pressure is not symmetric for model 1. As a result, in model 1, stresses are higher at the right wall (Wall 3) than the left wall (Wall 1). Due to this fact, the left wall is free to move, whereas the right wall is supported by the backfilling soil. A variation of the base shear force for each wall can be clearly seen in Table 17. Model 1 can be assumed to have a as semi-rigid basement, while model 2 has a rigid basement. This also suggests why the base shear force difference between these two models is high.

In this report, the fundamental period of vibration of the building T_1 is computed according to the equation (2.58). This is a simplified approach and gives an approximate value, which does not account for the building's stiffness. EC8 suggests three different approaches for computing of the fundamental period of vibration of the building T_1. Equations are discussed in section 2.5.3 Eurocode 8. As an example, equation (2.60) is used to compute T_1 for model 1.

Table 24: Base shear force-Alternative method for computation of fundamental period-Model 1

Description	$T_1[s]$	$S_d\ [m/s^2]$	$F_b\ [kN/m]$
Alternative 1 - T_1 , Eq (2.58)	0,572	0,416	25,6
Alternative 2 - T_1 , Eq (2.60)	0,525	0,452	27,8

The alternative 2 results shown in Table 24 are better than those from the alternative 1. The reason is that equation (2.60) considers building's stiffness. The derivation of equation (2.60) is illustrated in Appendix F, equation (8.1). According to "Dimensjonering for JORDSKJELV" (Øystein Løset, et al 2010), calculation of the fundamental period T_1 based on the Rayleigh method (equation (2.61)) provides better results than the two other alternatives. This is because the Rayleigh method considers lateral deformation of each floor, which means, the method also takes into consideration the building's stiffness more precisly than equation (2.60). Alternative 2, equation (2.60) also considers stiffness of the building, but presents a more simplified method than the Rayleigh method. Since the Rayleigh method requires an iterative process and is beyond the scope of this report, no further calculations have been performed according to this method.

5 CONCLUSION

The summary of the comparisons between PLAXIS 2D, DEEPSOIL and EERA presented in Table 15, suggests that PLAXIS 2D has provided the highest PSA value, and values obtained from DEEPSOIL and EERA are relatively close. Acceleration results suggest that there is a good agreement between PLAXIS 2D, and DEEPSOIL, and that EERA provided a highest ground acceleration peak than other two.

The results in Table 15 show that by defining the Rayleigh damping coefficients, peak ground acceleration decreases. This gives a better match with DEEPSOIL and EERA compared to the modelling without defining Rayleigh damping coefficients.

The simulation carried out for the *compliant base* boundary conditions did not match well with the input signal motion at the base of the model. Similarly, the effect of the dynamic time intervals has shown that defined *dynamic time interval* corresponds with an input signal motion interval.

The analysis method used in PLAXIS 2D (Nonlinear) is not the same as in DEEPSOIL and EERA (Equivalent Linear). However, EL analysis is a good approximation to nonlinear analysis. Although, results are not conclusively close, nevertheless, a good agreement of the results is obtained in PLAXIS, DEEPSOIL and EERA. Based on the findings, it can be concluded that selected material model in PLAXIS 2D, calculated material stiffness parameters, defined Rayleigh damping coefficients, selected boundary conditions, and dynamic time interval provided good match with DEEPSOIL and EERA. It can be said that PLAXIS 2D model is calibrated with DEEPSOIL and EERA. Therefore, the same material properties and defined settings are used for further analysis in section 4.3 Part 2.

In 4.3 Part 2, three different models are analyzed for the dynamic analysis in PLAXIS 2D and EC8, where model 1 presents a structure with earth pressure on one side, model 2 with a basement and earth pressure along both parallel basement walls, and model 3 on grade without a basement.

The findings show that the EC8 method provides better results for the structure on grade without a basement, model 3. When the structure has a rigid basement, the EC8 method is on the safe side and provides somewhat higher values than FEM program, PLAXIS 2D. Whereas, when earth pressure is at one of the longitudinal basement walls, the EC8 method provides lower base shear force than PLAXIS 2D.

According to the section 4.3.3 *Methods of analysis* in EC8, seismic design may be determined based on linear-elastic behavior of the structure. Depending on the structure characteristics, linear-elastic analysis either a *Lateral force method analysis* or a *Modal response spectrum analysis*, which is applicable to all type of buildings can be performed.

All three models analyzed in this report satisfies criteria according to the section 4.2.3.3 *Criteria for regularity in elevation*, and section 4.3.3.2.1(2) in EC8. Thus, the *Lateral force method analysis* has been used. This method is a simplified approach, where response spectrum considers the building's fundamental or first period is based on equivalent static analysis. Computing the fundamental period of the building in EC8 is based on empirical calculations.

Modal response spectrum analysis which is widely used by FEM analysis programs considers several modes. Therefore, a *Modal response spectrum analysis* will provide more reliable results than the *Lateral force method*. In *Lateral force method analysis*, total mass of the structure is used in the first mode shape as shown in Figure 25, and assumes that the structure is fixed at its base, this may result in higher or lower base shear force calculations. As shown, EC8 provided higher value for model 2, and lower for model 1 compare to FEM program.

Another factor which should be considered in EC8 method is, the value for the behavior factor q. In this report, calculations are carried out for $q = 1{,}5$. Another simulation is done for model 2 for different values of the behavior factor q. As shown in Table 25, lower q value provides higher base shear force, while higher q value provides lower base shear force.

Table 25: Base shear force for different behavior factor q, Model 2

PLAXIS 2D [kN/m]	EC 8 [kN/m]		
	$q = 1{,}0$	$q = 1{,}5$	$q = 2{,}0$
15,4	37,9	25,3	18,9

Based on the results for the selected time series, Kobe, it can be said that the *Lateral force method* can be used for symmetrical systems with regular elevation, where contribution from mode shape with rotation is little. Results from PLAXIS 2D and EC8 suggest that the closes match is obtained for model 3. It can be said that the EC8 method is not conservative when the structure is on grade and without a basement. However, when a basement is present and soil pressure is at both parallel basement walls, the EC8 method provides higher values than FEM program, and indeed EC8 is on the safe side. For model 1, with a semi-rigid basement where soil pressure is at one of the parallel basement walls, the EC8 method provides lower base shear force than PLAXIS 2D. Hence, it can be concluded that for case of model 1 and model 2, especially in case of asymmetric earth pressure, FEM analysis should be carried out to obtain more accurate results.

6 RECOMMENDATION FOR FURTHER WORK

In this report all simulations are done for one soil layer, simulations can be performed for several soil layers and possibly for soil type S_1 or S_2.

Further earthquake analysis can be carried out where the structure is partially on the rock and partially on the soil.

Consider additional *Time Series* and carry out analysis.

This Thesis used only the *Lateral force method of analysis* according to section 4.3.3.2 in the EC8, other analysis methods such as *Model response spectrum analysis* according to 4.3.3.3 in the EC8 can be carried out to assess comparison with *Lateral force method analysis*.

As discussed, computing of the fundamental period of vibration of the building T_1 according to section 4.3.3.2.2(5) in EC8 provided better base shear force, alternative method for computing of fundamental period of vibration T_1 according to section 4.3.3.2.2(3) in EC8 can be used in the further analysis.

The calculation of T_1 proposed by the EC8 is based on the assumption that the structure is fixed at its base (zero displacements and rotations), in other words, that the structure is supported by infinitely rigid soil springs. In reality, the soil stiffness is not infinite and a more realistic approach to account for this is to use equivalent natural frequency or period of the structure (Kramer, 1996). Equation (7.78) in Kramer, 1996 is based on *Soil-Structure Interaction* and it considers translation and rotation springs. This approach will result in a more realistic evaluation of the base shear force.

7 BIBLIOGRAPHY

A. Laera, R. B. (2017, August 4th). *Ground response analysis*. (Ground response analysis) Retrieved March 27th, 2021, from PLAXIS 2D: https://communities.bentley.com/products/geotech-analysis/w/plaxis-soilvision-wiki/46049/ground-response-analysis

Bentely-01. (2013, January 3rd). *Ground response analysis in case of linear soil*. Retrieved March 27th, 2021, from PLAXIS: https://communities.bentley.com/products/geotech-analysis/w/plaxis-soilvision-wiki/45532/ground-response-analysis-in-case-of-linear-soil

Bentley-02. (2012, April 16th). *Time Step Used in Dynamic Calculation*. Retrieved March 27th, 2021, from PLAXIS: https://communities.bentley.com/products/geotech-analysis/w/plaxis-soilvision-wiki/45936/time-step-used-in-dynamic-calculation

Bentley-03. (2013, January 4th). *Free vibration analysis of a dam*. Retrieved March 27th, 2021, from PLAXIS: https://communities.bentley.com/products/geotech-analysis/w/plaxis-soilvision-wiki/45533/free-vibration-analysis-of-a-dam

Bentley-04. (2014, July 23rd). *Fixed and Compliant base: what input motion is required?* Retrieved March 27th, 2021, from PLAXIS: https://communities.bentley.com/products/geotech-analysis/w/plaxis-soilvision-wiki/45985/fixed-and-compliant-base-what-input-motion-is-required

Bentley-05. (2014, July 23rd). *Compliant base and free field boundaries: check on input signal*. Retrieved March 27th, 2021, from PLAXIS: https://communities.bentley.com/products/geotech-analysis/w/plaxis-soilvision-wiki/45989/compliant-base-and-free-field-boundaries-check-on-input-signal

Bentley-06. (2014, July 23rd). *On the use of dynamic boundary conditions*. Retrieved March 27th, 2021, from PLAXIS: https://communities.bentley.com/products/geotech-analysis/w/plaxis-soilvision-wiki/45984/on-the-use-of-dynamic-boundary-conditions

Bentley-07. (2016, February 12th). *How to create a model for ground response analysis in PLAXIS 2D*. Retrieved March 27th, 2021, from PLAXIS: https://communities.bentley.com/products/geotech-analysis/w/plaxis-soilvision-wiki/46133/how-to-create-a-model-for-ground-response-analysis-in-plaxis-2d

Bentley-08. (2020, March 5th). *Manuals*. Retrieved March 27th, 2021, from PLAXIS: https://communities.bentley.com/products/geotech-analysis/w/plaxis-soilvision-wiki/46137/manuals---plaxis

Bentley-09. (2020, September 18th). *Dynamics Verifications*. Retrieved March 27th, 2021, from PLAXIS: https://communities.bentley.com/products/geotech-analysis/w/plaxis-soilvision-wiki/45396/verifications---plaxis

Bentley-10. (2020, December 1st). *Reference Manual.pdf*. Retrieved from PLAXIS 2D: https://communities.bentley.com/products/geotech-analysis/w/plaxis-soilvision-wiki/46137/manuals---plaxis

Bentley-11. (2021). PLAXIS 2D. *Version 20.04.00.790*.

Bentley-12. (2021, January 25th). *Material Models Manual.pdf*. Retrieved from Manuals-PLAXIS: https://communities.bentley.com/products/geotech-analysis/w/plaxis-soilvision-wiki/46137/manuals---plaxis

Bentley-13. (2021, June 1st). *Free vibration and earthquake analysis of a building*. Retrieved from PLAXIS: https://communities.bentley.com/products/geotech-analysis/w/plaxis-soilvision-wiki/45568/plaxis-2d-tutorial-16-free-vibration-and-earthquake-analysis-of-a-building

CEN, N. (2004). Eurocode 8: Design of structures for earthquake resistance NS-EN 1998-1:2004+A1:2013+NA:2014. European Committee for Normalization, Brussels.

K.Chopra, A. (2012). *Dynamics of Structures: Theory and Applications to Earthquake Engineering (Fourth Edition)*. California: Prentice Hall.

Kramer, S. L. (1996). *Geotechnical Earthquake Engineering*. Prentice Hall.

L.Humar, J. (2012). *Dynamics of Structures (Third Edition)*. Carleton University, Ottawa: CRC Press-Taylor & Francis Group.

L.Kramer, S. (2019). Advanced Analysis. In *Geodynamics, PhD Course BA8305, Lecture notes Part 2 & 3*. Trondheim: NTNU.

L.Kramer, S. (2019). One-Dimensiontal Site Response Analysis. In *Geodynamics, PhD Course BA8305, Lecture notes Part 2 & 3*. Trondheim: NTNU.

Nordal, S. (2019). *Geodynamics, PhD Course BA8305, Lecture notes Part 1*. Trondheim: NTNU.

PLAXIS. (2019, 12 24). *Bentley/Plaxis*. Retrieved from Fixed and Compliant base: what input motion is required?: https://communities.bentley.com/products/geotech-analysis/w/plaxis-soilvision-wiki/45985/fixed-and-compliant-base-what-input-motion-is-required

SEiSMOSOFT. (2021). SeismoMatch. https://seismosoft.com/products/seismomatch/.

SRBULOV, M. (2008). *Geotechnical Earthquake Engineering, Simplified Analysis with Case Studies and Examples*. Springer.

StruSoft. (2019). FEM-Design, Structural Analysis and Design Software. StruSoft.

University of Southern California, Department of Civil Engineering. (2000, August). *Equivalent-linear Earthquake site Response Analyses of Layered Soil Deposits*. Retrieved from EERAManual: http://www.ce.memphis.edu/7137/PDFs/EERA2/EERAManual2.pdf

Wikipedia-1. (2021, May 6th). *Seismic wave*. Retrieved from Wikipedia: https://en.wikipedia.org/wiki/Seismic_wave

Wikipedia-2. (2021, April 13th). *Geodynamics*. Retrieved from Wikipedia: https://en.wikipedia.org/wiki/Geodynamics

Øystein Løset, Max Milan Loo, Åse Lyslo Døssland, Morten Gjestvang, Amir M.Kaynia, Christian Bråten. (2010). *Dimensjonering for JORDSKJELV*. Rådgivende Ingeniørers Forening (RIF).

8 APPENDICES

8.1 Appendix A

PLAXIS Input

Table 26: Material parameter Hssmall model

Depth z (m)	$\sigma_v = \gamma * z$ [kN/m²]	$u = \gamma_w * z$ [kN/m²]	$\sigma_v' = \sigma_v - u$ [kN/m²]	$\sigma_h' = \sigma_v' * K_0$ [kN/m²]	G_0 factor	G_0^{ref} [kN/m²]	G_0 [kN/m²]	$Vs = \sqrt{G/\rho}$ [m/s]
0	0	0	0	0,00	0,314	66 450	20885,7	101,2
1	20	0	20	13,82	0,423	66 450	28100,3	117,4
2	40	0	40	27,64	0,525	66 450	34873,6	130,8
3	60	0	60	41,46	0,622	66 450	41330,7	142,4
4	80	0	80	55,28	0,715	66 450	47543,7	152,7
5	100	0	100	69,10	0,806	66 450	53559,5	162,1
6	120	10	110	76,01	0,850	66 450	56503,9	166,5
7	140	20	120	82,92	0,894	66 450	59410,4	170,7
8	160	30	130	89,83	0,937	66 450	62281,8	174,8
9	180	40	140	96,74	0,980	66 450	65120,5	178,7
10	200	50	150	103,65	1,022	66 450	67928,6	182,5
11	220	60	160	110,56	1,064	66 450	70707,9	186,2
12	240	70	170	117,47	1,105	66 450	73460,2	189,8
13	260	80	180	124,38	1,147	66 450	76186,9	193,3
14	280	90	190	131,29	1,187	66 450	78889,4	196,7
15	300	100	200	138,20	1,228	66 450	81569,0	200,0

$\gamma = 20\ kN/m^3$
$c' = 10\ kN/m^2$
$\varphi' = 18°$
$K_0 = 1 - sin\varphi = 0{,}691$
$p_{ref} = 100\ kN/m^2$
$m = 0{,}8$
$GW = 5{,}0\ m$
$\rho = \frac{\gamma}{g} = 2038{,}7\ kN/m^3$
$\nu = 0{,}2$

Recommendations on Stiffness parameters

In section 3 METHODOLOGY, computation of stiffness parameters is discussed.

$$G_0^{ref} = 66450\ kN/m^2$$

$$G_u^{ref} = \frac{G_0^{ref}}{7{,}8} = 8519\ kN/m^2$$

$$E_{ur}^{ref} = G_u^{ref}\ (2 * (1 + v)) = 20446\ kN/m^2 \qquad \text{Refers to equation (3.1)}$$

$$E_{50}^{ref} = \frac{E_{ur}^{ref}}{3} = 6815\ kN/m^2$$

$$E_{oed}^{ref} = E_{50}^{ref} = 6815\ kN/m^2$$

Dynamic time interval

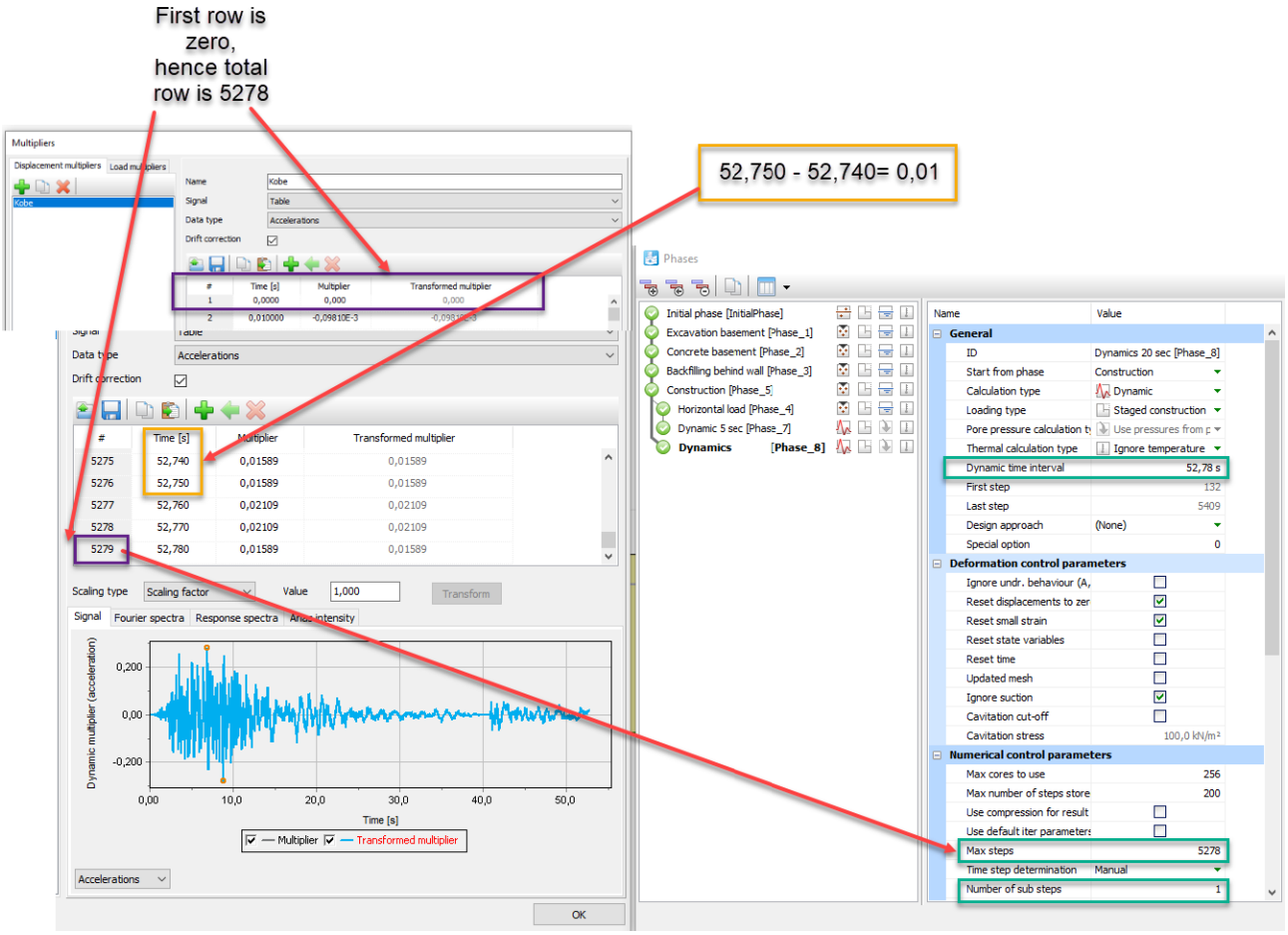

Figure 57: Dynamic time interval

According to equation (2.29), chosen values for δt should correspond with input signal motion interval

$$\delta t = \frac{\Delta t}{n * m} = \frac{52{,}78}{5278 * 1} = 0{,}01$$

Rayleigh Damping Coefficient

- Calculate fundamental frequency, use equation (2.28)
- Input signal motion, define node at the bottom of the model and run analysis in PLAXIS 2D
- From Curve Manager, plot Fourier spectrum graph from the node selected at the bottom of the model
- Find maximum frequency from the graph,f_2
- Find the ratio of $\frac{f_2}{f_1}$ and select closest odd number for f_2
- Keep ξ =1% both for Target 1 and Target 2
- Input values for f_1 and f_2 in PLAXIS 2D

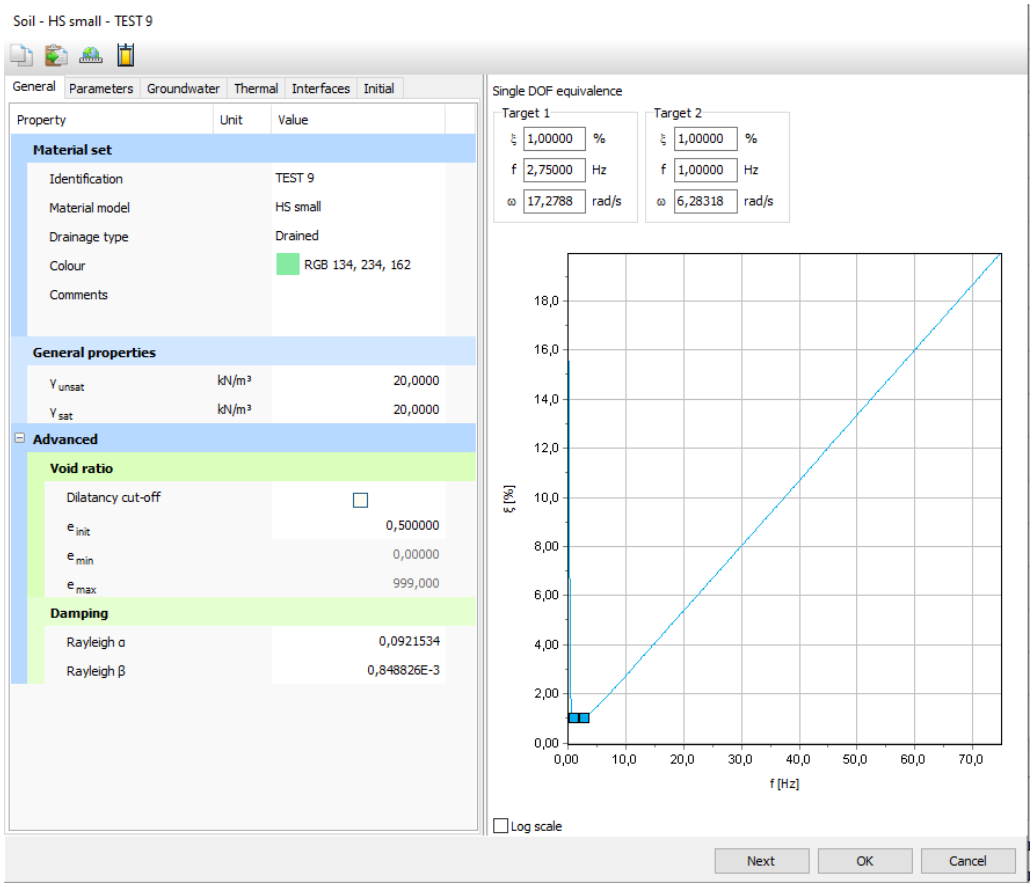

Figure 58: Rayleigh damping coefficients

$$f_1 = \frac{V_{s,average}}{4 * H} = \frac{165{,}4}{4 * 15} = 2{,}75\ Hz$$

$$\frac{f_2}{f_1} = \frac{0{,}79}{2{,}75} = 0{,}28 \rightarrow f_2 = 1\ Hz$$

8.2 Appendix B

PLAXIS Output

Base Shear Force

Figure 59: Base Shear Force, Model 1

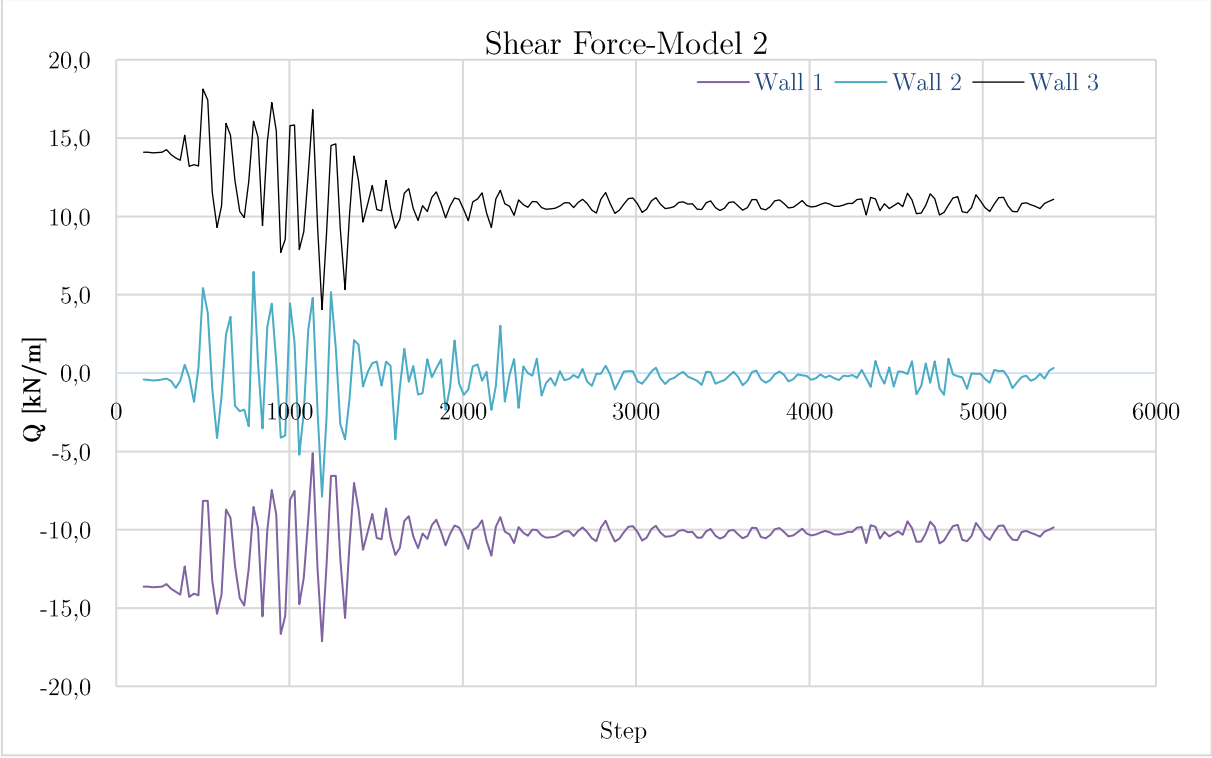

Figure 60: Base Shear Force, Model 2

Figure 61: Base Shear Force, Model 3

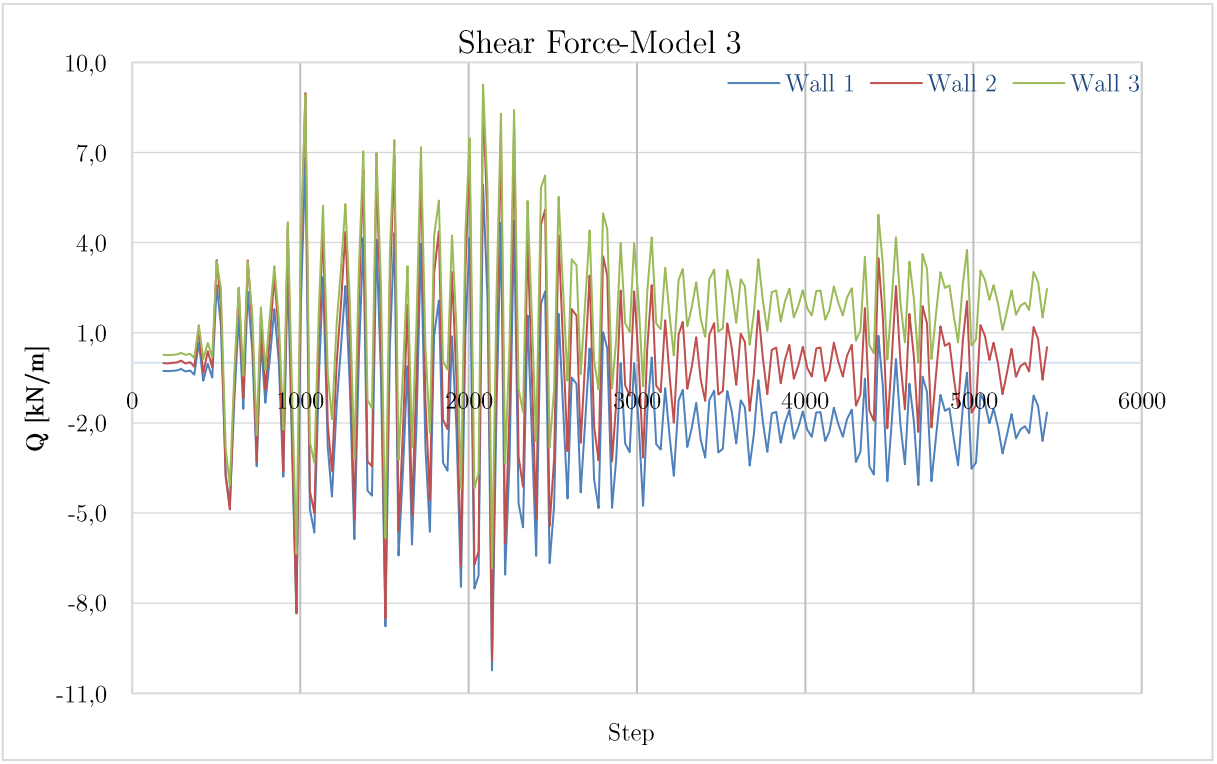

Figure 62: Base Shear Force-Model 3 for interface R=0,6

Table 27: Summary Base Shear Force-Model 3 for interface R=0,6

Wall	Wall 1	Wall 2	Wall 3
Shear Force [kN/m]	5,9	8,8	9,3
Step	2085	2085	2085

Total: 24,0 kN/m

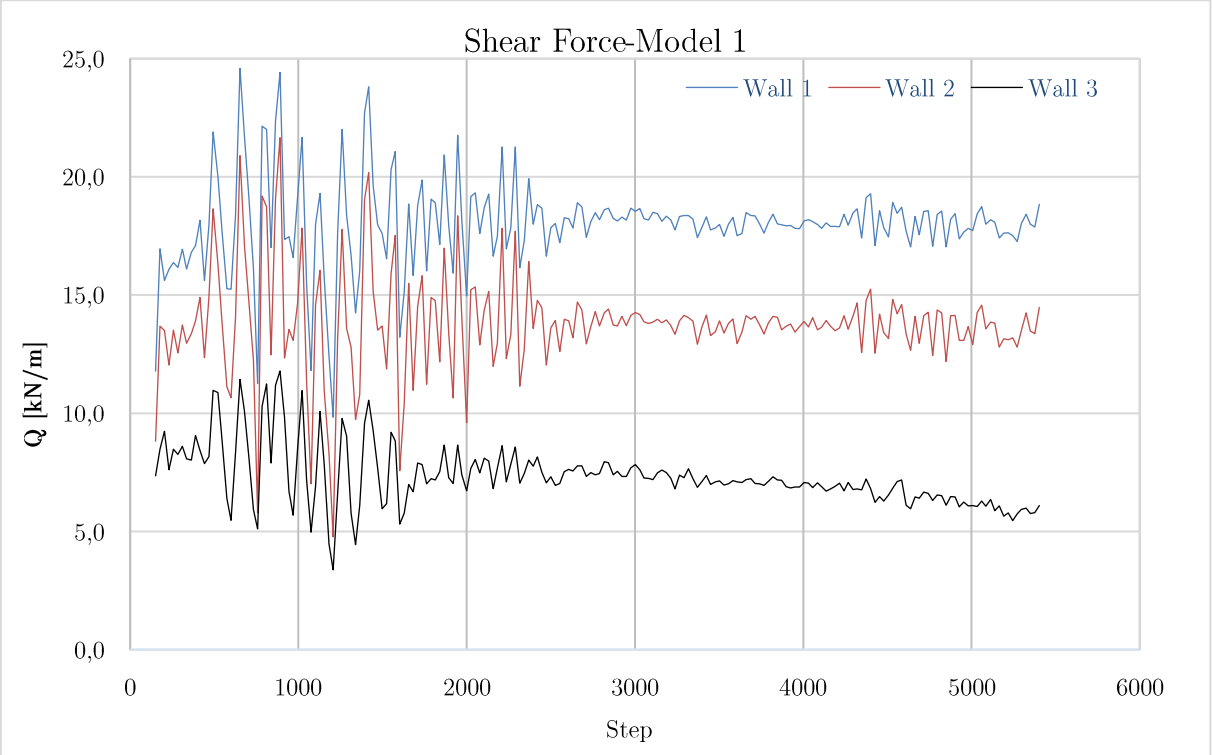

Figure 63: Base Shear Force, Model 1 without Rayleigh damping

Table 28: Summary Base Shear Force, Model 1 without Rayleigh damping

Wall	Wall 1	Wall 2	Wall 3
Shear Force [kN/m]	24,4	21,7	11,8
Step	890	890	890

Total: 57,9 kN/m

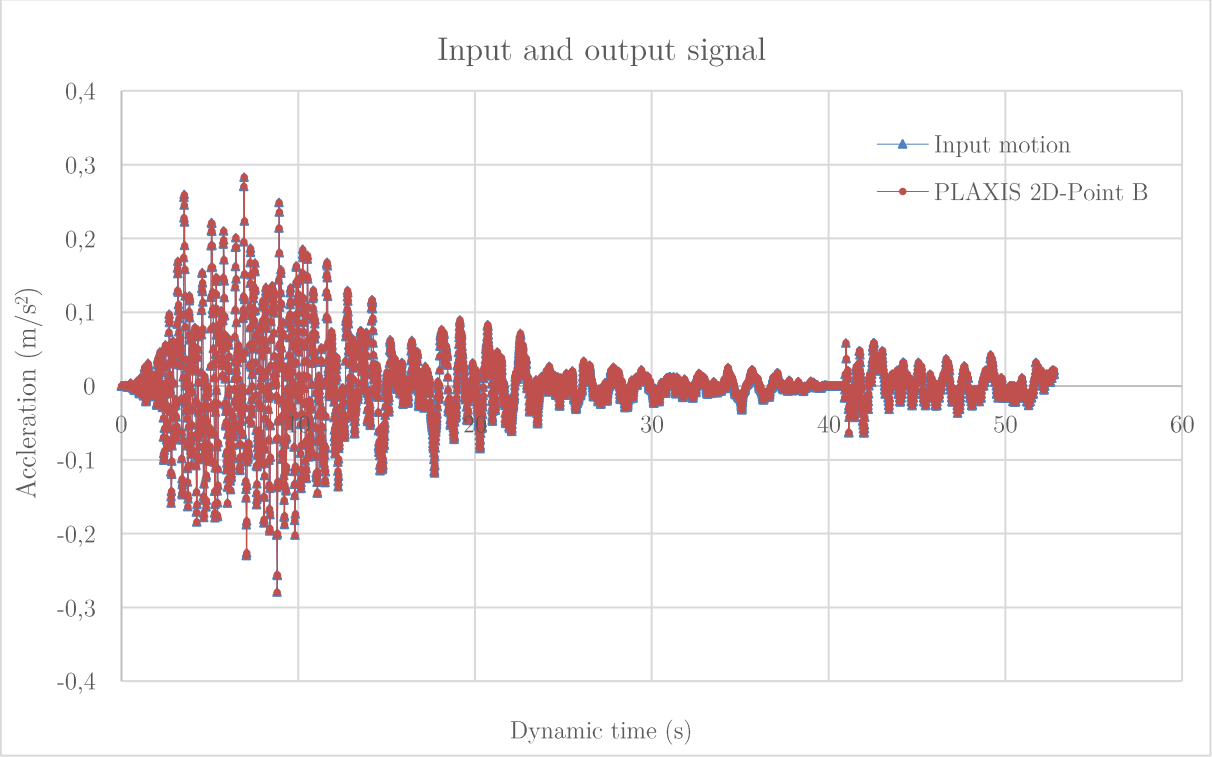

Figure 64: Input and output signal at point B-Part 1

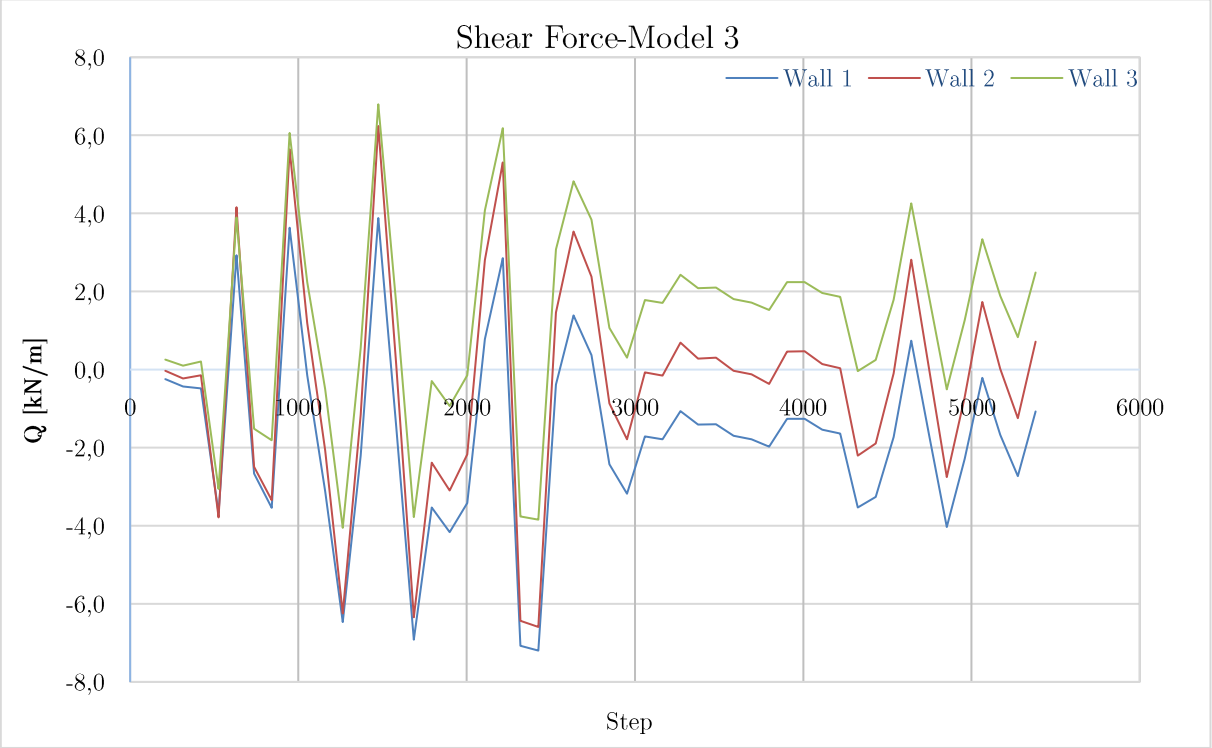

Figure 65: Base Shear Force-Model 3 for Max number of steps store=50

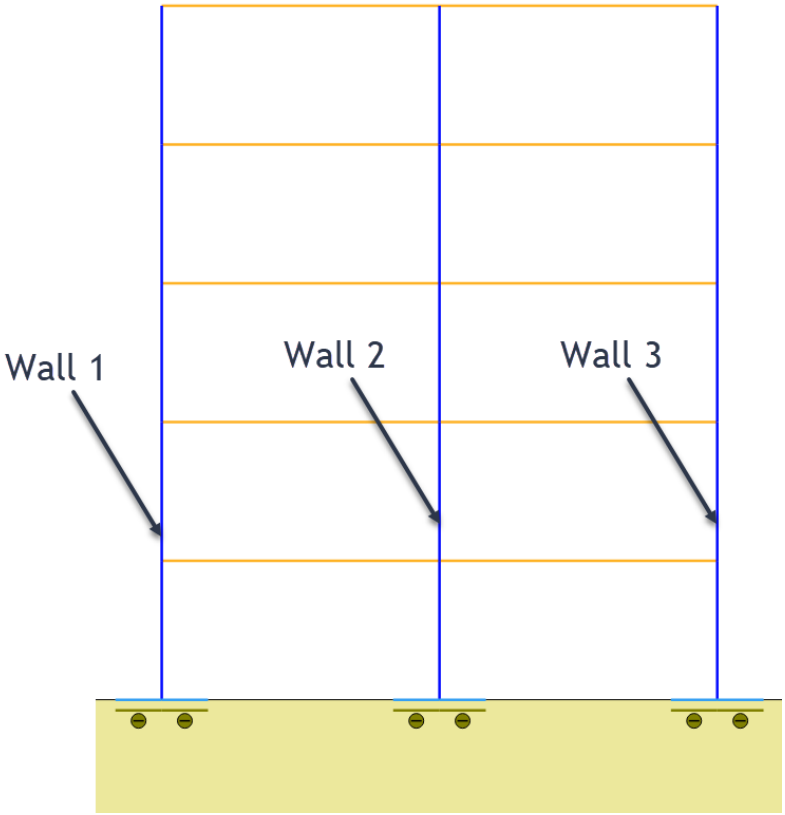

Figure 66: Wall numbering

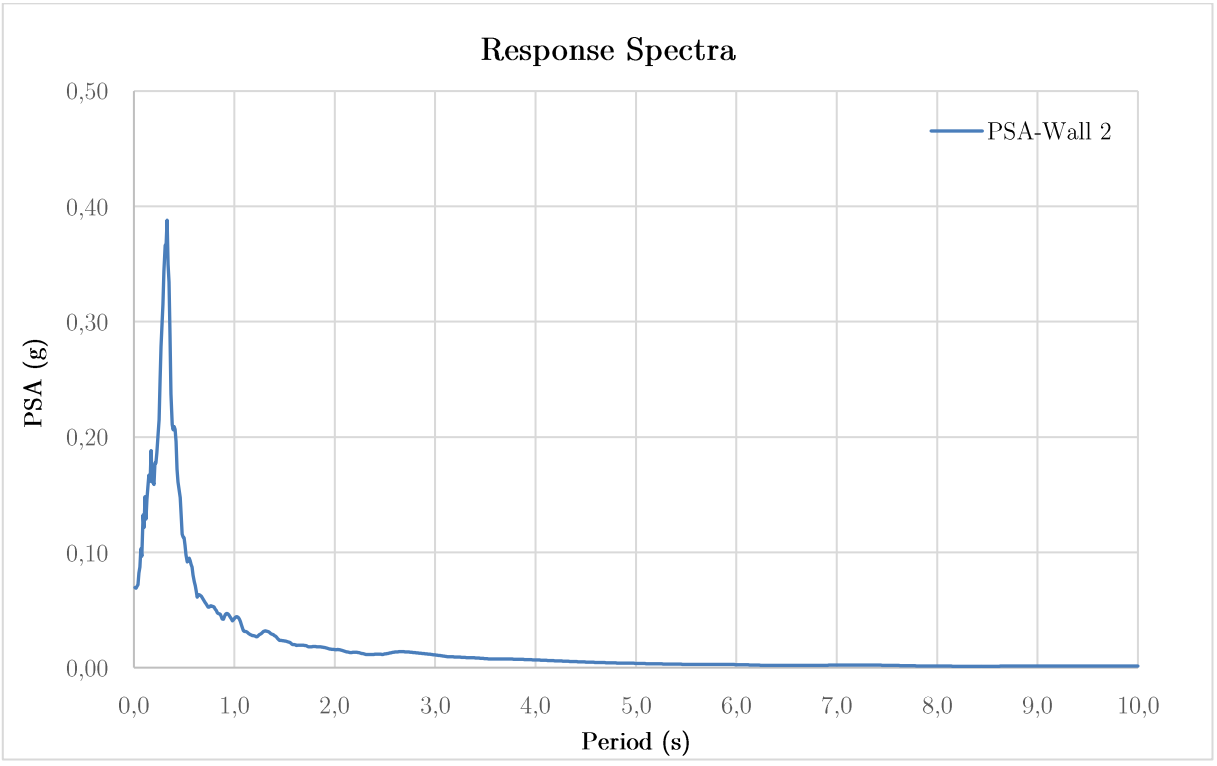

Figure 67: PSA Model 1

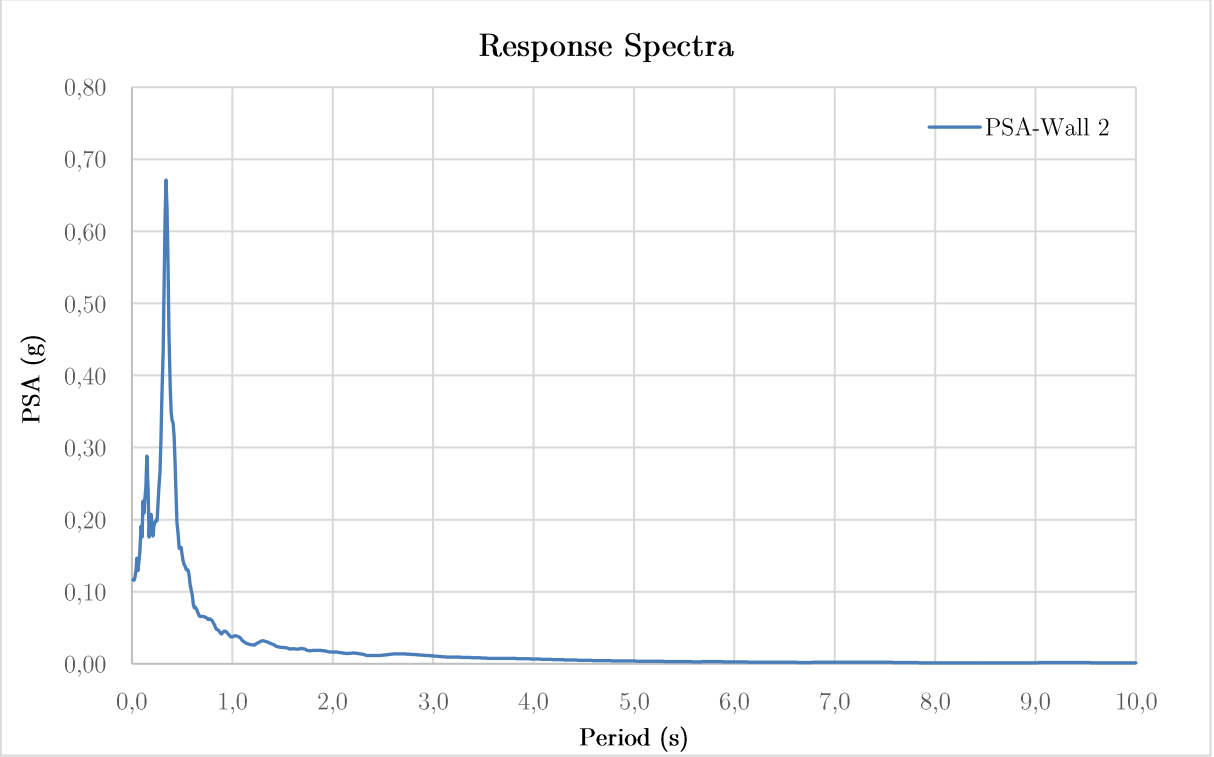

Figure 68: PSA Model 2

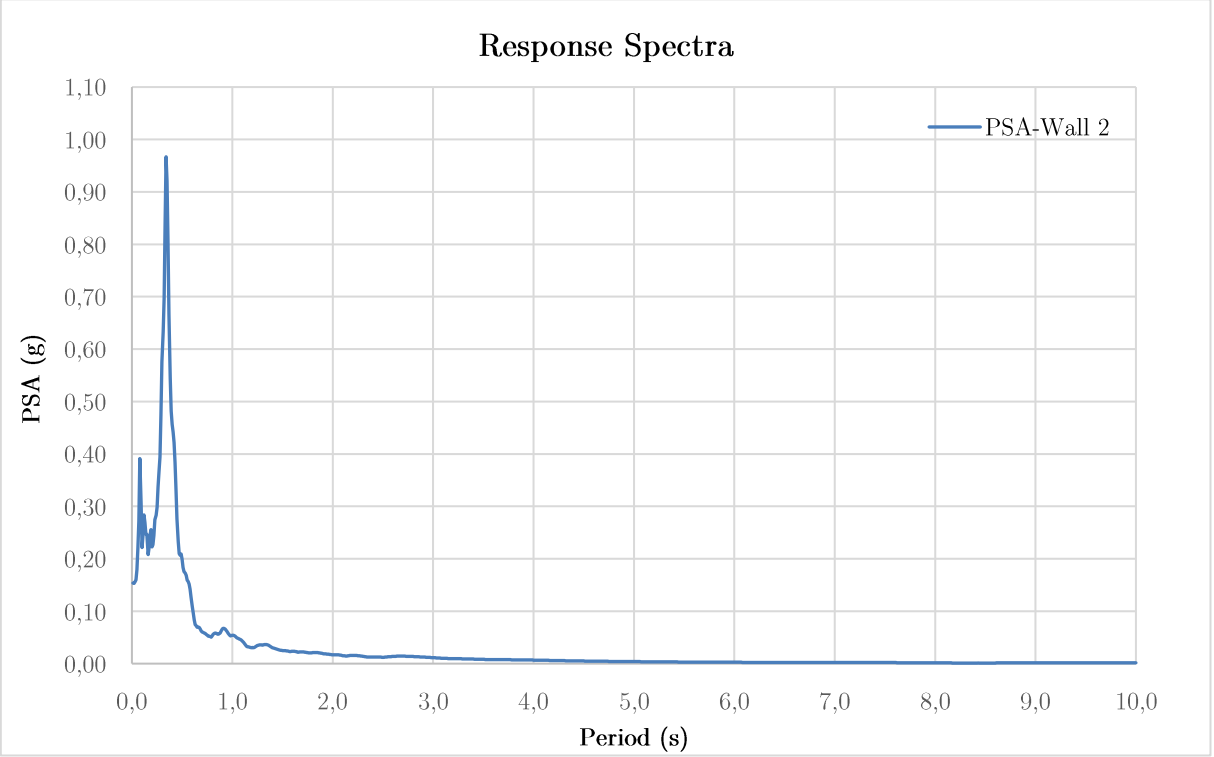

Figure 69: PSA Model 3

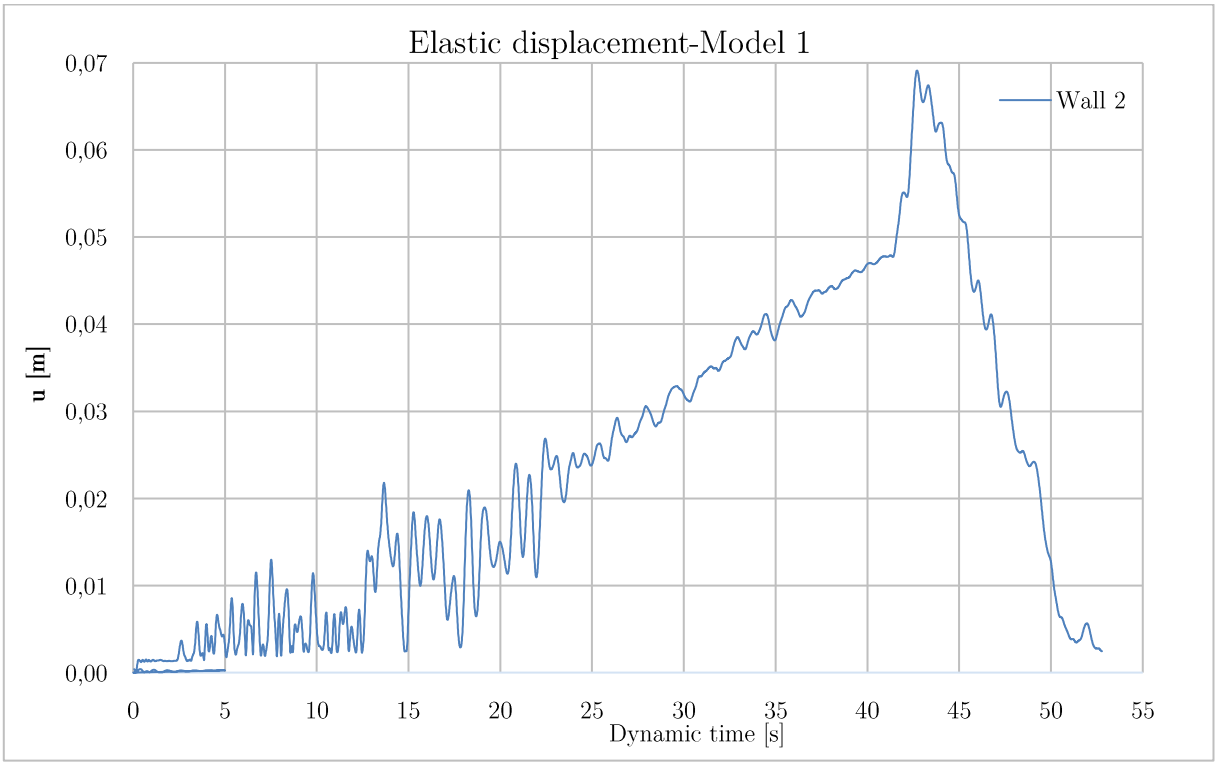

Figure 70: Displacement at top of Model 1

8.3 Appendix C

SeismoMatch

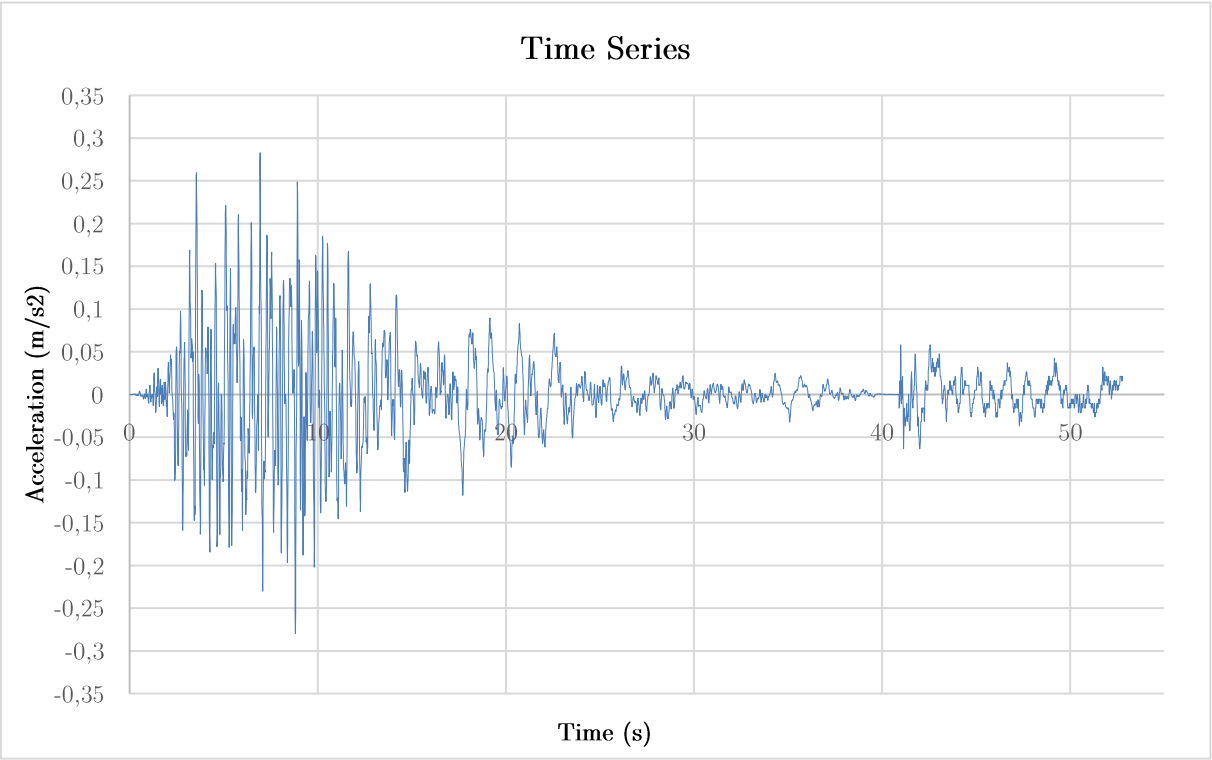

Figure 71: Output Time Series at point B, SeismoMatch

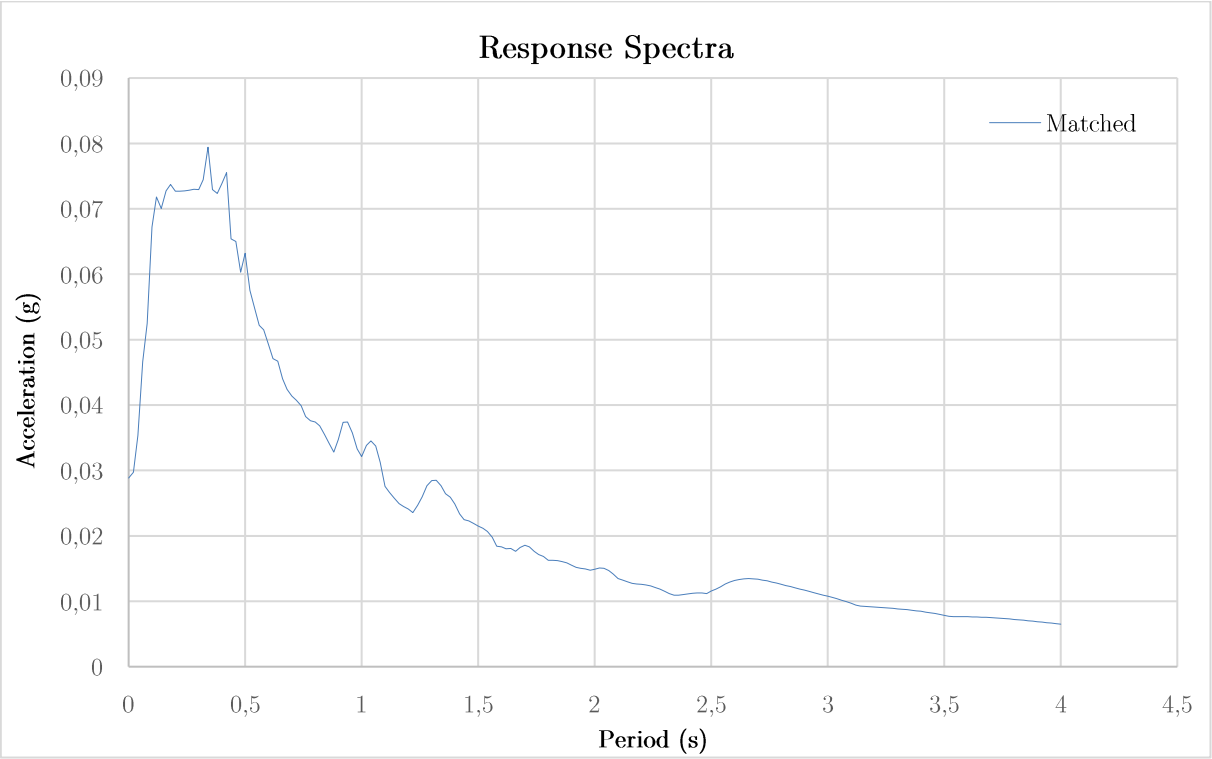

Figure 72: Output Response Spectra at point B, SeismoMatch

8.4 Appendix D

DEEPSOIL

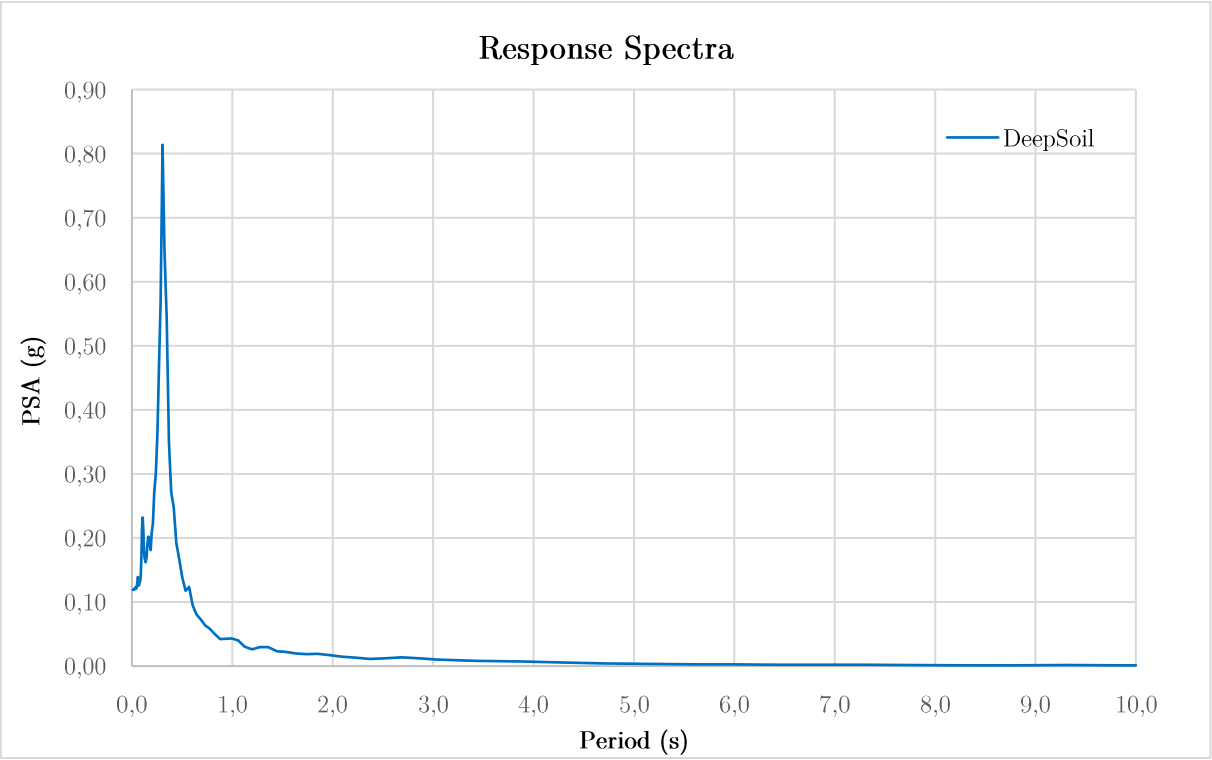

Figure 73: PSA at point A, DEEPSOIL

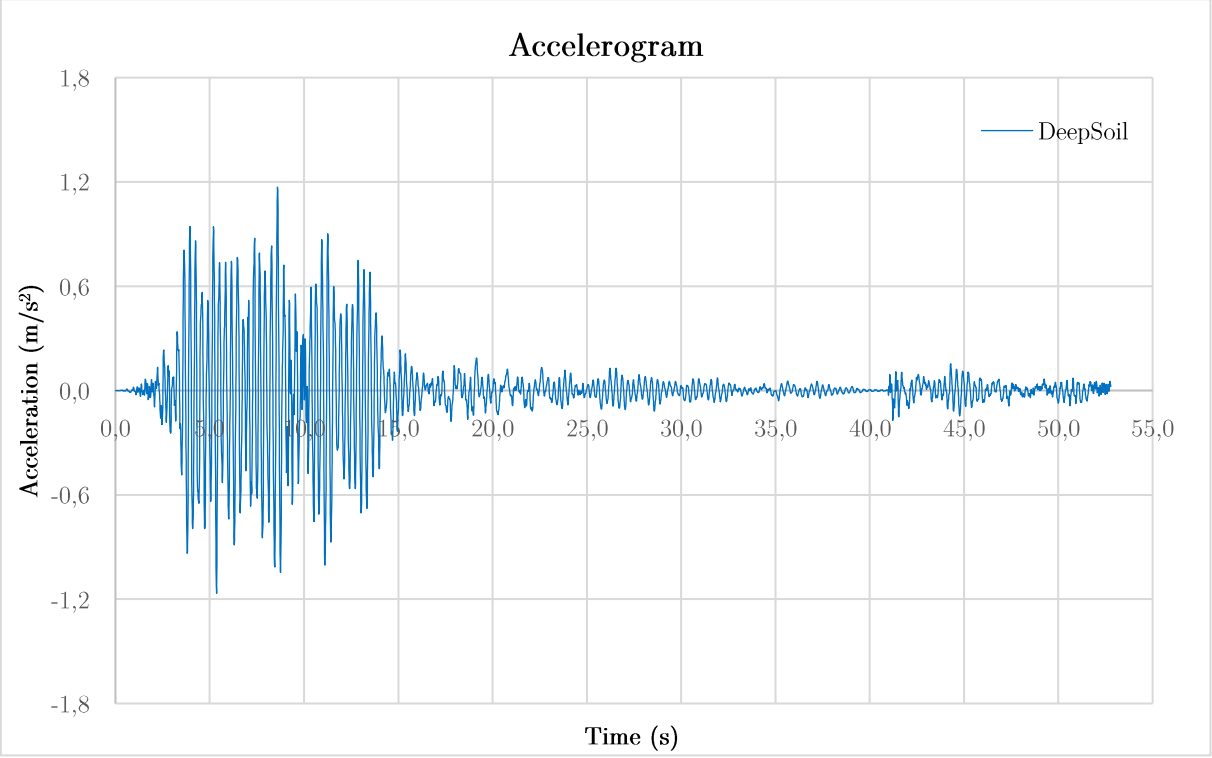

Figure 74: Acceleration at point A, DEEPSOIL

8.5 Appendix E

EERA

	A	B	C	D
1	*Loma Prieta Earthquake:Diamond Height*			
2	Time step ΔT (sec) =	0,01		
3	Desired maximum acceleration (g) =			
4	Maximum frequency cut-off (Hz) =	25		
5	Use frequency cut-off in calculation ?	No		
6	Number of points for FFT =	5279		
7	Import input motion from external file ?	No		
8	Name of input file =	Kobe		
9	Total number of values read =	5279		
10	Peak Acceleration in input file (g) =	0,0288		
11	Time of peak acceleration (sec) =	6,950		
12	Mean Square Frequency (Hz) =	3,538		
13	Peak acceleration after filtering (g) =	0,029		
14	Time (sec)	Input Acceleration (g)	Scaled Acceleration (g)	Filtered Acceleration (g)
15	0,000	0	0,00	0,00
16	0,010	-1E-05	0,00	0,00
17	0,020	-1E-05	0,00	0,00
18	0,030	-1E-05	0,00	0,00
19	0,040	-1E-05	0,00	0,00
20	0,050	-1E-05	0,00	0,00
21	0,060	-1E-05	0,00	0,00
22	0,070	-1E-05	0,00	0,00
23	0,080	0	0,00	0,00
24	0,090	0	0,00	0,00
25	0,100	-1E-05	0,00	0,00
26	0,110	-1E-05	0,00	0,00
27	0,120	-2E-05	0,00	0,00
28	0,130	-2E-05	0,00	0,00
29	0,140	-2E-05	0,00	0,00
30	0,150	-2E-05	0,00	0,00
31	0,160	-2E-05	0,00	0,00
32	0,170	-2E-05	0,00	0,00
33	0,180	-2E-05	0,00	0,00
34	0,190	0	0,00	0,00
35	0,200	2E-05	0,00	0,00
36	0,210	3E-05	0,00	0,00
37	0,220	3E-05	0,00	0,00
38	0,230	4E-05	0,00	0,00
39	0,240	5E-05	0,00	0,00
40	0,250	6E-05	0,00	0,00
41	0,260	5E-05	0,00	0,00

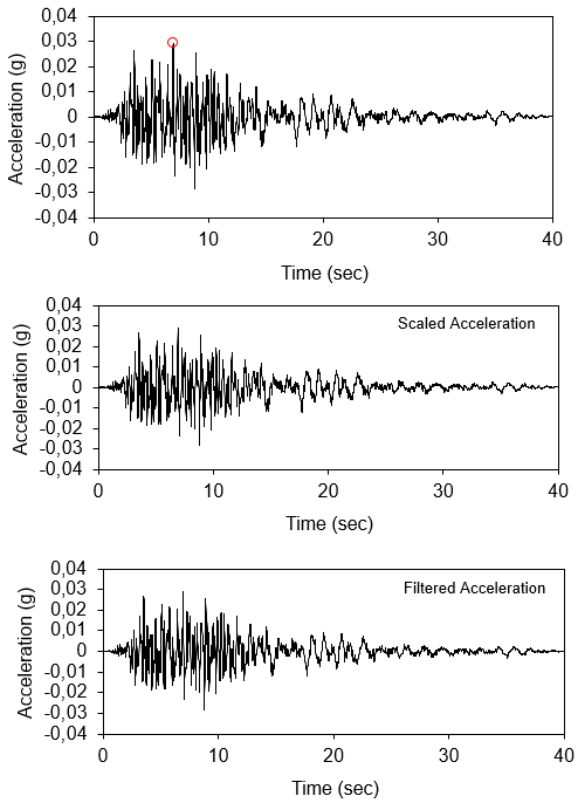

Figure 75: Earthquake tab sheet, (EERA)

	A	B	C	D	E	F	G	H	I	J	K	L	M
1													
2				Fundamental period (s) = 0,37									
3				Average shear wave velocity (m/sec) = 163,05									
4				Total number of sublayers = 16									
5		Layer Number	Soil Material Type	Number of sublayers in layer	Thickness of layer (m)	Maximum shear modulus G_{max} (MPa)	Initial critical damping ratio (%)	Total unit weight (kN/m^3)	Shear wave velocity (m/sec)	Location and type of earthquake input motion	Location of water table	Depth at middle of layer (m)	Vertical effective stress (kPa)
6	Surface	1	1		1,0	20,88		20,00	*101,2*			0,5	10,00
7		2	1		1,0	28,10		20,00	*117,4*			1,5	30,00
8		3	1		1,0	34,88		20,00	*130,8*			2,5	50,00
9		4	1		1,0	41,34		20,00	*142,4*			3,5	70,00
10		5	1		1,0	47,54		20,00	*152,7*		*W*	4,5	90,00
11		6	1		1,0	53,57		20,00	*162,1*			5,5	105,10
12		7	1		1,0	56,52		20,00	*166,5*			6,5	115,29
13		8	1		1,0	59,41		20,00	*170,7*			7,5	125,48
14		9	1		1,0	62,29		20,00	*174,8*			8,5	135,67
15		10	1		1,0	65,10		20,00	*178,7*			9,5	145,86
16		11	1		1,0	67,90		20,00	*182,5*			10,5	156,05
17		12	1		1,0	70,68		20,00	*186,2*			11,5	166,24
18		13	1		1,0	73,44		20,00	*189,8*			12,5	176,43
19		14	1		1,0	76,18		20,00	*193,3*			13,5	186,62
20		15	1		1,0	78,88		20,00	*196,7*			14,5	196,81
21	Bedrock	16	0			101,94		25,00	*200*	Inside		15,0	201,90
22													
23													

Figure 76: Profile tab sheet, (EERA)

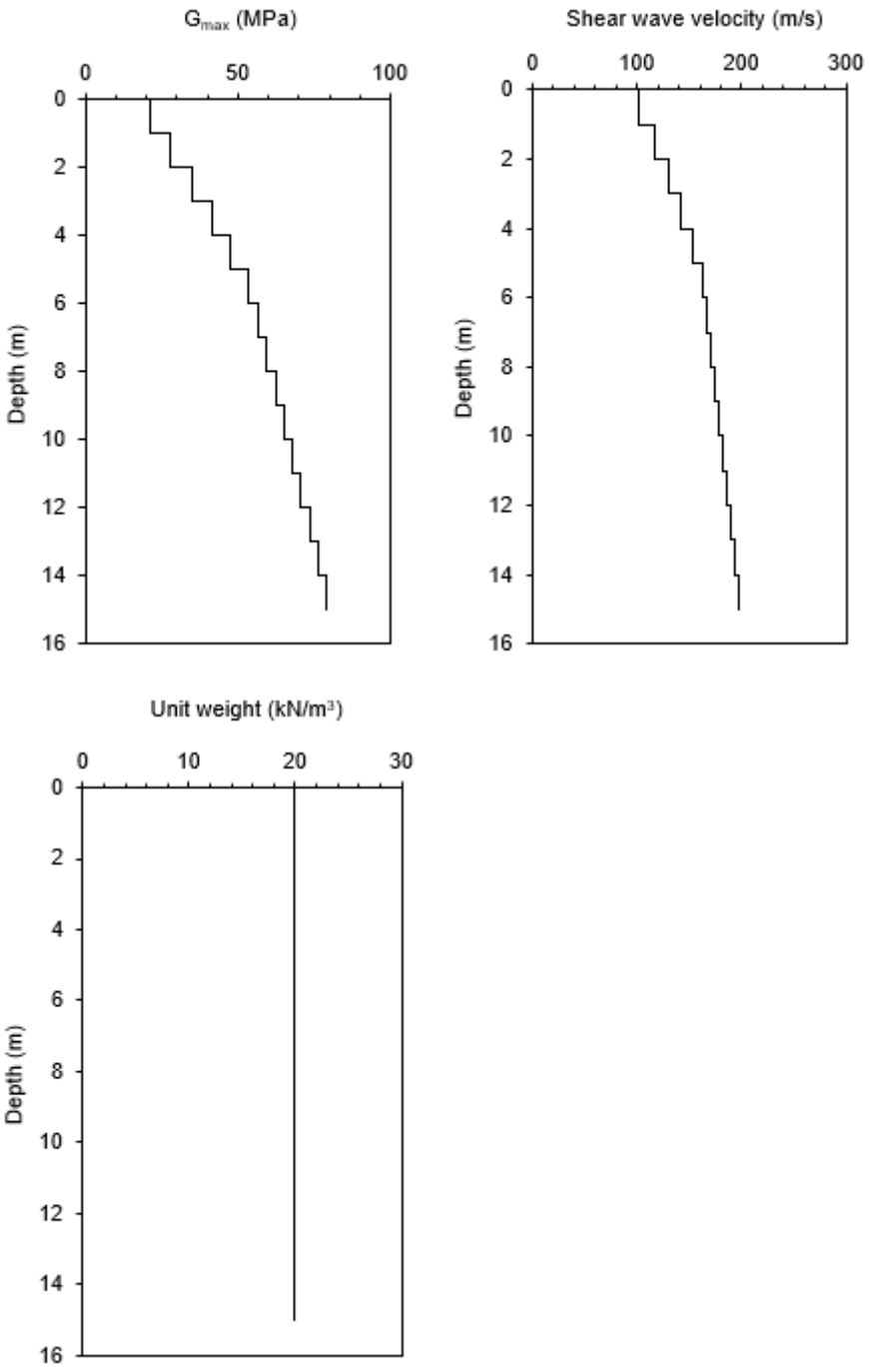

Figure 77: Variation of G, V_s and unit weight of soil with depth. Profile tab sheet, (EERA)

Modulus for clay (Seed and Sun, 1989) upper range and damping for clay (Idriss 1990)

Strain (%)	G/G_{max}	Strain (%)	Damping (%)
0,0001	1	0,0001	0,24
0,0003	1	0,0003	0,42
0,001	1	0,001	0,8
0,003	0,981	0,003	1,4
0,01	0,941	0,01	2,8
0,03	0,847	0,03	5,1
0,1	0,656	0,1	9,8
0,3	0,438	0,3	15,5
1	0,238	1	21
3	0,144	3,16	25
10	0,11	10	28

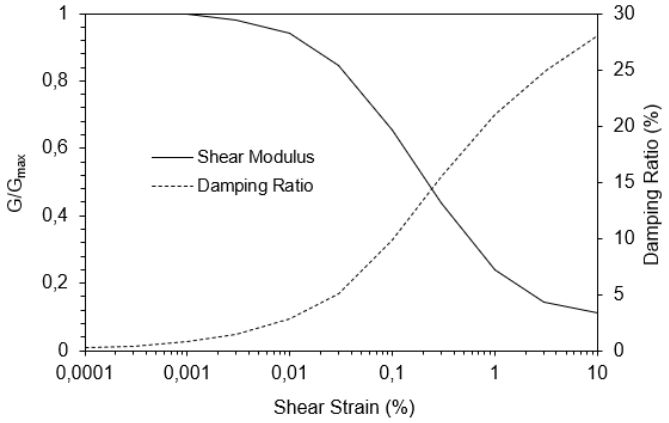

Figure 78: Mat1 tab sheet, (EERA)

Number of iterations : 8
Ratio of effective and maximum shear strain : 0,5
Type of shear modulus = Shake91
Convergence achieved (%) = 1,664894

Iteration Number	Sublayer Number	Type	Depth (m)	Maximum Strain (%)	Time of Maximum Strain (sec)	Shear Modulus	G/G_{max}	Damping (%)	Convergence on Shear Modulus (%)	Convergence on Damping (%)	Maximum stress (kPa)	Depth at top of sublayer (m)	Maximum acceleration (g)
1	1	1	0,5	0,024073	12,16	20,87959	1	0,24	0	0	5,02629		
	2	1	1,5	0,052206	12,16	28,09941	1	0,24	0	0	14,66948		
	3	1	2,5	0,067202	12,16	34,88	1	0,24	0	0	23,44015		
	4	1	3,5	0,075499	12,16	41,34099	1	0,24	0	0	31,21215		
	5	1	4,5	0,080131	12,51	47,53779	1	0,24	0	0	38,09261		
	6	1	5,5	0,082408	12,51	53,57066	1	0,24	0	0	44,14677		
	7	1	6,5	0,088326	12,17	56,51834	1	0,24	0	0	49,92055		
	8	1	7,5	0,092584	12,17	59,40568	1	0,24	0	0	55,00022		
	9	1	8,5	0,095314	12,18	62,29366	1	0,24	0	0	59,37464		
	10	1	9,5	0,097598	12,18	65,10435	1	0,24	0	0	63,54046		
	11	1	10,5	0,098571	12,18	67,90265	1	0,24	0	0	66,93259		
	12	1	11,5	0,09938	12,01	70,68387	1	0,24	0	0	70,24569		
	13	1	12,5	0,099341	12,01	73,4435	1	0,24	0	0	72,95943		
	14	1	13,5	0,098172	12,01	76,17715	1	0,24	0	0	74,78499		
	15	1	14,5	0,095965	12,01	78,8805	1	0,24	0	0	75,69762		
	16	0	15	0,073929	12,01	101,9368	1	0	0	0	75,36058		
2	1	1	0,5	0,005148	7,4	19,31657	0,925141	3,188036	7,485888004	1228,348267	0,994491		
	2	1	1,5	0,012152	7,4	24,13476	0,858906	4,808675	14,1093626	1903,614624	2,932785		
	3	1	2,5	0,016359	7,4	28,91608	0,829016	5,542537	17,0983963	2209,390625	4,730384		
	4	1	3,5	0,019049	7,39	33,50884	0,810548	5,996996	18,94523811	2398,748779	6,382968		
	5	1	4,5	0,020752	7,39	38,08261	0,801102	6,229434	19,88982773	2495,597656	7,902851		
	6	1	5,5	0,021661	7,39	42,67739	0,796656	6,338829	20,33439255	2541,178711	9,244187		
	7	1	6,5	0,023394	7,39	44,40389	0,785654	6,60955	21,43455505	2653,979248	10,38783		
	8	1	7,5	0,024499	7,39	46,22865	0,778186	6,793338	22,18143463	2730,557617	11,32571		
	9	1	8,5	0,025035	7,39	48,18885	0,773575	6,906781	22,64245224	2777,825684	12,0642		
	10	1	9,5	0,025213	7,38	50,11858	0,769819	6,999214	23,01808357	2816,339355	12,63657		
	11	1	10,5	0,025439	9,07	52,16584	0,768245	7,037961	23,17553902	2832,483887	13,27055		
	12	1	11,5	0,025853	9,07	54,21088	0,766948	7,069857	23,30515862	2845,773682	14,0149		

Figure 79: Iteration tab sheet, (EERA)

8.6 Appendix F

Eurocode 8

Base Shear Force

Model 1

$a_{g\ 40\ Hz}$	=	0,36	m/s²
a_g	=	0,288	g
γ_I	=	1,0	
Ground type	=	E	
ξ	=	5	%
β	=	0,2	
η	=	1,0	
S	=	1,65	
T_B	=	0,10	
T_C	=	0,30	
T_D	=	1,40	
q	=	1,5	
H	=	15	m
C_t	=	0,075	
T_1	=	0,572	s
m	=	72360	kg
λ	=	0,85	
S_d	=	0,416	m/s²
F_b	=	25,6	kN/m

Using building frequency obtained from PLAXIS 2D:

T_1	=	0,714	s

T1 is greater than 2Tc, hence λ=1,0

λ	=	1,0	
S_d	=	0,333	m/s²
F_b	=	24,1	kN/m

Elastic S_e (T) and Design S_d (T) Response Spectrum

f (Hz)	T (s)	S_e (T)	S_d (T)
	0,00	0,475	0,317
10,00	**0,10**	1,188	0,792
5,00	0,20	1,188	0,792
3,33	**0,30**	1,188	0,792
2,50	0,40	0,891	0,594
2,00	0,50	0,713	0,475
1,67	0,60	0,594	0,396
1,54	0,65	0,548	0,366
1,25	0,80	0,446	0,297
0,91	1,10	0,324	0,216
0,71	**1,40**	0,255	0,170
0,63	1,60	0,195	0,130
0,56	1,80	0,154	0,103
0,50	2,00	0,125	0,083
0,40	2,50	0,080	0,058
0,33	3,00	0,055	0,058
0,25	4,00	0,031	0,058

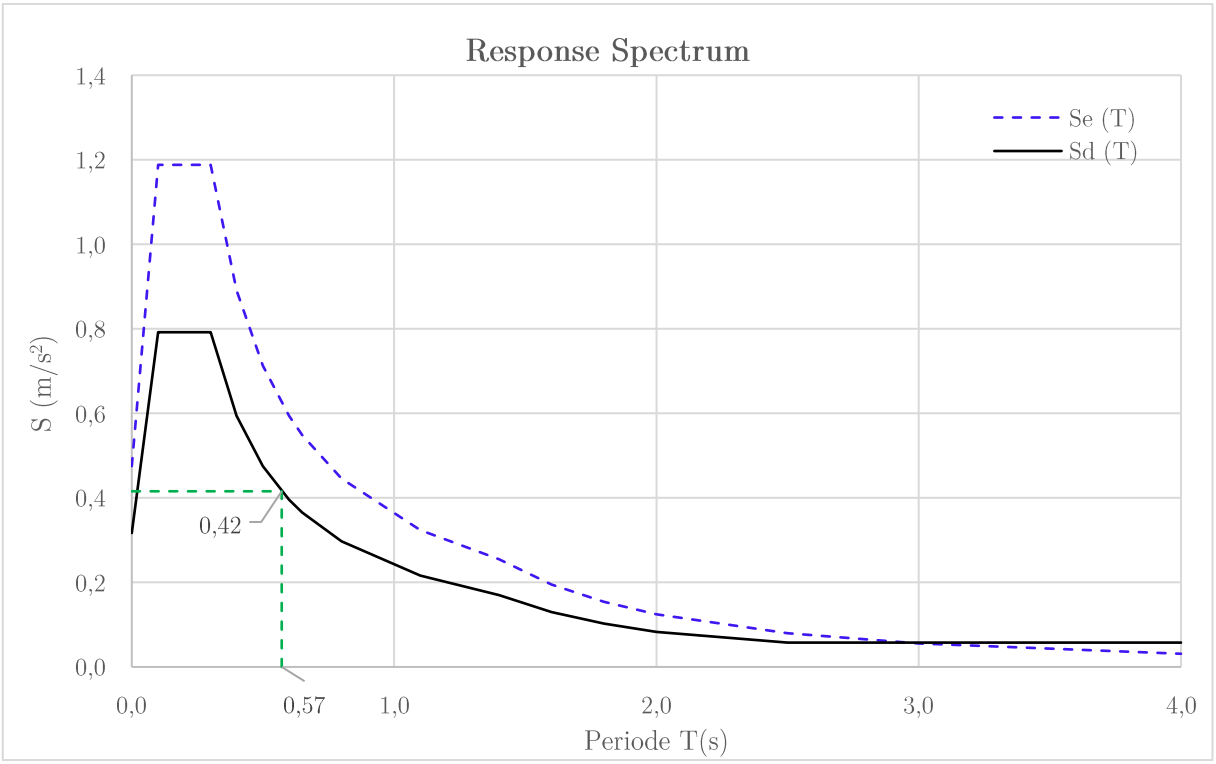

Figure 80: Design Spectrum-Model 1

Model 2

$a_{g\ 40\ Hz}$	=	0,36	m/s^2
a_g	=	0,288	g
γ_I	=	1,0	
Ground type	=	E	
ξ	=	5	%
β	=	0,2	
η	=	1,0	
S	=	1,65	
T_B	=	0,10	
T_C	=	0,30	
T_D	=	1,40	
q	=	1,5	
H	=	12	m
C_t	=	0,075	
T_1	=	0,484	s
m	=	60480	kg
λ	=	0,85	
S_d	=	0,491	m/s^2
F_b	=	25,3	kN/m

Using building frequency obtained from PLAXIS 2D:

T_1	=	0,714	s

T1 is greater than 2Tc, hence λ=1,0

λ	=	1,0	
S_d	=	0,333	m/s^2
F_b	=	20,1	kN/m

Elastic S_e (T) and Design S_d (T) Response Spectrum

f (Hz)	T (s)	S_e (T)	S_d (T)
	0,00	0,475	0,317
10,00	**0,10**	1,188	0,792
5,00	0,20	1,188	0,792
3,33	**0,30**	1,188	0,792
2,50	0,40	0,891	0,594
2,00	0,50	0,713	0,475
1,67	0,60	0,594	0,396
1,54	0,65	0,548	0,366
1,25	0,80	0,446	0,297
0,91	1,10	0,324	0,216
0,71	**1,40**	0,255	0,170
0,63	1,60	0,195	0,130
0,56	1,80	0,154	0,103
0,50	2,00	0,125	0,083
0,40	2,50	0,080	0,058
0,33	3,00	0,055	0,058
0,25	4,00	0,031	0,058

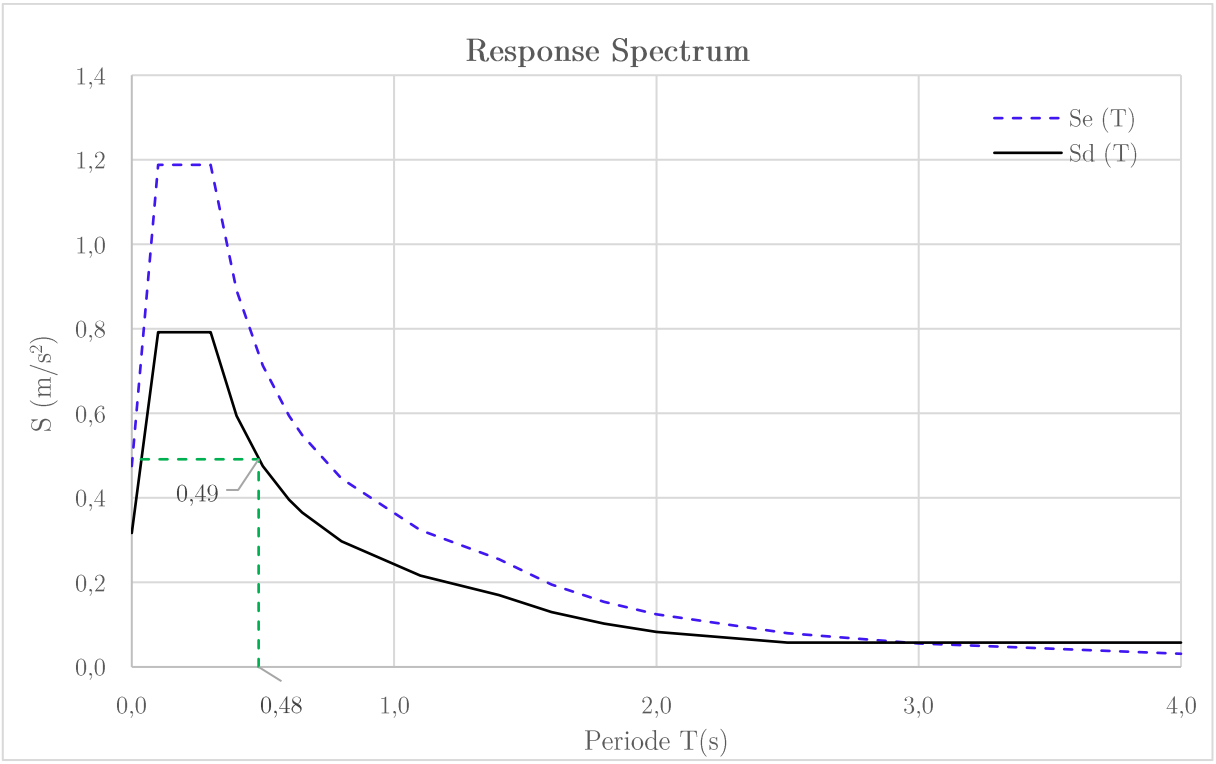

Figure 81: Design Spectrum-Model 2

Model 3

$a_{g\ 40\ Hz}$	=	0,36	m/s^2
a_g	=	0,288	g
γ_I	=	1,0	
Ground type	=	E	
ξ	=	5	%
β	=	0,2	
η	=	1,0	
S	=	1,65	
T_B	=	0,10	
T_C	=	0,30	
T_D	=	1,40	
q	=	1,5	
H	=	15	m
C_t	=	0,075	
T_1	=	0,572	s
m	=	72360	kg
λ	=	0,85	
S_d	=	0,416	m/s^2
F_b	=	25,6	kN/m

Using building frequency obtained from PLAXIS 2D:

T_1	=	0,833	s

T1 is greater than 2Tc, hence λ=1,0

λ	=	1,0	
S_d	=	0,285	m/s^2
F_b	=	20,6	kN/m

Elastic S_e (T) and Design S_d (T) Response Spectrum

f (Hz)	T (s)	S_e (T)	S_d (T)
	0,00	0,475	0,317
10,00	**0,10**	1,188	0,792
5,00	0,20	1,188	0,792
3,33	**0,30**	1,188	0,792
2,50	0,40	0,891	0,594
2,00	0,50	0,713	0,475
1,67	0,60	0,594	0,396
1,54	0,65	0,548	0,366
1,25	0,80	0,446	0,297
0,91	1,10	0,324	0,216
0,71	**1,40**	0,255	0,170
0,63	1,60	0,195	0,130
0,56	1,80	0,154	0,103
0,50	2,00	0,125	0,083
0,40	2,50	0,080	0,058
0,33	3,00	0,055	0,058
0,25	4,00	0,031	0,058

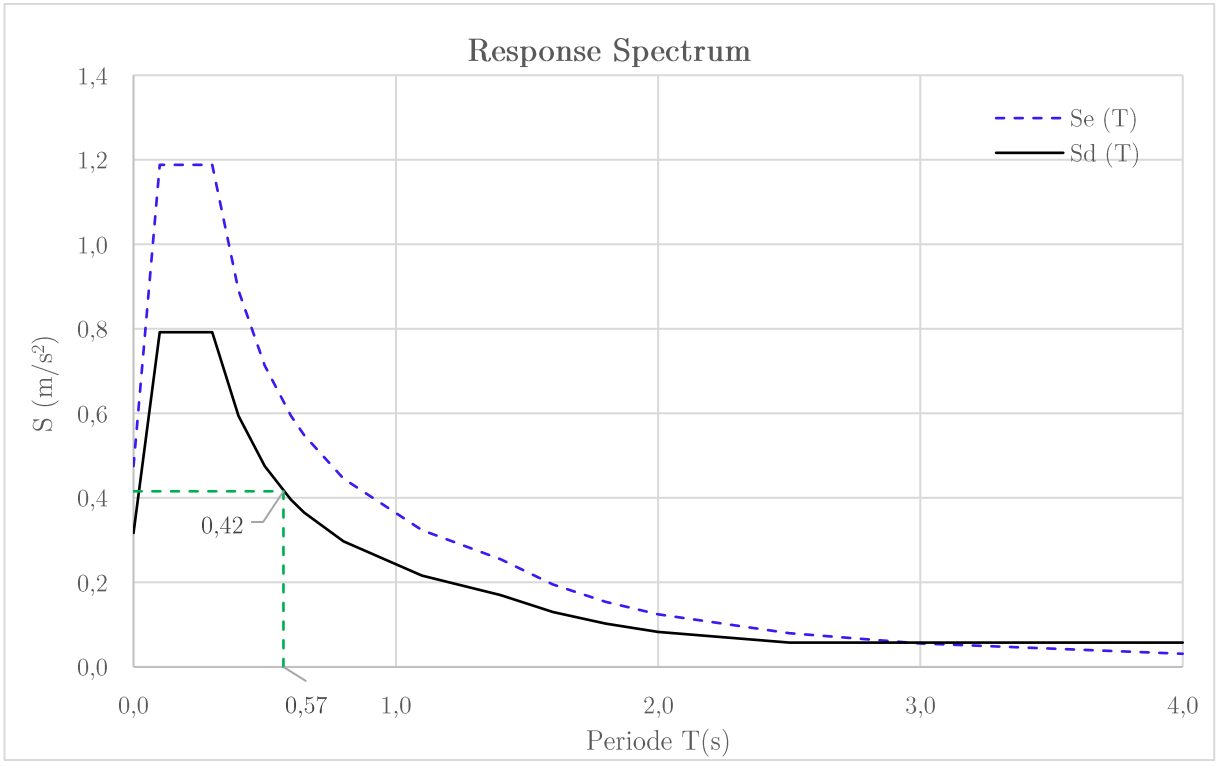

Figure 82: Design Spectrum-Model 3

Model 1- Alternative method for computation of fundament period $\mathbf{T_1}$

The lateral elastic displacement of the top of the building "d" is obtained from PLAXIS 2D for Model 1. Figure 70

$T_1 = 2\sqrt{d} = 2\sqrt{0{,}069} = 0{,}52\ s$

m	=	72360	kg
λ	=	0,85	
S_d	=	0,452	m/s^2
F_b	=	27,8	kN/m

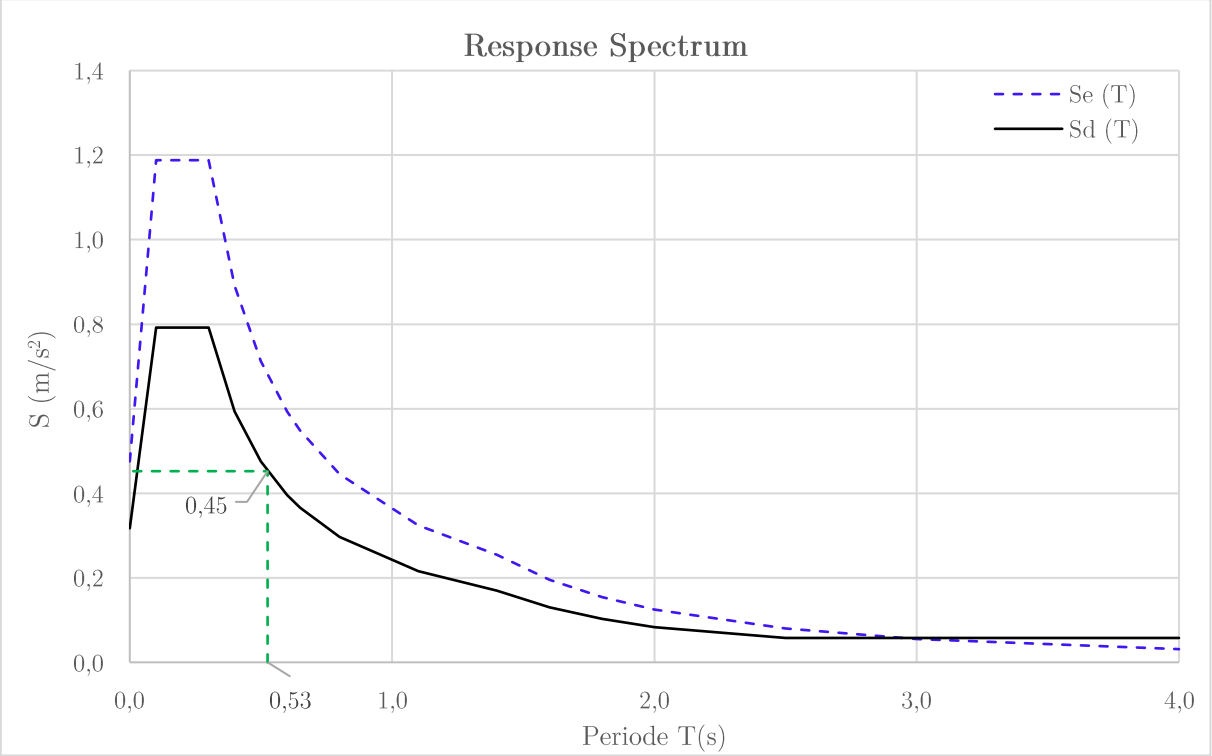

Figure 83: Design Spectrum for alternative computation of fundamental period (T_1)-Model 1

Deriving equation (2.60) according to RIF Veiledning, (Øystein Løset, Max Milan Loo, Åse Lyslo Døssland, Morten Gjestvang, Amir M.Kaynia, Christian Bråten, 2010)

$$T_1 = 2\pi\sqrt{\frac{M}{K}} = 2\pi\sqrt{\frac{F_h}{g * K}} = 2\pi\sqrt{\frac{d}{g}} \cong 2\sqrt{d} \tag{8.1}$$

Mass (M) converts to horizontal force F_h followed by gravitation (g).

Model 2-For behavior factor $q = 2,0$

q	=	2	
H	=	12	m
C_t	=	0,075	
T_1	=	0,484	s
m	=	60480	kg
λ	=	0,85	
S_d	=	0,369	m/s^2
F_b	=	18,9	kN/m

Using building frequency obtained from PLAXIS 2D:

T_1	=	0,714	s

T1 is greater than 2Tc, hence λ=1,0

λ	=	1,0	
S_d	=	0,249	m/s^2
F_b	=	15,1	kN/m

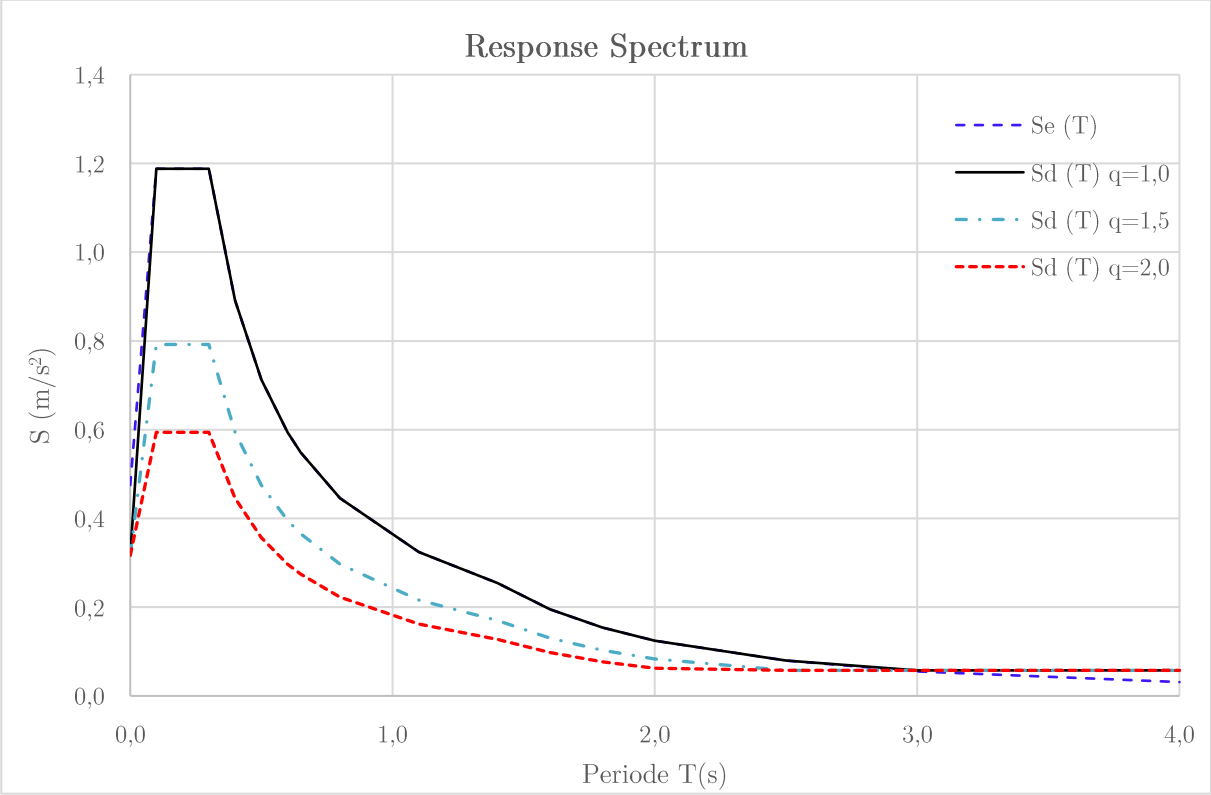

Figure 84: Design Spectrum, for behavior factor $q = 2,0$ -Model 2

Mass of the structure

Model 1 & 3

Total mass of model 1 and model 3 is assumed to be above foundation level.
Self-weight of members is shown in Table 9.

$m_1 = 108{,}0\ kN/m$
$m_2 = 129{,}6\ kN/m$
$m_3 = 129{,}6\ kN/m$
$m_4 = 129{,}6\ kN/m$
$m_5 = 151{,}2\ kN/m$
$Base\ plate\ =\ 75{,}6\ kN/m$
$Total\ =\ 723{,}6\ kN/m$

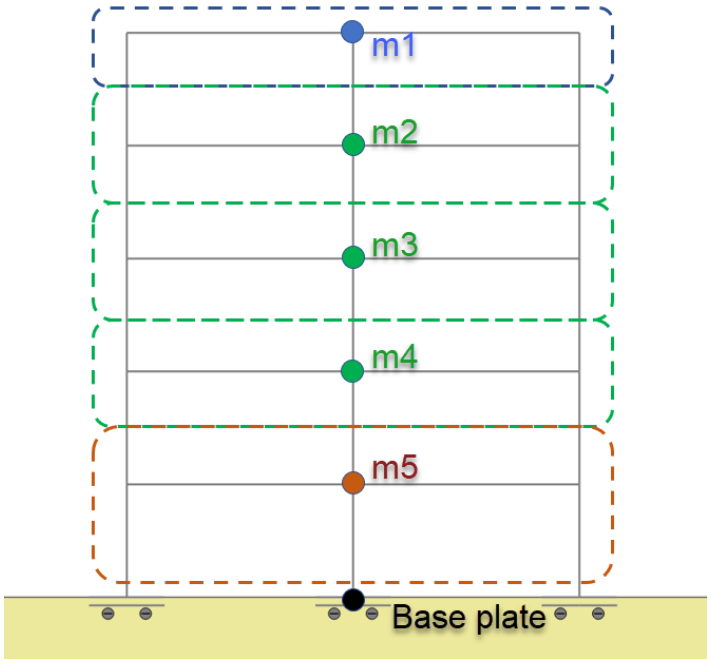

Figure 85: Mass of Model 1 and Model 3, illustration by Hijratullah Niazi

Model 2

$m_1\ = 108{,}0\ kN/m$
$m_2\ = 129{,}6\ kN/m$
$m_3\ = 129{,}6\ kN/m$
$m_4\ = 129{,}6\ kN/m$
$m_5\ = 108{,}0\ kN/m$
$Total\ =\ 604{,}8\ kN/m$

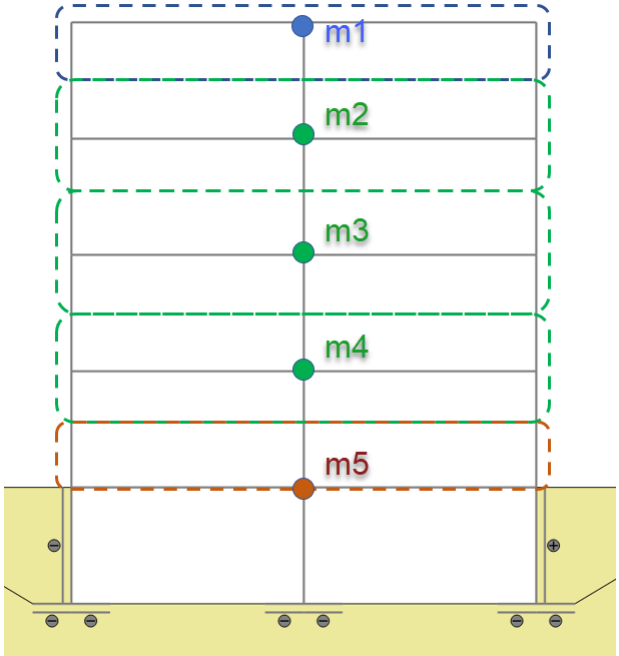

Figure 86: Mass of Model 2, illustration by Hijratullah Niazi

Total mass of Model 2 is assumed to be above top of rigid basement.

Ground types

Ground type	Description of stratigraphic profile	Parameters [2), 3)]		
		$v_{s,30}$ (m/s)	N_{SPT}(blows/ 30cm)	c_u (kPa)
A	Rock or other rock-like geological formation, including at most 5 m of weaker material at the surface.	> 800	–	–
B	Deposits of very dense sand, gravel, or very stiff clay, at least several tens of metres in thickness, characterised by a gradual increase of mechanical properties with depth.	360 – 800	> 50	> 250
C	Deep deposits of dense or medium-dense sand, gravel or stiff clay with a thickness from several tens to many hundreds of metres.	180 – 360	15 - 50	70 – 250
D	Deposits of loose-to-medium cohesionless soil (with or without some soft cohesive layers), or of predominantly soft-to-firm cohesive soil.	120 – 180	10 – 15	30 – 70
E	A soil profile consisting of a surface alluvium layer with v_s values of type C or D and a thickness varying between about 5 m and 20 m, underlain by stiffer material with v_s > 800 m/s.			
S1	Deposits consisting of or containing a layer at least 10 m thick of soft clays/silts with a high plasticity index (PI > 40) and high water content	< 100 (indicative)	–	10 – 20
S2	Deposits of liquefiable soils, of sensitive clays, or any other soil profile not included in types A – E or *S1*			

[1)] If at least 75 % of the structure rests on rock and the rest on other soil conditions, and the structure has a continuous plate foundation, ground type A may be selected.

[2)] The selection of ground type may be based either on $v_{s,30}$, N_{SPT} or c_u. $v_{s,30}$ is regarded as the most relevant parameter to be used.

[3)] If there is doubt on which ground type to select, the most unfavourable ground type shall be selected.

Figure 87: Ground types, (CEN, 2004), (TableNA.3.1)

Structural ductility class

Design concept	Structural ductility class	Range of the reference values of the behaviour factor, q
Concept a) Low dissipative structural behaviour	DCL (Low)	≤ 1,5
Concept b) Dissipative structural behaviour	DCM (Medium)	≤ 4 also limited by the values for DCM in Table 6.2
	DCH (High)	Same as for DCM

Figure 88: Design concepts, structural ductility classes and upper limit reference values of the behavior factors, (CEN, 2004), (Table NA.6.1)

Seismic Zone

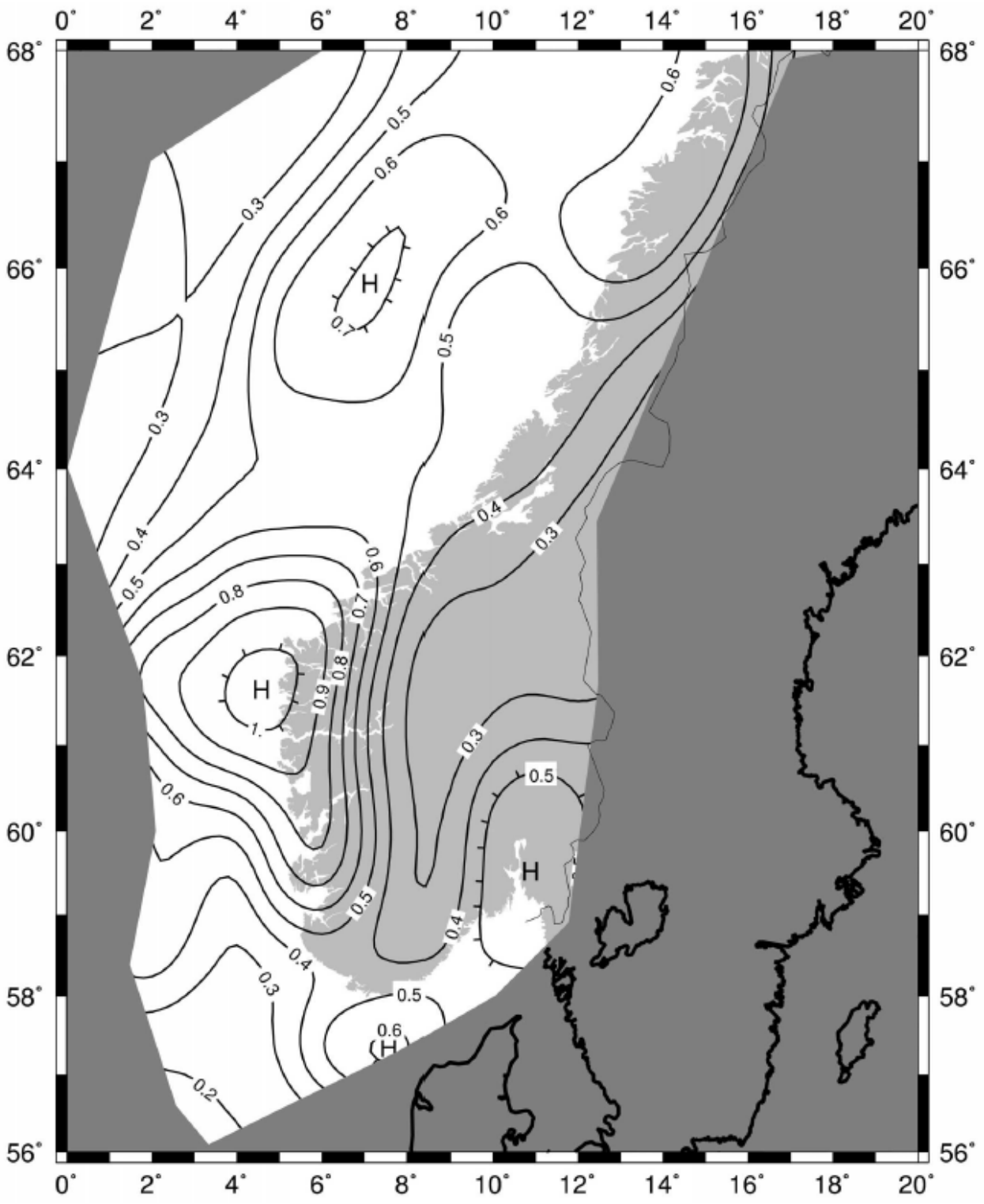

Figure 89: Seismic zones in southern Norway, $a_{g\,40Hz}$ in m/s^2, (CEN, 2004), Fig NA.3(901)

8.7 Appendix G

PLAXIS 2D Tips

Ground Response Analysis

1. In the *Soil* menu, Create borehole, input all necessary information or chose the one which is already made
2. Select Site_response, Edit displacement multipliers, and select input signal/time series which is already input in the model, then OK
3. From Site_response, select Calculate for Borehole
4. Start server, Close
5. Save the file as PLAXIS asks, and follow the steps. 1D Response Analysis modell will be created after awhile. All necessary nodes will be generated automatically, proper dynamic time interval, mesh and boundaries will be selected.
6. When calculation is done, open PLAXIS 2D Output from Windows Start menu and generated file will on the top of the Recent porjects list

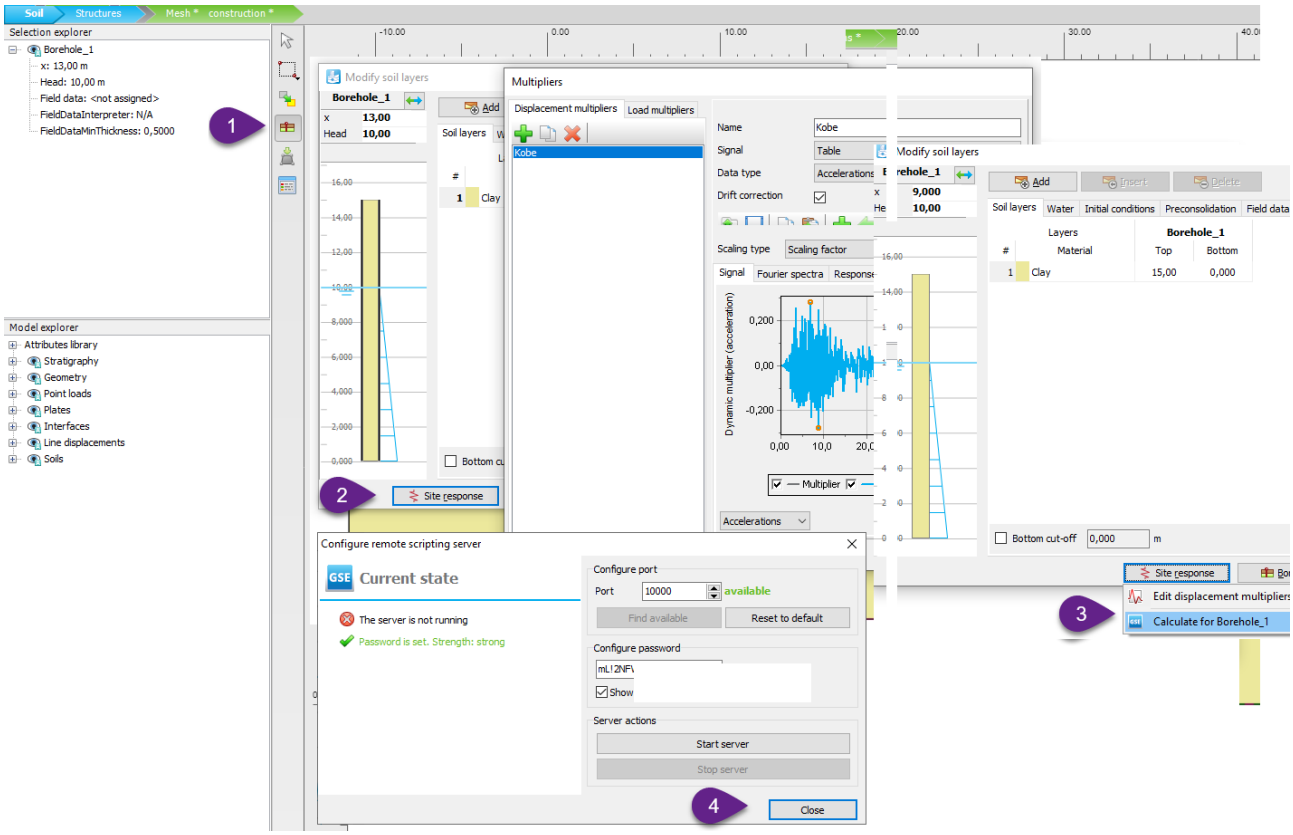

Figure 90: Generating Ground Response Analysis

Check Dynamic Time Interval

1. Open View Calculation Result, and open accleration at the bottom of the model
2. Open input signal motion file

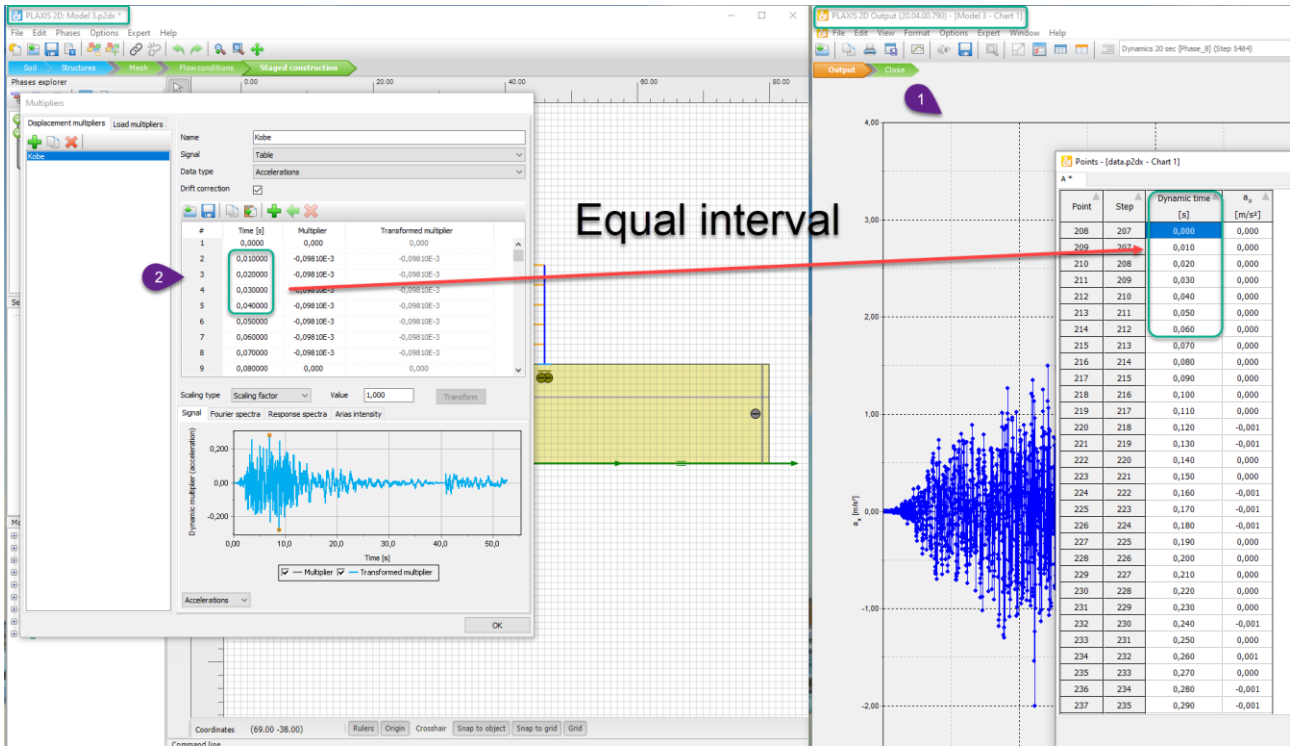

Figure 91: Check Dynamic Time Interval at the base of model

Frequency Representation (Spectrum)

1. Open Curve generation menu, select *Dynamic time* for X-axis and ax or ux for Y-axis
2. Generate the curve for correct phase and selected point for the structure, chose middle top of the structure
3. In the setting menu, right after curve is generated, in *Chart* menu choose *Standard frequency (Hz)*
4. Frequency representation (Spectrum) is generated

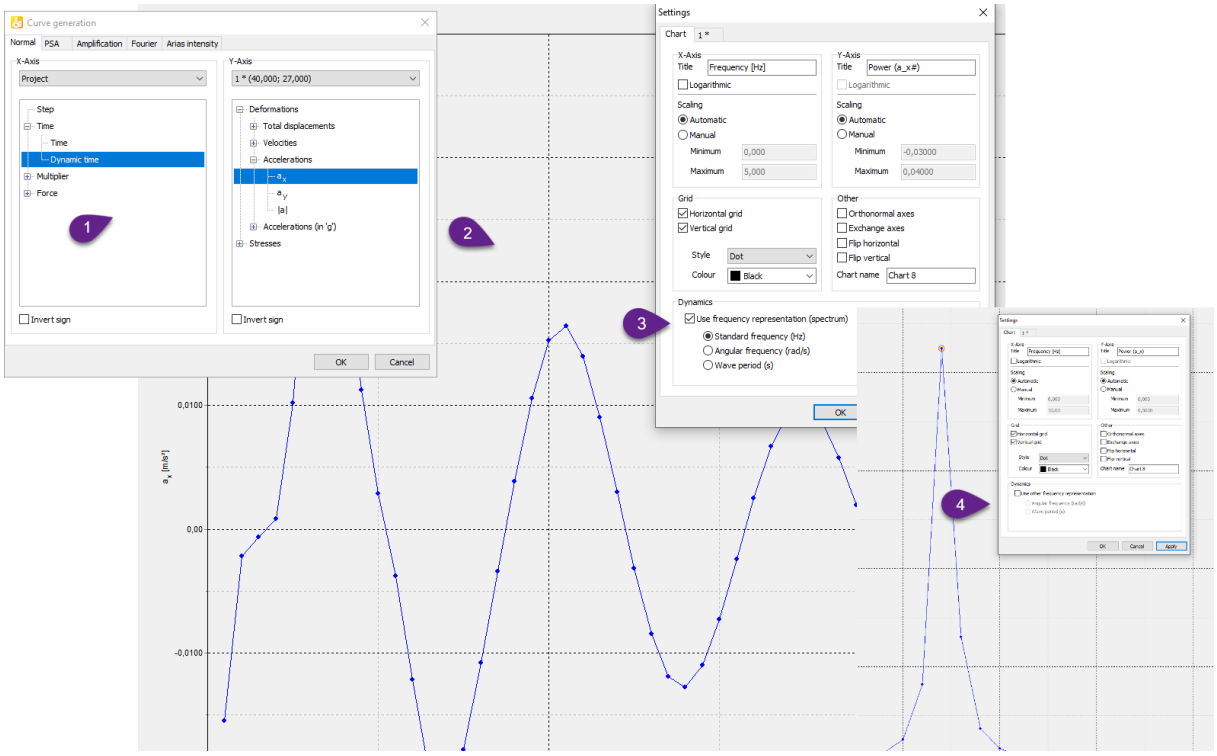

Figure 92: Plotting Frequency Representation (Spectrum)

Base Shear Force

1. Run analysis and save file before opening calculation results
2. Select point for curves (Post-calculation point)
3. Open Curve generation, New, chose Step for X-axis, and chosen node for Y-axis
4. Generate curve, chose correct phase
5. Extreme values sub menu also shows envelope forces with step

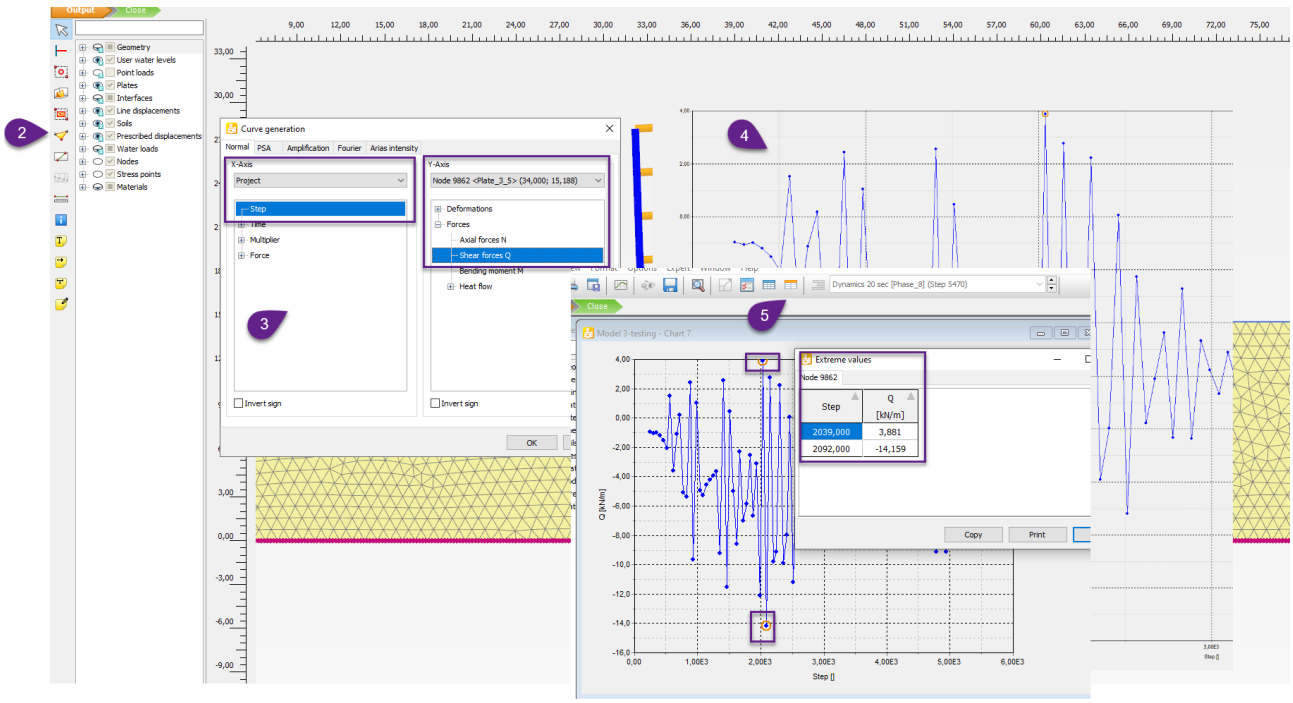

Figure 93: Plot Base Shear Force